THE PHYSICAL REVIEW

VOLUME 47 | Second Series | NUMBER 1

JANUARY 1, 1935

Published for the

AMERICAN PHYSICAL SOCIETY

by the

AMERICAN INSTITUTE OF PHYSICS

Incorporated

LANCASTER, PA., AND NEW YORK, N. Y.

The American Physical Society

OFFICERS OF THE SOCIETY

President
The Johns Hopkins University
Baltimore, Maryland

F. K. Richtmyer, *Vice-President*
Cornell University
Ithaca, New York

W. [illegible] Duane, *Secretary*
Columbia University
New York, New York

G. B. Pegram, *Treasurer*
Columbia University
New York, New York

John T. Tate, *Editor*
University of Minnesota
Minneapolis, Minnesota

L. B. Loeb, *Local Secretary for the Pacific Coast*
University of California
Berkeley, California

The Physical Review

BOARD OF EDITORS

John T. Tate, *Editor*

J. W. Buchta, *Assistant Editor*

Associate Editors

[illegible] Darrow	A. Ellett	W. V. Houston
[illegible] C. Hubbard	L. A. Turner	R. S. Mulliken
A. E. Ruark	G. E. Uhlenbeck	I. I. Rabi

The Physical Review, which was established [illegible], is a journal of experimental and [illegible] physics. It is published for the American Physical Society by the American Institute of Physics Incorporated. There are two volumes annually with twelve issues in each volume.

Papers for publication should be submitted to [illegible] University of Minnesota, Minneapolis, Minnesota.

All correspondence concerning papers in the [illegible] section, should be addressed to the Editorial [illegible] American Institute of Physics, 11 East 38th [illegible] New York, New York.

Subscriptions: United States and Possessions and [illegible] Foreign, $16.50. Subscriptions and orders [illegible] should be addressed to Prince and [illegible] Lancaster, Pennsylvania, or to the American [illegible] of Physics, 11 East 38th Street, New York, [illegible] York.

[illegible] not accepted for the *Physical Review* but [illegible] to the *Review of Scientific Instruments* [illegible] *and Views*, a companion publication of [illegible] and a medium through which the field of physics can be reached most effectively. Rates and other information will be furnished on request to the Editorial Secretary.

Changes of address and complaints of failure to receive the *Physical Review*, in the case of members of the American Physical Society, should be addressed to the Treasurer; in the case of other subscribers, to the Editorial Secretary. New copies can be sent free in response to complaints of non-delivery only if notice of non-delivery is received within three months of date of issue.

The Physical Review is published semi-monthly at Prince and Lemon Streets, Lancaster, Pennsylvania.

Entered at the Post Office at Lancaster, Pennsylvania, as second class matter.

Acceptance for mailing at special rate of postage provided for in section 1103, Act of October 3, 1917, authorized September 6, 1924.

THE
PHYSICAL REVIEW
A Journal of Experimental and Theoretical Physics
VOL. 47, NO. 1 JANUARY 1, 1935 SECOND SERIES

Ultraviolet Absorption of Iodine Vapor

DANA T. WARREN, *Sloane Physics Laboratory, Yale University**

(Received November 13, 1934)

The regularity of development of the ultraviolet absorption spectrum of iodine between λ1900 and λ3413 from shorter to longer wave-lengths with increasing temperature and pressure indicates that the bands all belong to one system. The large range of conditions under which bands studied by Pringsheim and Rosen and those found by Kimura and Miyanishi are both found leads to the same conclusion. The "long thin bridge" joining these two regions is explained as the result of the coincidence of $\Delta G' = 70$ cm^{-1} and $\Delta G'' = 210$ cm^{-1}, causing successive v' progressions to coincide. This is supported by the manner in which successive v' progressions join on to the single series. A similar explanation probably holds for the single series of spacing 90 cm^{-1} at the red end of the Pringsheim and Rosen bands, which breaks up near λ2850 into the bands found associated with the λ3413 "continuum" in fluorescence, emission and absorption. This continuum forms the absorption maximum at the long wave-length limit of the spectrum, the red end. It is therefore neither an electron affinity nor ionic recombination nor any other atomic spectrum. These results agree well with Mulliken's theory of this system.

THE existence of ultraviolet absorption in iodine vapor was indicated, according to the theory of Lenz,[1] by the ultraviolet fluorescence found by McLennan,[2] Oldenberg[3] and Wychodil.[4] This absorption was studied by three different groups of investigators in 1928–29. The region λλ2080–2760 was studied by Pringsheim and Rosen.[5] They used a sphere of 6 cm diameter, and unstated temperatures in the range 200–800°C. They found two series of bands: one at λλ2500–2760 spaced uniformly at 90 cm^{-1}, the second λλ2080–2200 spaced at 70 cm^{-1}. These they called the $v'=0$ and $v''=0$ progressions, respectively, and analyzed the intervening welter of bands according to these two frequencies, which they could readily do within the limits of their accuracy. This necessitated the identification of their lower state with an excited state of the molecule ($\omega = 90$ cm^{-1}, $\omega x = 0$) rather than the ground state ($\omega = 214$ cm^{-1}, $\omega x = 0.6$ cm^{-1}). Kimura and Miyanishi[6] extended the absorption, obtaining bands with an absorption tube 15 cm long at temperatures 35–120°C in the region λλ1950–2150. These they analyzed according to the equation

$$\nu = 52{,}800 + 78v' - v'^2 - 210v'' \text{ cm}^{-1}.$$

The value $\omega' = 78$ cm^{-1} they identified with that (70 cm^{-1}) of the upper state of the Pringsheim-Rosen bands, and the lower state they identified with the ground state of the molecule. However, their intensity distribution was incomprehensible and their method of determining v'' incorrect, hence their results are not very convincing.

* Portion of a dissertation presented for the degree of Doctor of Philosophy at Yale University.

[1] W. Lenz, Phys. Zeits. **21**, 691 (1920); Zeits. f. Physik **25**, 299 (1924).

[2] J. C. McLennan, Proc. Roy. Soc. **A88**, 289 (1913); **A91**, 23 (1914).

[3] O. Oldenberg, Zeits. f. Physik **18**, 1 (1923).

[4] P. Pringsheim, Die Naturwiss. **16**, 131 (1928); E. Hirschlaff, Zeits. f. Physik **75**, 325 (1932).

[5] P. Pringsheim and B. Rosen, Zeits. f. Physik **50**, 1 (1928).

[6] M. Kimura and M. Miyanishi, Sci. Papers Inst. Chem. and Phys. Res. Tokyo **10**, 33 (1929).

TABLE I. *Dependence of ultraviolet absorption on temperature and pressure.* Data for the observations plotted in Fig. 1 are given here.

Temp. (°C)	Pressure (mm Hg)	Bands	Region (Å)	Temp. (°C)	Pressure (mm Hg)	Bands	Region (Å)
23	0.41	K–M and S–W	1930–1960	190	27	P–R	2130–2210
30	.50	K–M " S–W	1925–1960	190	157	None	
30	.50	K–M " S–W	1900–2000 (2 hrs.)	190	521	None	
31	.70	K–M " S–W	1930–1970	330	5.8	None	
39	1.05	K–M	1930–2010	326	8.2	P–R and K–M	2100–2200
47	1.1	K–M	2040–2125	330	18	P–R	2120–2210
120	0.9	None		330	105	P–R	2200–2250
120	1.3	P–R and K–M	2010–2120	335	217	P–R	2280–2340
120	1.9	P–R " K–M	2050–2140	330	570	P–R	2270–2330
120	2.5	P–R " K–M	2060–2150	505	27	None	
120	4.7	P–R " K–M	2070–2150	545	55	P–R	2220–2270
120	8.0	P–R " K–M	2110–2180	502	105	P–R	2220–2330
120	8.2	P–R " K–M	2080–2160	510	150	P–R	2300–2370
120	11	P–R " K–M	2080–2160	498	350	P–R	ca 2330
120	30	P–R	2100–2190	498	680	None	
190	.25	None		690	157	P–R	2350–2450
190	.75	None		640	170	P–R	2350–2480
190	1.4	P–R and K–M	2060–2140	644	294	P–R	2400–2630
190	6.0	P–R " K–M	2100–2160	630	350	P–R	2440–2630
				690	815	P–R	2500–2700

Note: K–M = bands in the Kimura-Miyanishi region; S–W = bands in the Sponer-Watson region; P–R = bands in the Pringsheim-Rosen region.

Sponer and Watson[7] carried the observations into the Schumann region, and found at least two absorption systems. The one lying at longer wave-lengths, λλ1770–1950, apparently formed a continuation of the Kimura-Miyanishi bands. However their temperatures, pressures and path lengths differed greatly from those of Kimura and Miyanishi.

The Sponer and Watson bands seemed to form two long v' progressions, and were certainly related to the ground state of the iodine molecule, since they were obtained at room temperature. They showed a $\Delta G'$ value varying in the range 35–55 cm^{-1}. Their relation to the Kimura-Miyanishi bands left little room to doubt that the value 78 cm^{-1} for the $\Delta G'$ of the latter was incorrect. Hence Sponer and Watson re-analyzed the Kimura and Miyanishi data, obtaining a value of $\Delta G'$ of 50–70 cm^{-1}. Their intensity distribution also seemed more probable than the solid block shown by Kimura and Miyanishi. Sponer and Watson also attempted to include the long series called by Pringsheim and Rosen their $v''=0$ progression. But here the relation was not so clear, and it was very difficult to make the connection between the two groups of bands consist of a single progression. However, it seemed quite possible that these bands all belonged to one system. These and some other relations of these bands have recently been discussed by Curtis and Evans.[8]

The chief difficulty concerning these bands is the relation between the bands observed by Pringsheim and Rosen and those found by Kimura and Miyanishi. This is due chiefly to the diversity in path length, temperatures, and pressures of the experimental conditions of the different investigations, and to the peculiar relation of the "long thin bridge," Pringsheim and Rosen's $v''=0$ progression, uniting them. Hence the first step in studying the relation of these bands was to investigate their dependence on temperature and pressure. For this purpose a 15 cm absorption tube with an electrically wound furnace and an appendix with a separate furnace were prepared. The temperatures of the main tube and the side limb were read by means of thermocouples. The absolute values are probably not in error by more than 10°C. The pressures were obtained from the temperature of the appendix tube by means of vapor pressure tables.

The results are shown in Fig. 1 and Table I. Table I gives the values of the quantities plotted

[7] H. Sponer and W. W. Watson, Zeits. f. Physik **56**, 184 (1929).

[8] W. E. Curtis and S. F. Evans, Proc. Roy. Soc. **A141**, 603 (1933).

in the figure. The region in which bands are found under the corresponding conditions of temperature and pressure is roughly indicated by the type of point entered, corresponding to the original investigators who found bands in the region of some of those found under those conditions, and by the contour lines. There are two important conclusions to be drawn from Fig. 1. First is the regularity of development of

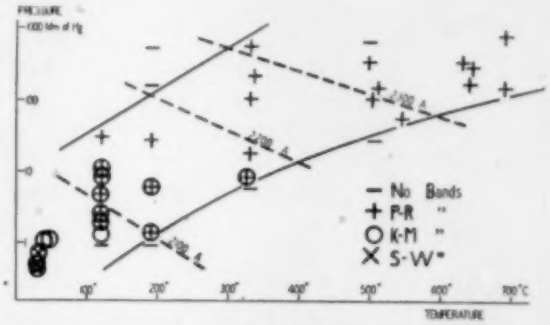

FIG. 1. Contour diagram of ultraviolet absorption bands obtained as a function of temperature and pressure. The data are for a 15 cm path length and low dispersion. The solid lines delineate the region in which bands are found, the dotted lines are wavelength contour lines. The type of point entered indicates whether the corresponding bands were observed by Pringsheim and Rosen,[5] Kimura and Miyanishi,[6] or Sponer and Watson.[7]

the system from shorter to longer wavelengths with increasing temperature and pressure within the limits where discrete bands are visible. There is no irregularity or discontinuity corresponding to the transition from Kimura-Miyanishi to Pringsheim-Rosen bands. This extends the regularity of development found by the various investigators in their own regions. Second is the large number of different conditions under which both Kimura-Miyanishi and Pringsheim-Rosen bands are found. This is partly due to the fact that the two wavelength regions overlapped considerably, but in any case it shows that there must be a close connection between the two groups of bands.

Since the results so far indicated that the bands belong to a single system, it was thought possible that other progressions could be found connecting the two groups of bands. For this purpose measurements were made at medium dispersion (100 cm^{-1}/mm at $\lambda 2200$) on bands in the intermediate region. A few new bands were found, but the single series with spacing 70 cm^{-1} remained. It was concluded that this series was due to the superposition of successive v' progressions, due to the coincidence of values $\Delta G' = 70$ cm^{-1}, $\Delta G'' = 210$ cm^{-1}. This could be tested by studying the manner in which different v' progressions are related to the single series. This is shown in Table II, which gives a partial

TABLE II.

TABLE II. *Kimura-Miyanishi bands and the long thin bridge.*

This gives a matrix diagram showing the relation of the single series (above the line in each column) to several progressions in the Kimura-Miyanishi region. Some new measurements are included. Other progressions in this region lie to the left of those given.

46726	*206*	46520	*207*	46313	*207*	46106
73		*71*		*70*		*67*
46799	*208*	46591	*208*	46383	*210*	46173
74		*68*		*68*		*68*
46873	*214*	46659	*211*	46448	*207*	46241
78		*67*		*72*		*78*
46948	*222*	46726	*206*	46520	*207*	46313
69		*73*		*71*		*70*
47017	*218*	46799	*208*	46591	*208*	46383
70		*74*		*68*		*68*
47087	*214*	46873	*214*	46659	*211*	46448
63		*75*		*67*		*78*
47150	*202*	46948	*222*	46726	*206*	46520
67		*69*		*78*		*71*
47217	*200*	47017	*218*	46799	*208*	46591
68		*70*		*74*		*68*
47285	*198*	47087	*214*	46873	*214*	46659
71		*63*		*75*		*67*
47356	*206*	47150	*202*	46948	*222*	46726
69		*67*		*69*		*73*
47425	*208*	47217	*200*	47017	*218*	46799
68		*68*		*70*		*65*
47493	*208*	47285	*198*	47087	*223*	46862
		71		*63*		*70*
		47356	*206*	47150	*218*	46932
		69		*62*		*68*
47636	*211*	47425	*213*	47212	*218*	47000
63		*68*		*68*		*70*
47699	*206*	47493	*213*	47280	*210*	47070
65				*60*		*67*
47764				47340	*208*	47137
66				*65*		
47830	*210*	47620	*213*	47405		
66		*61*		*65*		
47896	*213*	47681	*211*	47470	*213*	47257
60		*68*		*69*		
47936	*207*	47749	*210*	47539		
66		*67*		*66*		
48022	*206*	47816	*211*	47605		
74		*71*		*66*		
48096	*200*	47887	*216*	47671		
67		*57*		*65*		
48163	*219*	47944	*208*	47736		
		62		*61*		
		48006	*209*	47797		

matrix diagram of measured frequencies in the region where the Kimura-Miyanishi bands merge into the single series. The bands at the top (lower v' values) belong to the single series and are repeated in successive columns, as far down as the underlined band. Beyond this band, the individual progressions are clearly distinguished. It will be readily seen that the series regarded by Pringsheim and Rosen as a $v'' = 0$ progression

TABLE III. *Band measurements in the region of the Kimura-Miyanishi and Sponer-Watson overlap.* The measurements were made at low dispersion, partly by extrapolation, and are not of great accuracy. However, the general agreement indicates the close connection of the two sets of bands.

Measured	K–M	Measured	K–M	Measured	S–W	Measured	S–W
50008	50015 (5)	50943	50942 (6)	51224	51224	51937	51939
041	045 (6)		961 (6)	291	281	990	982
075	075 (5)		983 (u)	349	334	52042	52032
109	105 (5)	50994	51007 (7)		387	094	082
	126 (u)		026 (7)	(masked)	430	148	136
139	140 (6)		033 (5)	51459		200	182
164	168 (5)	51050	044 (5)		476	250	235
	173 (u)		059 (6)	509		288 ?	289
200	198 (7)		086 (7)	522 ?	526	356	339
238	234 (6)	106	117 (8)	564	569	403	389
(masked)	259 (5)		130 (u)	589 ?		459	439
50281	287 (7)	167		616	623	517	492
(These bands	50314 (7)		185 (8)	663	673	562	542
visible but	—		206 (u)	693 ?		616	591
too weak to	—						
measure.)	50741 (7)	224		720	724		640
CH_3I Absorption							
	50847 (8)		237 (8)	777	777	686	691
50898	896 (6)		258 (u)	835	828	710	740
	911 (6)	291	298 (8)	889	885	761	787
						811	840

actually belongs to three or four progressions with different v'' values. The conditions are similar at the other end of the long thin bridge where the Pringsheim and Rosen bands merge into the single series.

It seemed desirable also to investigate the relation of the Sponer-Watson and Kimura-Miyanishi bands by means of overlapping measurements. The results are given in Table III, and show the continuity of the two groups of bands.

The analysis of the Pringsheim and Rosen bands is not very satisfactory in any case. An attempt was made to improve it by the use of high dispersion (40 cm^{-1}/mm at λ2300), but it was found that the rotational structure, though incompletely resolved, made the bands too diffuse for accurate measurement. Hence the relation of the bands to the other single series (Pringsheim and Rosen's $v'=0$ series, with a spacing of 90 cm^{-1}) is not clear. However, if the series is due to the coincidence of $\Delta G'=90$ cm^{-1} and $\Delta G''=180$ cm^{-1}, the series should break up at the long wavelength end. For this purpose high pressures and temperatures were used to extend the system as far as possible. It was found that the series breaks up in the neighborhood of λ2850. This is interpreted as being due to the simultaneous increase of $\Delta G'$ and decrease of $\Delta G''$ till the progressions no longer coincide.

Still further increase of temperature and pressure gave, as found by Skorko,[9] two "continua" with intensity maxima at λ3413 and λ3270. At the highest temperatures obtained, 1115°C, the bands visible in the absorption edge have progressed until they reach the region of strong absorption at λ3413, but go no farther.

[9] E. Skorko, Nature **131**, 366 (1933).

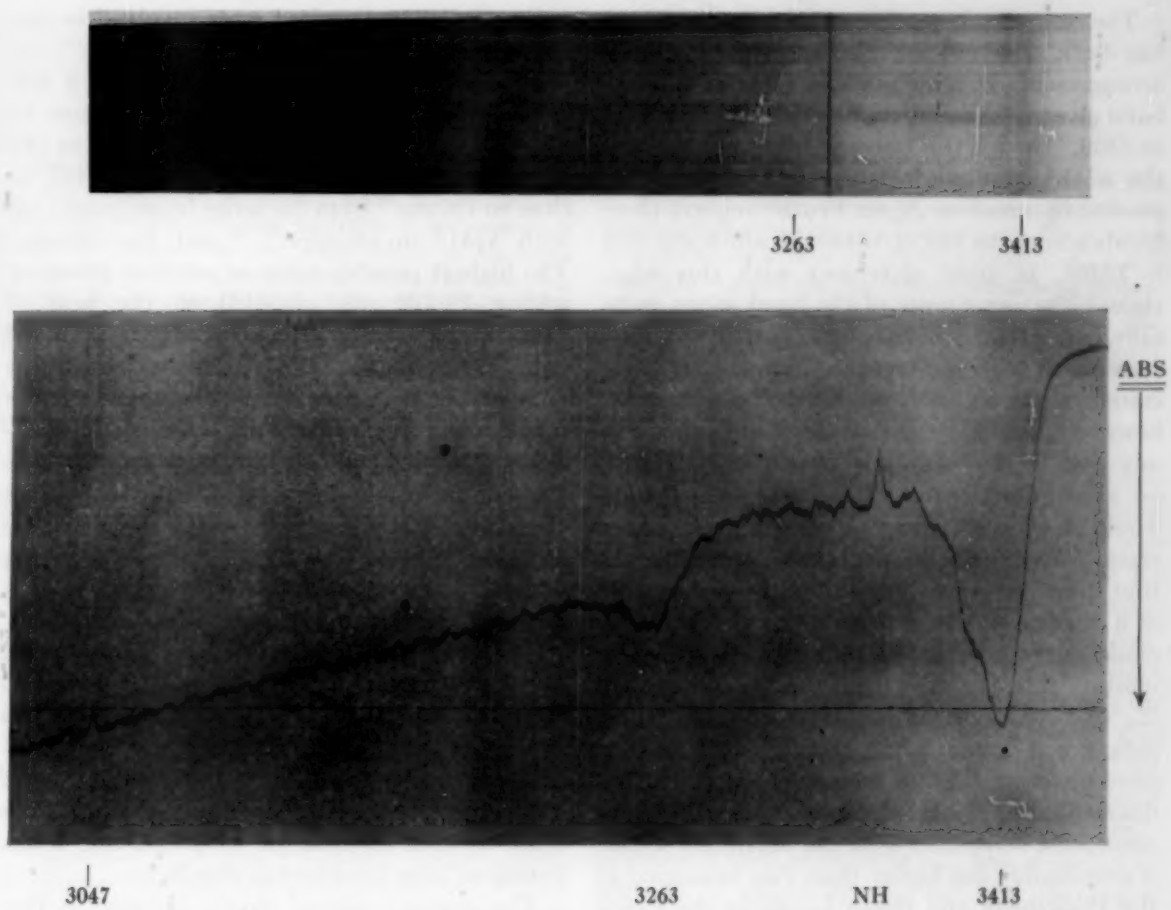

FIG. 2. Enlargement (4×) and microphotometer trace (6×) of two plates showing the absorption bands of iodine at the red end of the ultraviolet absorption system.

This condition is illustrated in Fig. 2. It will be noticed that there is no visible absorption at wavelengths greater than λ3413. Hence this "continuum," which has been the subject of much discussion,[8] appears to be the red end[10] of this strong absorption system. Naturally, when it is observed in emission the bands with lowest values of v' are most strongly developed, and these correspond to the red end. That the "continuum" and the discrete bands belong to the same system is indicated by their being found associated under such diverse circumstances (fluorescence at high temperatures[4] and pressures,[11] electrical discharge,[12] and absorption). Hence the upper state involved is that of the ultraviolet absorption, not electron+atom[13] or ions.[11] Its presence in fluorescence with conditions of high collision probability must be because collisions favor the emission of these bands over the McLennan bands. This may also be the reason why these bands appear so strongly in heated vapor in the discharge.[13, 14]

The bands measured in absorption have been compared with previous measurements, but it has not been possible to obtain a satisfactory quantum analysis. Further work in fluorescence is under way, and it is hoped to obtain an analysis of these bands by relating them to the fluorescence series.

[10] F. W. Loomis and S. W. Nile, Jr., Phys. Rev. **32**, 873 (1928).
[11] O. Oldenberg, Zeits. f. Physik **25**, 136 (1924).
[12] G. Cario and O. Oldenberg, Zeits. f. Physik **31**, 914 (1925).
[13] W. Gerlach and F. Gromann, Zeits. f. Physik **18**, 239 (1923).
[14] H. F. Fruth, Phys. Rev. **31**, 614 (1928).

The second absorption maximum at λ3263 has been observed by Skorko with a similar arrangement. It may possibly correspond to a band given by Konen[15] as "continuous maximum at 3300," though this latter seems more probably the λ3413 continuum, which is almost always present in emission. Again Fruth[14] reports three bands across the tail of λ3460, of which the first is λ3265, in good agreement with this edge, though the appearance of the band seems to be different. Hirschlaff[4] has obtained it in fluorescence at high temperatures, apparently associated with six narrow bands, which may, however, belong to the absorption system. In any case, it may similarly form the red end of an absorption system. If so, the upper state would lie about 1400 cm^{-1} higher than the upper state of the discrete bands. It was at first thought that these two states might form the components of a multiplet, presumably $^3\Pi_{0,1u}$. But the conclusions reached by Mulliken[16] make it seem unlikely that the upper state can be other than $^1\Sigma_u^+(0_u^+)$, with no multiplicity. In any case, it indicates a second excited state of the iodine molecule lying close to the one concerned in the discrete absorption. If there is any discrete absorption connected with the maximum λ3263, it presumably lies higher than that belonging to the Pringsheim and Rosen bands, in the region of total absorption (to which it would contribute) under given conditions of temperature and pressure.

[15] H. Konen, Ann. d. Physik **65**, 257 (1898).

[16] R. S. Mulliken, Phys. Rev. **46**, 549 (1934) and private communication.

Concerning the excited state involved in this absorption (called by Jevons[17] C and C', by Mulliken[16] and Curtis and Evans[8] D) a few conclusions may be drawn. The ω value must be at least as great as 90 cm^{-1} as found in the single progression, and may be estimated as close to 100 cm^{-1} from the series found connected with λ3413 in emission[11, 12] and fluorescence.[4] The highest possible value of $\nu(0,0)$ is given by adding 29,229 cm^{-1} (λ3413) to the heat of dissociation of the ground state, $D''=12{,}439$ cm^{-1}, giving $\nu(0,0)\leq 41{,}670$. This is because the r_e value of the excited state is so large that the transitions corresponding to the intensity maximum of the red end belong to very low v' values. Extrapolation of Oldenberg's intervals[11] gives the value 41,210 cm^{-1} for $\nu(0,0)$. The corresponding heat of dissociation (based on a long and doubtful extrapolation in the vacuum region) is 19,000 cm^{-1}.

These unusual characteristics lead to an absorption system covering a very long spectral region (3.3 volts), which is unusual for such a heavy molecule. This difficulty has been explained by Mulliken,[16] who shows that these characteristics are due to the relation of this state to ionic dissociation with Coulomb forces acting at large internuclear distances.

The author's sincere thanks are due to Professor W. W. Watson who suggested the problem and gave constant assistance in the investigation and in interpretation of results.

[17] W. Jevons, *Report on Band-Spectra of Diatomic Molecules*, London, The Physical Society (1932).

The Analysis of the Hydrogen Sulfide Band at 10,100A

PAUL C. CROSS,* *Gates Chemical Laboratory, California Institute of Technology*†

(Received November 8, 1934)

Details of the measurement and procedure of analysis of the $\nu_\sigma+3\nu_\pi$ band of H_2S are given. An approximate correction for the rotational distortion of the molecule is included. Assignments are made which satisfactorily account for 84 of the 91 measured lines. The remaining 7 lines are considered spurious. The theory for a rigid rotator plus the distortion correction gives a very good approximation to the rotational energy levels of the H_2S molecule, but many deviations are observed which are definitely larger than the experimental error. The moments of inertia in the normal vibrational state are 2.667, 3.076, 5.845×10^{-40} g cm^2, the axis of least inertia being perpendicular to the symmetry axis of the molecule. The bond angle is 92° 20′ and the H−S distance 1.345A.

I. INTRODUCTION

PREVIOUS work on the infrared absorption of hydrogen sulfide has been confined to the thermocouple region, and has not as yet yielded data capable of complete rotational analysis.[1–4] A brief summary of the vibrational spectrum is given here which is essentially that suggested by Mecke.[5]

Combination	Frequency (cm^{-1})	Reference	Combination	Frequency (cm^{-1})	Reference
ν_δ	1260	1	$\nu_\sigma+\nu_\delta$	3790	2
ν_π	2615	6	$\nu_\sigma+\nu_\pi$	5130	2
ν_σ	2630	2, 3	$\nu_\sigma+3\nu_\pi$	9911	7, 8, 9
			$3\nu_\sigma+\nu_\pi$	10100	7, 8, 9

It is proposed to describe here the details of the rotational analysis of the band designated above as $\nu_\sigma+3\nu_\pi$, of which a preliminary report has recently been given.[7]

II. EXPERIMENTAL

Photographs of this band were taken in the first order spectrum of a 21-foot grating having 15,000 lines to the inch. The dispersion was approximately 2.5A per mm. Eastman type 1Q infrared plates, supersensitized in 4 percent ammonia were used. The absorption cell consisted of five sections of polished stainless steel one inch in diameter, and a brass section with valves for filling. The total length of the cell was about 71 feet. The source of light was a 32–32 candle power double filament Mazda automobile headlight, burned at 16 volts with the filaments in series. A very short focus lens was mounted on the end of the absorption cell and the source adjusted to give a maximum intensity at the slit as determined by a photronic cell.

Due to the weakness of the absorption it was necessary to take a large number of photographs under various conditions of pressure and exposure. Of these, 14 were selected for detailed measurements. In some instances contact prints were used for measuring. Everything that had any possibility of representing an absorption line was recorded and the results from the 14 plates arranged in series. Real lines were then readily identified by the near coincidence of measurements on several different plates, and the wave numbers were calculated from the mean positions of the groups. The first column of Table III shows the results and includes lines that were observed on at least three plates.

Most of the useful plates were taken with the pressure of hydrogen sulfide at three-quarters of an atmosphere. At pressures of over one and a half atmospheres the lines were so broad that

* National Research Fellow in Chemistry.
† No. 440.
[1] A. H. Rollefson, Phys. Rev. **34**, 604 (1929).
[2] H. H. Nielsen and E. F. Barker, Phys. Rev. **37**, 727 (1931).
[3] A. D. Sprague and H. H. Nielsen, Phys. Rev. **43**, 375 (1933).
[4] W. Mischke, Zeits. f. Physik **67**, 106 (1931). These results are falsified by impurities.
[5] R. Mecke, Zeits. f. physik. Chemie **B16**, 431 (1932).
[6] K. W. F. Kohlrausch, Phys. Zeits. **33**, 165 (1932).
[7] P. C. Cross, Phys. Rev. **46**, 536 (1934). Note that $3\nu_\sigma+\nu_\pi=11{,}000$ cm^{-1} is incorrect.
[8] W. Weizel, Zeits. f. Physik **88**, 214 (1934). The intensities of the vibrational combinations of water type molecules are discussed. The results are that the parallel type of bands are very weak in comparison to the perpendicular type. The electric moment changes along the axis perpendicular to the symmetry axis of the molecule only for combinations containing an odd multiple of ν_σ. Combinations with $1\nu_\sigma$ are stronger than those with $3\nu_\sigma$,[9] hence the identification given here.
[9] R. Mecke, *et al.*, Zeits. f. Physik **81**, 313, 445, 465 (1933). Much of the discussion in connection with this analysis of the water spectrum is equally applicable to the hydrogen sulfide spectrum.

there was no advantage over the weaker but sharper lines. The well-defined lines appeared to the eye to be about 0.4A in breadth on the average plate used for measurement.

III. Predicted Structure from Other Considerations

The interpretation of a complex spectrum is greatly facilitated by a knowledge of the approximate value of the molecular constants which determine the spectrum. Such a knowledge may now be obtained from certain principles of theoretical and empirical origin. The additivity of atomic radii in covalent bonds gives an estimate of 1.33A for the H–S separation in H_2S.[10] The theory of directed valence and qualitative considerations similar to those used by Van Vleck and Cross[11] in a treatment of the H_2O molecule lead to an estimate of the bond angle as about 95°. This structure requires that the axis of least inertia be perpendicular to the symmetry axis of the molecule.

A second estimate of the H–S separation may be made by assuming that the Badger relation[12] between force constant and interatomic distance may be extended to polyatomic molecules. The value of ν_e^0 for H_2S may be estimated as about 2700 cm^{-1}, and k_1 obtained from the linear factor, $4\pi^2c^2(\nu_e^0)^2\ (a_{11}-a_{12})-k_1+k_{12}=0$, of the Eqs. (11) of reference 11, assuming $k_{12}=0$ and by using appropriate approximate values of a_{11} and a_{12}. k_1 is found to be about 4.2×10^5 dynes cm^{-1}, corresponding to an H–S separation of about 1.35A. Uses of these estimates will be mentioned later.

IV. The Rigid Rotator

The theory of the rigid rotator has been thoroughly discussed in the literature, so reference will be made only to the review article by Dennison[13] and the treatise by Casimir[14] for the details of the results and further references.

The energies are obtained from the equations

$$E(\text{cm}^{-1})=\tfrac{1}{2}(A+B)j(j+1)+[C-\tfrac{1}{2}(A+B)]W_{\epsilon_C}, \quad (1)$$

$$A=h/8\pi^2cI_A,\quad B=h/8\pi^2cI_B,\quad C=h/8\pi^2cI_C, \quad (2)$$

$$\epsilon_C=(B-A)/4[C-\tfrac{1}{2}(A+B)]=-\tfrac{1}{2}b, \quad \text{(Wang}^{15}\text{)}, \quad (3)$$

where I_A, I_B, and I_C are the three principal moments of inertia ($I_A<I_B<I_C$) and the W_{ϵ_C} are the roots of the secular determinant given by Wang.[15] Eqs. (1) and (3) are based on a choice of the C axis as the unique axis of the limiting symmetric rotator $\epsilon_C=0$ ($I_A=I_B$). In some instances it is more convenient to choose the A axis as the unique axis in the limiting case, and the energies are obtained by interchanging A and C throughout Eqs. (1) and (3). The constants of H_2S are such that we shall always employ the former choice, and we shall drop the subscript of ϵ for the remainder of the discussion.

The symmetries of the levels and the selection rules are easily obtained from the simple rules formulated by Dennison.[13] Levels having the symmetries $+-$ and $-+$ are antisymmetric with respect to a rotation of π about the B axis (i.e., an interchange of the hydrogen atoms) and hence have statistical weights three times those of analogous symmetric levels $++$ and $--$. Transitions originating in antisymmetric levels thus tend to average about three times as intense as those originating in symmetric levels.

For the band in question the electric moment oscillates perpendicular to the symmetry axis of the molecule, along the A axis.[8] The selection rules are $+-\rightleftharpoons--$ and $-+\rightleftharpoons++$. For practical purposes, one need consider only the transitions which also satisfy the selection rules of the limiting symmetrical rotator.[9]

V. Approximate Values of C and C′ [16]

An investigation of the intensities for a hypothetical symmetrical H_2S rotator with $r=1.35$A ($I_A=I_B$; $\theta=88°\ 16'$) shows the most intense lines in the spectrum to be $j_j=(j+1)_{j+1}$ in the symmetric rotator notation. For the actual

[10] L. Pauling, Proc. Nat. Acad. Sci. **18**, 293 (1932).
[11] J. H. Van Vleck and P. C. Cross, J. Chem. Phys. **1**, 357 (1933).
[12] R. M. Badger, J. Chem. Phys. **2**, 128 (1934).
[13] D. M. Dennison, Rev. Mod. Phys. **3**, 280 (1931).
[14] H. B. G. Casimir, *Rotation of a Rigid Body in Quantum Mechanics*, J. B. Wolters, The Hague (1931).
[15] S. C. Wang, Phys. Rev. **34**, 247 (1929).
[16] The structural constants for the excited vibrational state are designated by the primes.

molecule, provided θ is not too different from 88° 16′, the degeneracy of these levels will not be effectively removed for moderate j values, and the intensities should approximate closely those for the hypothetical symmetric rotator.[17] The strongest lines will be the unresolved doublets

$$\left\{\begin{matrix} j_{-j}=(j+1)_{-(j+1)} \\ j_{-(j-1)}=(j+1)_{-j} \end{matrix}\right\}$$

in the asymmetrical rotator notation. In the following paragraph the notation j^* will be used to designate the nearly coincident pair of energy levels j_{-j} and $j_{-(j-1)}$. The energies are given approximately by the equation

$$Ej^*=Cj^2+\tfrac{1}{2}(A+B)j+\frac{(B-A)\epsilon}{4}\cdot\frac{j(2j-1)}{j-1}. \quad (4)$$

The outstanding feature of the band is the series of strong lines of rapidly converging parabolic spacing which extends throughout the band except for some missing members near the center. These may be identified as specific transitions of the type $j^*=(j+1)^*$ after a choice of the position of the center of the band, ν_0, has been made. The difference between the energies of the lines corresponding to the transitions $j^{*\prime}-(j-1)^*$ and $j^{*\prime}-(j+1)^*$ gives directly the energy difference $(j+1)^*-(j-1)^*$ between two pairs of levels of the normal vibrational state. In terms of the structural constants this difference is

$$E(j+1)^*-E(j-1)^*=4jC+A+B$$
$$+\frac{(B-A)\epsilon}{4}\left\{\frac{(j+1)(2j+1)}{j}-\frac{(j-1)(2j-3)}{j-2}\right\}. \quad (5)$$

Subtracting the value of this energy difference for $j=n$ from that for $j=n+1$ gives a value of $4C$. (The contribution of the final term of Eq. (5) is found to be negligible for values of $(B-A)\epsilon$ which seem probable from the considerations of Section III.) The constancy of these values of $4C$ obtained from different values of n upholds the validity of the assumptions that were necessary.

[17] G. H. Dieke and G. B. Kistiakowsky, Phys. Rev. **45**, 4 (1934). This article contains a discussion of the relative positions of the energy levels and intensities for nearly symmetrical rotators. The formula $(J-K+1)(J-K)/(J+K)(J+K-1)$ of the Eqs. (7) should read $(J-K+1)\times(J-K)/8J$. (reference 14, p. 53).

The value of r can be obtained from that of C without accurate knowledge of the angle since

$$I_C=2mr^2(M+2m\sin^2\phi)/(M+2m) \quad (6)$$

is not strongly dependent upon $\phi(M/2m=16)$. The two choices for the position of the band center which seem most likely from the intensities and distribution of lines in the band lead to the values 1.35A and 1.39A for r. Again, referring to Section III, strong preference is found for the value 1.35A. The corresponding value of C is 4.73 (cm^{-1}). By an analogous treatment the value of C' is found to be 4.47. These values were used with but little variation throughout the numerous approximations in the determination of the remaining constants of the band.

VI. Approximate Determination of A, B, A', B' and ν_0

The energy levels considered in the preceding section are those for which the rotation is chiefly about the C axis and are little dependent upon the angle. To determine the angle and obtain a complete analysis of the band it is necessary to consider weaker lines and, in particular, those near the band center. The strongest lines arising from transitions between levels for which the rotation is chiefly about the A and B axes are, for the hypothetical symmetrical H_2S rotator,

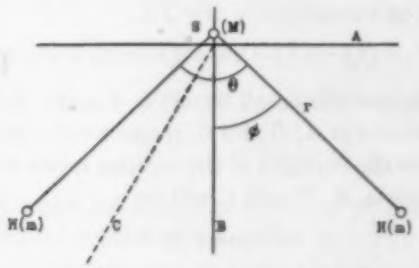

FIG. 1. H_2S rotator.

those between the two upper levels of a given j value. If the molecule were symmetrical with $2C=A=B=2C'=A'=B'$, these transitions would fall into two groups displaced from the band center by C wave numbers on either side. The asymmetry, however, causes the transitions for higher j values to approach the center, as

shown in the charts of Dennison.[18] The difference in the moments of inertia of the normal and excited states causes a shift toward the low frequency side which may be roughly approximated by $2j(j+1)(C-C')$. These simple considerations enabled the recognition of the transitions between the two upper levels of a given j state which originated in antisymmetric levels. From this point the procedure was largely one of trial and error to determine values of the constants which would fit the already identified lines and enable identification of additional ones. Considerable use was made of the differentials derived in the following section.

VII. Dependence of Energy Levels on the Individual Constants

After the identification of the majority of the lines was obtained, and values of the constants determined which gave the positions within a wave number of two, the rotational energies up to $j=8$ were calculated for both vibrational states. A simple method of solving the factors of the Wang equation by numerical approximation to the desired accuracy greatly reduced the labor involved in these calculations.[19]

The problem thus became one of adjusting these levels in accordance with the theory to give the best fit to the observed spectrum. Let

$$\alpha=\partial E/\partial A=\tfrac{1}{2}j(j+1)-\tfrac{1}{2}W_\epsilon+\tfrac{1}{4}(B-C)[C-\tfrac{1}{2}(A+B)]^{-1}(dW_\epsilon/d\epsilon), \quad (7)$$

$$\beta=\partial E/\partial B=\tfrac{1}{2}j(j+1)-\tfrac{1}{2}W_\epsilon+\tfrac{1}{4}(C-A)[C-\tfrac{1}{2}(A+B)]^{-1}(dW_\epsilon/d\epsilon), \quad (8)$$

$$\gamma=\partial E/\partial C=W_\epsilon+\tfrac{1}{4}(A-B)\times[C-\tfrac{1}{2}(A+B)]^{-1}(dW_\epsilon/d\epsilon). \quad (9)$$

The values of $dW_\epsilon/d\epsilon$ were calculated by the approximate formulas

$$\begin{aligned}
dW_\epsilon(j_i)/d\epsilon &= 4\epsilon J_1^2/[W_\epsilon(j_i)-W_\epsilon(j_{i-4})],\\
dW_\epsilon(j_{i-1})/d\epsilon &= -J_0+2\epsilon J_2^2/[W_\epsilon(j_{i-1})-W_\epsilon(j_{i-5})],\\
dW_\epsilon(j_{i-2})/d\epsilon &= J_0+2\epsilon J_2^2/[W_\epsilon(j_{i-2})-W_\epsilon(j_{i-6})],\\
dW_\epsilon(j_{i-3})/d\epsilon &= 2\epsilon J_3^2/[W_\epsilon(j_{i-3})-W_\epsilon(j_{i-7})],\\
dW_\epsilon(j_{i-4})/d\epsilon &= 4\epsilon J_1^2/[W_\epsilon(j_{i-4})-W_\epsilon(j_i)]+2\epsilon J_3^2/[W_\epsilon(j_{i-4})-W_\epsilon(j_{i-8})],\\
dW_\epsilon(j_{i-\kappa})/d\epsilon &= 2\epsilon J^2_{i\kappa-1}/[W_\epsilon(j_{i-\kappa})-W_\epsilon(j_{i-\kappa+4})]+2\epsilon J^2_{i\kappa+1}/[W_\epsilon(j_{i-\kappa})-W_\epsilon(j_{i-\kappa-4})].
\end{aligned} \quad (10)$$

$\kappa(\text{even})>4$. If κ is odd, substitute $\frac{1}{2}(\kappa+1)$ for $\frac{1}{2}\kappa$ in the subscripts of the J's.

$$J_x=[(j-x)(j-x+1)(j+x)(j+x+1)]^{\frac{1}{2}}.$$

If we use the small letters a, b and c to denote increments in A, B and C, respectively, the increment in the energies of the various levels for small changes in A, B and C will be

$$\Delta E=\alpha a+\beta b+\gamma c. \quad (11)$$

Further discussion of the use of these formulas will be postponed until after the discussion of the effect of the non-rigidity of the molecule.

VIII. Correction for the Rotational Distortion of the Molecule

The centrifugal force of rotation will alter both r and θ. To determine the approximate magnitude of the energy change due to these distortions it will be assumed that the molecule is rotating as would a classical rotator having the same values of α, β and γ.[20] α, β and γ may be considered as representing the square of the component of the angular momentum along the A, B and C axes, respectively ($\alpha+\beta+\gamma=j(j+1)\propto$ square of the total angular momentum). Thus the energy may be divided into three components representing the energy of rotation about the three principle axes.

$$E=\alpha A+\beta B+\gamma C. \quad (12)$$

Since the center of gravity is so near the S atom,

[18] Fig. 19 of reference 13.

[19] The author is indebted to Professor Badger for suggesting this procedure.

[20] This may be partially justified by considering that the distortion will be important for only large values of the quantum number, where the results of classical theory are more likely to be good approximations.

we may further simplify the treatment by assuming that the rotation takes place about the S atom.

The centrifugal force on each H atom due to rotation about the A, B and C axes, respectively, is

$$f_A=\alpha A/r\cos\phi,\ f_B=\beta B/r\sin\phi,\ f_C=\gamma C/r. \quad (13)$$

Resolving these forces into components $\parallel$ and $\perp$ to the direction of the H−S bond gives

$$f_\parallel=\alpha A\cos\phi/r\cos\phi+\beta B\sin\phi/r\sin\phi+\gamma C/r=E/r. \quad (14)$$

$$f_\perp=-\alpha A\sin\phi/r\cos\phi+\beta B\cos\phi/r\sin\phi=(-\alpha A\tan\phi+\beta B\cot\phi)/r. \quad (15)$$

These forces must be in equilibrium with the restoring forces of the distorted molecule, which may be approximated by the "valence" force system. Thus

$$E/r=k_1(\Delta r) \quad (16)$$

$$(-\alpha A\tan\phi+\beta B\cot\phi)/r=k_2r(\Delta\theta), \quad (17)$$

and

$$\Delta r=E/k_1r, \quad (18)$$

$$\Delta\theta=(-\alpha A\tan\phi+\beta B\cot\phi)/k_2r^2. \quad (19)$$

The change in the kinetic energy due to each of these displacements may be readily obtained.[21]

$$\Delta E_{\text{kin.}}=[\alpha\partial A/\partial r+\beta\partial B/\partial r+\gamma\partial C/\partial r](\Delta r)+[\alpha\partial A/\partial\theta+\beta\partial B/\partial\theta](\Delta\theta) \quad (20)$$

$$=-2E^2/k_1r^2-(\alpha A\tan\phi-\beta B\cot\phi)^2/k_2r^2. \quad (21)$$

The change in the potential energy is

$$\Delta E_{\text{pot.}}=2\times\tfrac{1}{2}k_1(\Delta r)^2+\tfrac{1}{2}k_2r^2(\Delta\theta)^2 \quad (22)$$

$$=E^2/k_1r^2+(\alpha A\tan\phi-\beta B\cot\phi)^2/2k_2r^2.$$

Hence the total change in energy due to rotational distortion is

$$\Delta E=[-E^2/k_1r^2-(\alpha A\tan\phi-\beta B\cot\phi)^2/2k_2r^2]\times1.963\times10^{-16}. \quad (23)$$

[21] The derivatives of A, B and C with respect to r and θ are calculated for the assumed rotation about the S atom.

The factor $hc=1.963\times10^{-16}$ is introduced to reduce the dimensions to cm^{-1}.

IX. Determinations of Molecular Constants by Least Squares

In applying the results of the two preceding sections to the $\nu_\sigma+3\nu_\pi$ band of H_2S the following procedure was used. Since the distortion corrections are small, it was assumed that they could be calculated from the approximate values of the molecular constants which were obtained as described in Section VI. The correction due to the change in r was applied numerically, with the value of k_1 given in Section III. Inasmuch as there has been some controversy[2] over the existence of the ν_3 band measured by Rollefson,[1] the value of k_2 was introduced as a constant to be determined.

The energy of the line $j'_{\tau'}-j_\tau$ from our nearly correct values of molecular constants is (corrected for stretching of r by rotation)

$$E_{\text{calc.}}=\nu_0+E(j'_{\tau'})-E(j_\tau). \quad (24)$$

By knowing the dependence of the energy levels upon the individual molecular constants and the correction for angular distortion in terms of k_2, it is possible to form an equation which must be satisfied in order to bring $E_{\text{calc.}}$ into coincidence with $E_{\text{obs.}}$.

$$\Delta\nu_0+\alpha'a'+\beta'b'+\gamma'c'-\alpha a-\beta b-\gamma c+\{(\alpha A\tan\phi-\beta B\cot\phi)^2/2r^2-(\alpha'A'\tan\phi'-\beta'B'\cot\phi')^2/2r'^2\}(hc/k_2)=E_{\text{obs.}}-E_{\text{calc.}}. \quad (25)$$

Seventy-eight equations of the type of Eq. (25) were formed involving energy levels up to $j=8$. In some instances two or more transitions were correlated with a single observed line. These equations were then solved by least squares to obtain the best values of the increments in ν_0, A', B', C', A, B, C and a value of k_2.

X. Results

The value of k_2 was found to be $(4.7\pm1.0)\times10^4$ dynes cm^{-1}. The corresponding value of ν_3^0 may

be approximated from the equation

$$2\pi^2c^2m(M+m)(\nu_3^0)^2-(M+2m)k_3=0;$$

$$\nu_3^0=1280\pm140\ \text{cm}^{-1}. \quad (26)$$

This value is in excellent agreement with the value estimated from Rollefson's measurements. It should be pointed out, however, that the agreement is in a certain measure fortuitous, as is seen by the large probable error. This calculation cannot be expected to be very accurate because of the smallness of the distortional effect. That it is even of the proper order of magnitude gives some encouragement.

The value of ν_0, the position of the center of the band ($\nu_s+3\nu_r$ of H_2S), was found to be $9911.05\pm0.03\ \text{cm}^{-1}$.

In Table I there is given for $j=3$ and $j=6$, the energies of a rigid rotator having the molecular constants which were used for the normal vibrational state of H_2S in the final approximation, the corresponding values of α, β, γ and the corrections to the energy due to the distortion in τ and θ. Due to the use of approximate formulas, the errors in α, β and γ may be as large as 2 percent. Errors in the correction $E(\Delta\theta)$ are possibly as large as 25 percent. Table II gives the rotational energies as finally determined by the least squares solution for the increments in the molecular constants and corrected for rotational distortion. The symmetries of the levels are also included.

TABLE I. *Energy of rigid rotator.*
($A=10.38$, $B=8.97$, $C=4.726$.)

Level	E	α	β	γ	$-E(\Delta\tau)$	$-E(\Delta\theta)$
3_3	117.51	7.7	4.0	0.3	0.03	0.03
3_2	115.55	8.7	2.3	1.0	0.03	0.07
3_1	107.13	2.8	8.2	1.0	0.03	0.02
3_0	96.30	4.0	4.0	4.0	0.02	0.00
3_{-1}	94.90	2.3	6.0	3.7	0.02	0.01
3_{-2}	71.39	1.3	1.8	9.0	0.01	0.00
3_{-3}	71.35	1.3	1.8	9.0	0.01	0.00
6_6	419.57	33.9	6.9	1.2	0.44	1.09
6_5	419.35	34.9	5.5	1.6	0.44	1.27
6_4	392.56	16.7	23.5	1.8	0.38	0.00
6_3	388.74	21.8	15.8	4.4	0.38	0.12
6_2	375.71	9.6	29.0	3.4	0.35	0.24
6_1	359.71	13.9	19.5	8.6	0.32	0.00
6_0	356.89	11.2	22.4	8.4	0.31	0.06
6_{-1}	325.31	10.6	15.7	15.7	0.26	0.01
6_{-2}	325.12	10.0	16.5	15.5	0.26	0.01
6_{-3}	281.59	7.1	10.1	24.8	0.20	0.00
6_{-4}	281.58	7.1	10.1	24.8	0.20	0.00
6_{-5}	227.85	2.6	3.5	35.9	0.13	0.00
6_{-6}	227.85	2.6	3.5	35.9	0.13	0.00

TABLE II. *Rotation energy and symmetry.*

Level	Symmetry	Rotational Energy (cm^{-1}) Normal state	Rotational Energy (cm^{-1}) Excited state
0_0	++	0.00	0.00
1_1	+−	19.36	18.22
1_0	−−	15.11	14.36
1_{-1}	−+	13.72	12.81
2_2	++	58.37	55.04
2_1	−+	55.20	52.33
2_0	−−	51.06	47.71
2_{-1}	+−	38.29	36.12
2_{-2}	++	38.01	35.74
3_3	+−	117.48	111.04
3_2	−−	115.44	109.23
3_1	−+	107.24	100.32
3_0	++	96.36	90.77
3_{-1}	+−	95.00	89.00
3_{-2}	−−	71.46	67.38
3_{-3}	−+	71.42	67.32
4_4	++	197.08	186.66
4_3	−+	195.92	185.84
4_2	−−	182.56	171.02
4_1	+−	173.98	163.91
4_0	++	170.27	159.23
4_{-1}	−+	148.41	139.63
4_{-2}	−−	148.14	139.21
4_{-3}	+−	114.18	107.70
4_{-4}	++	114.18	107.69
5_5	+−	297.29	281.96
5_4	−−	296.66	281.53
5_3	−+	277.49	260.46
5_2	++	271.30	255.74
5_1	+−	263.73	246.50
5_0	−−	244.48	229.88
5_{-1}	−+	243.47	228.33
5_{-2}	++	210.30	197.93
5_{-3}	+−	210.26	197.85
5_{-4}	−−	166.37	156.99
5_{-5}	−+	166.37	156.99
6_6	++	417.96	396.78
6_5	−+	417.52	396.47
6_4	−−	392.57	369.33
6_3	+−	388.46	366.44
6_2	++	375.68	351.26
6_1	−+	359.65	338.22
6_0	−−	356.96	334.17
6_{-1}	+−	325.39	305.93
6_{-2}	++	325.22	305.59
6_{-3}	−+	281.70	265.25
6_{-4}	−−	281.69	265.25
6_{-5}	+−	227.99	215.20
6_{-6}	++	227.99	215.20
7_7	+−	558.89	530.97
7_6	−−	558.37	530.47
7_5	−+	528.26	498.04
7_4	++	525.55	496.16
7_3	+−	506.59	474.20
7_2	−−	494.40	464.87
7_1	−+	488.29	456.52
7_0	++	459.42	431.67
7_{-1}	+−	458.71	430.49
7_{-2}	−−	415.98	391.25
7_{-3}	−+	415.96	391.20
7_{-4}	++	362.52	341.51
7_{-5}	+−	362.52	341.51
7_{-6}	−−	299.06	282.33
7_{-7}	−+	299.06	282.33
8_8	++	719.67	683.85
8_7	−+	718.92	683.19
8_6	−−	684.77	646.68
8_5	+−	682.59	644.96
8_4	++	657.10	616.05
8_3	−+	648.35	610.06
8_2	−−	637.49	595.71
8_1	+−	612.33	575.20
8_0	++	610.42	572.00
8_{-1}	−+	569.11	534.88
8_{-2}	−−	568.95	534.62
8_{-3}	+−	516.03	485.53
8_{-4}	++	516.03	485.52
8_{-5}	−+	452.77	426.67
8_{-6}	−−	452.77	426.67
8_{-7}	+−	379.53	358.38
8_{-8}	++	379.53	358.38
9_{-2}	++	688.29	647.11
9_{-3}	+−	688.29	647.11
9_{-4}	−−	625.36	588.68
9_{-5}	−+	625.36	588.68
9_{-6}	++	552.38	520.69
9_{-7}	+−	552.38	520.69
9_{-8}	−−	469.39	443.31
9_{-9}	−+	469.39	443.31
10_{-5}	+−	744.11	700.72
10_{-6}	++	744.11	700.72
10_{-7}	−+	661.38	623.61
10_{-8}	−−	661.38	623.61
10_{-9}	+−	568.67	537.16
10_{-10}	++	568.67	537.16
11_{-8}	++	779.70	735.38
11_{-9}	+−	779.70	735.38
11_{-10}	−−	677.31	639.83
11_{-11}	−+	677.31	639.83
12_{-9}	−+	907.46	856.00
12_{-10}	−−	907.46	856.00
12_{-11}	+−	795.33	751.39
12_{-12}	++	795.33	751.39

Table III gives the positions of the observed lines in comparison with the spectrum calculated from the rotational term values of Table II and the above value of ν_0. The calculated positions of a number of unobserved lines which should first be observed on increasing the path of absorbing H_2S are included. In cases where a transition is between unresolved doublets, only the strong component is specifically designated. The strong components are those having odd τ values in the normal state. (Transitions are written in the customary form of excited state—normal state.) The column headed I gives an approximate intensity which is a composite of estimated

TABLE III. *Transition values, calculated and observed.*

Observed (cm^{-1})	I	Calculated (cm^{-1})	$\Delta j = \pm 1$ Transitions	$\Delta j = 0$ Transitions
		9987.46	$7_2 - 6_2$	
		87.35	$12_{-10} - 11_{-9}$	
9987.09	2	86.96	$8_{-2} - 7_{-1}$	
85.96	1	86.41	$10_{-6} - 9_{-5}$	
		85.13	$12_{-13} - 11_{-11}$	
85.01	4	85.05	$11_{-3} - 10_{-2}$	
		84.82	$6_2 - 5_3$	
		83.70	$9_{-4} - 8_{-3}$	
83.44	4	83.09	$6_4 - 5_3$	
		83.07	$7_0 - 6_1$	
82.25	5	82.28	$10_{-3} - 9_{-2}$	
		82.21	$11_{-10} - 10_{-9}$	
81.33	2	81.49	$6_0 - 5_1$	
80.30	4	80.61	$8_{-4} - 7_{-3}$	
		78.97	$9_{-6} - 8_{-5}$	
78.86	5	78.82	$10_{-10} - 9_{-8}$	
76.57	1	76.91	$7_{-3} - 6_{-1}$	
74.93	5	75.20	$8_{-8} - 7_{-3}$	
		74.83	$9_{-4} - 8_{-2}$	
73.30	3	73.17	$6_{-3} - 5_{-1}$	
71.93	1	72.50	$6_{-1} - 5_0$	
		70.87	$5_2 - 4_2$	
70.73	3	70.86	$7_{-4} - 6_{-2}$	
70.45	5	70.37	$8_{-3} - 7_{-2}$	
67.42	1	66.95	$5_0 - 4_1$	
65.94	4	66.04	$6_{-4} - 5_{-3}$	
65.40	5	65.39	$7_{-6} - 6_{-5}$	
		64.59	$4_2 - 3_2$	
62.96	1	63.04	$4_0 - 3_1$	
		60.76	$5_{-3} - 4_{-2}$	
60.46	4	60.57	$5_{-2} - 4_{-1}$	
59.87	5	59.88	$6_{-6} - 5_{-5}$	
55.54	4	55.26	$4_{-2} - 3_{-1}$	
54.63	1	54.32	$4_{-1} - 3_0$	
53.88	5	53.86	$5_{-4} - 4_{-3}$	
52.11	1	52.37	$2_2 - 1_{-1}$	
		48.31		$6_{-4} - 6_{-3}$
47.30	5	47.32	$4_{-4} - 3_{-3}$	
		47.29	$4_{-3} - 3_{-3}$	
		46.62	$3_0 - 2_1$	
42.62	1	42.61		$5_{-3} - 5_{-4}$
		40.36	$3_{-3} - 2_{-2}$	
40.07	4	40.14	$3_{-2} - 2_{-1}$	
		39.78		$7_{-2} - 7_{-3}$
		39.40	$2_0 - 1_1$	
		36.08		$4_{-2} - 4_{-3}$
		34.94		$6_{-2} - 6_{-3}$
34.89	1	34.93		$7_2 - 7_3$
33.31	2	33.07	$2_{-2} - 1_{-1}$	
32.01	1	32.06	$2_{-1} - 1_0$	
		30.67		$5_0 - 5_{-3}$
30.41	1	30.40		$3_0 - 3_{-2}$
		28.85		$5_1 - 5_1$
		25.37		$2_1 - 2_{-2}$
25.24	1	25.28		$3_2 - 3_{-1}$
		23.86	$1_{-1} - 0_0$	
23.14	1	23.32		$5_2 - 5_{-1}$
21.84	1	21.87		$4_0 - 4_{-1}$
20.48	1	20.47		$2_0 - 2_{-1}$
		19.83		$6_0 - 6_{-1}$
14.20	1	14.16		$1_1 - 1_0$
12.18	1			
10.87	4	10.89		$2_2 - 2_1$
08.02	2	08.09		$4_2 - 4_1$
06.72	1	06.65		$3_2 - 3_2$
06.07	1	06.05		$1_0 - 1_1$
		05.01		$2_1 - 2_2$
04.44	1			
02.99	4	02.80		$3_2 - 3_2$

Observed (cm^{-1})	I	Calculated (cm^{-1})	$\Delta j = \pm 1$ Transitions	$\Delta j = 0$ Transitions
		02.66		$6_2 - 6_1$
01.77	4	01.79		$4_4 - 4_3$
9899.89	2	9899.81		$4_3 - 4_4$
97.25	3	97.33	$0_0 - 1_{-1}$	
95.47	4	95.29		$5_4 - 5_2$
94.59	1	94.58		$3_0 - 3_1$
94.01	2			
92.61	2	92.40		$4_3 - 4_2$
		91.92		$6_4 - 6_3$
91.34	1	91.59		$2_{-2} - 2_1$
90.43	2	90.31		$6_0 - 6_1$
88.78	1	89.30		$5_3 - 5_2$
87.03	1	87.12	$1_0 - 2_{-1}$	
85.88	1	85.85	$1_{-1} - 2_{-2}$	
83.30	1	83.43		$3_{-2} - 3_{-1}$
		82.63		$7_0 - 7_1$
82.22	1	82.01		$3_{-3} - 3_0$
80.09	2	80.41		$4_{-1} - 4_0$
78.90	1	78.95		$7_4 - 7_2$
		77.20		$5_0 - 5_1$
76.72	3	76.28		$4_{-2} - 4_1$
		75.71	$2_{-1} - 3_{-2}$	
75.47	4	75.37	$2_{-2} - 3_{-3}$	
74.28	1	74.36		$4_0 - 4_0$
73.47	1			
72.22	1			
70.37	1	70.33		$4_{-4} - 4_{-3}$
69.36	1	69.33		$7_2 - 7_3$
65.38	2	65.51		$5_{-2} - 5_{-3}$
		64.25	$3_{-3} - 4_{-2}$	
64.18	4	64.19	$3_{-2} - 4_{-3}$	
		63.76	$2_0 - 3_{-1}$	
58.63	1	58.85	$2_2 - 3_1$	
57.78	1	57.78		$5_{-4} - 5_{-3}$
		56.99		$6_{-3} - 6_{-2}$
		56.76		$6_0 - 6_2$
53.38	3	53.41	$3_0 - 4_{-1}$	
52.40	4	52.37	$4_{-4} - 5_{-3}$	
51.57	1	51.91	$3_{-3} - 4_{-2}$	
		50.91		$6_{-4} - 6_{-3}$
46.41	2	46.30	$3_2 - 4_1$	
44.70	2	44.79		$6_2 - 6_3$
		44.55		$6_{-6} - 6_{-5}$
43.80	1	43.59		$7_{-2} - 7_{-3}$
41.19	1	41.28	$2_2 - 3_2$	
		41.10	$3_1 - 4_0$	
40.08	3	40.38	$4_{-1} - 5_{-2}$	
		40.05	$5_{-4} - 6_{-4}$	
27.21	5	40.00	$4_{-2} - 5_{-3}$	
		27.28	$5_{-3} - 6_{-4}$	
		27.19	$6_{-6} - 7_{-7}$	
		26.81	$4_0 - 5_{-1}$	
20.04	1	20.22	$4_3 - 5_2$	
18.19	3	18.34	$4_2 - 5_3$	
15.40	1	15.54	$5_0 - 6_{-1}$	
13.90	4	13.85	$7_{-6} - 8_{-7}$	
		13.78	$6_{-4} - 7_{-5}$	
06.96	1	07.14	$5_2 - 6_3$	
		04.12	$5_4 - 6_4$	
02.32	2			
01.10	3	00.68	$6_{-2} - 7_{-3}$	
9800.00	3	9800.04	$8_{-3} - 9_{-4}$	
		9799.79	$7_{-4} - 8_{-4}$	
9791.53	1			
86.45	1	86.51	$6_0 - 7_{-1}$	
		86.27	$7_{-2} - 8_{-3}$	
85.52	2	85.69	$9_{-6} - 10_{-8}$	
		85.34	$8_{-6} - 9_{-7}$	
79.04	1			

intensities and the number of times the lines were observed. Because of the extreme weakness of the absorption the accuracy of these estimates is very low. The probable error in the positions of the lines varies from about 0.03 cm^{-1} for the best lines to about 0.15 cm^{-1} for the poorest. Seven lines are reported for which no transitions can be assigned. These need not cause any concern over the validity of the analysis since they are all weak and the method of measuring would readily admit a few spurious lines.

The mean deviation of the calculated values from the observed is about 0.13 cm^{-1}. That so many of the deviations are of larger magnitude than the probable error of the experimental measurements is probably due to the failure of the theory, and may be anticipated from some of the assumptions which are necessary in order

to set up the theoretical treatment in a form capable of solution. It should be mentioned that there are deviations of the same order of magnitude in Mecke's results for the water spectrum, but they are not so evident because Mecke's term values are experimental, and comparison with theory requires a calculation of the term values from the molecular constants which Mecke obtained from sum rules.

A summary of the results of the determination of the molecular constants will be found in Table IV.

TABLE IV. *Constants of H_2S molecule.*

	Normal State	Excited State
A	10.373 ± 0.005 cm^{-1}	9.883 ± 0.005 cm^{-1}
B	8.991 ± 0.004	8.340 ± 0.004
C	4.732 ± 0.003	4.474 ± 0.003
I_A	2.667×10^{-40} g cm^2	2.799×10^{-40} g cm^2
I_B	3.076	3.317
I_C	5.845	6.182
Bond angle	92° 20′	93° 10′
H−S distance	1.345A	1.383A
	$\omega(\nu_2+3\nu_3) = 9911.05 \pm 0.03$ cm^{-1}	

XI. Structure of the H_2S Molecule

It will be observed from the "effective" moments of inertia that $I_A+I_B \neq I_C$, which is also true for H_2O. This is not compatible with any planar structure, so Mecke's example will be followed and r and θ calculated from the equations

$$r=[(M+2m)I_C/2m(M+2m\sin^2\phi)]^{\frac{1}{2}}. \quad (27)$$

$$\theta=2\tan^{-1}[MI_B/(M+2m)I_A]^{\frac{1}{2}}. \quad (28)$$

The results are given in Table IV.

It has been supposed for some time that the angle in the H_2S molecule was about 90° since this angle was given by Kohlrausch[6] from an interpretation of the Raman spectrum. It was purely fortuitous that Kohlrausch's result was so nearly correct, as can readily be seen by applying the same reasoning to the water molecule. Cross and Van Vleck[22] have discussed reasons why structures cannot be determined from the vibrational frequencies when the central mass is much larger than the attached masses. Furthermore, when the attached masses are very small, the amplitudes will be large and the anharmonic factors so large that the mechanical frequencies (i.e., the frequencies corresponding to infinitesimal amplitude) may be quite different from the observed fundamentals.[23] Calculations of structures using the observed frequencies instead of the mechanical frequencies would in such cases be meaningless.

In using structures given with the precision of those in Table IV, it must be borne in mind that they are only "effective" structures for the particular type of experiment used in their determination. For a molecule such as H_2S the atoms are vibrating over paths which admit displacements of the interatomic distances of as much as a tenth of the equilibrium values. The particular path of vibration depends to a certain extent on the rotational state of the molecule. The instantaneous structure may vary widely from these effective structures, especially in excited vibrational states, where the atoms spend more time near the extremes of their vibration paths.

In conclusion the author wishes to acknowledge the kind cooperation and the helpful suggestions given by Professor R. M. Badger during the progress of this work.

[22] P. C. Cross and J. H. Van Vleck, J. Chem. Phys. **1**, 350 (1933).
[23] L. G. Bonner, Phys. Rev. **46**, 458 (1934).

Theories of the Spectral Selective Photoelectric Effect

CLARENCE ZENER, *H. H. Wills Physics Laboratory, Bristol, England, and The Institute for Advanced Study, Princeton*

(Received October 18, 1934)

Clean alkali surfaces emit less than one photoelectron for every 10,000 incident light quanta in the visible spectrum. A monomolecular layer of gas can greatly increase this yield. In this paper it is shown that mechanisms in which the metal electrons directly absorb the light can never give high efficiencies. A process is discussed in which alkali atoms *outside* the gas layer absorb light, their excitation energy then being transferred to the metal electrons. This process is shown capable of giving an efficiency comparable with the highest which has been observed.

THE photoelectric efficiency of a metal frequently has a maximum in the visible spectrum, i.e., the efficiency is *spectral selective*.[1] The interpretation of this maximum has been the basis of considerable speculation. The models of three different theories are represented schematically in Figs. 1–3. The purpose of the present letter is to discuss the relative efficiency of these models. We conclude that the highest observed efficiency can be obtained only with the third model.

In the first theory the wall of the Sommerfeld free electron gas model acts as the third body which is necessary for the simultaneous conservation of energy and of momentum. The photoelectric yield of such a model has been the subject of numerous calculations.[2] The result pertinent to our discussion is that the efficiency at the peak is not greater than 2×10^{-4} (the efficiency is the reciprocal of the number of incident photons required for the ejection of one photoelectron). Although cases of such low efficiency have been observed, the efficiency at the peak may in certain cases be as high as 0.05.[1]

Campbell[3] has proposed that the most efficient surfaces are obtained when an alkali metal is covered first by a monomolecular layer of electronegative gas, then by a monatomic layer of alkali atoms. Fowler[4] suggested that the potential of such a surface, Fig. 2, would be such as to allow the transmission of electrons having a normal velocity only within certain bands. The wide acceptance of this theory is surprising in view of the simplicity of the argument that may be advanced against it. Now when the selective effect is absent, as is apparently the case for clean surfaces,[5] the photoelectric efficiency is exceedingly low in the visible region,

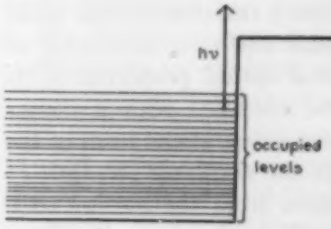

FIG. 1. Free electron model. The surface wall acts as the third body in the absorption of light quanta.

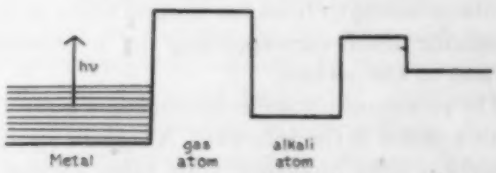

FIG. 2. Velocity filter model. Only electrons whose normal velocities lie within certain bands may escape from the metal.

FIG. 3. Bound surface electron model. Electrons bound to the surface absorb the light, and then transfer their energy of excitation to metal electrons.

[1] A comprehensive review of the spectral selective effect is given by R. Suhrmann, Ergebnisse der Exakten Naturwissenschaften **13**, 148–223 (1934).

[2] G. Wentzel, *Sommerfeld-Festschrift*, 79 (1928).
H. Frölich, Ann. d. Physik **7**, 109 (1930).
I. Tamm and S. Schubin, Zeits. f. Physik **68**, 97 (1931).
K. Mitchell, Proc. Roy. Soc. **A146**, 442 (1934).

[3] N. R. Campbell, *Photoelectric Cells and Their Applications* (London), p. 10, 1930.

[4] R. H. Fowler, Proc. Roy. Soc. **A128**, 123 (1930).

[5] Hughes and Dubridge, *Photoelectric Phenomena*, p. 160, 1932.

of the order of 10^{-5}.[1] This low efficiency is due to the small number of electrons striking the surface with sufficient energy to escape, and is *not* due to a small reflection coefficient. This conclusion is reached upon observing that in the equation for the thermionic current

$$I=120(1-r)T^2e^{-\varphi/kT} \text{ amperes cm}^{-2},$$

the reflection coefficient r of clean surfaces is found experimentally to be of the order of $\frac{1}{2}$.[6] A velocity filter at the surface can thus only *lower* the photoelectric efficiency on both sides of a band. The efficiency at a peak in the visible spectrum would thus be of the order of 10^{-5}.

The idea has been advanced, particularly by Suhrmann,[1] that the light is absorbed by atoms isolated from the main body of the metal. A model for a monatomic layer of such atoms is schematized in Fig. 3. The constancy of the potential in the plane of the surface is the representation of the idea that the monatomic alkali layer forms a two dimensional alkali metal. For in the visible and near ultraviolet we know that the essential optical properties of the alkali metals may be obtained with a constant potential.[7] The nearly parabolic form of the valley insures us that the oscillator strength (f value) for the transition from the normal to the first excited state will be nearly unity. We assume essentially that the binding of an alkali atom to the surface does not appreciably affect its oscillator strength from the normal state to that resonance level corresponding to a vibration normal to the surface.

The process of photoelectric emission according to this model is the following. A surface electron absorbs a light quantum, thus being excited to the resonance level. The excitation energy is next transferred to an electron in the metal, which then escapes from the metal. We shall now calculate the efficiency of this model.

Let f, $\Delta\nu$, A be the oscillator strength, line breadth, and effective cross section at the center of an absorption line, respectively, for a transition of a single electron. Then

$$A\Delta\nu=(4e^2/mc)f=0.034f.$$

Taking the line breadth to be such that $h\Delta\nu=1$ electron volt (approximately the breadth of the selective effect) and setting $f=1$, we obtain the effective cross section at center of line to be 0.14×10^{-14} cm^2. Hence *a surface layer of 7×10^{14} electrons cm^{-2} may have an absorption line 1 electron volt broad with a maximum absorption efficiency of 0.1.* Hence this third model can give an efficiency as high as has been observed.

The spectral selective effect is dependent upon the state of polarization of the incident light. For optically smooth surfaces no spectral selective effect is observed when the light is so polarized that the electric vector is parallel to the surface.[8] Irrespective of the model used, we must expect from optical considerations[9] that light so polarized will be less effective than light polarized so that the electric vector is in the plane of incidence. As the angle of incidence approaches 90°, the ratio of the square of the electric vector normal to the surface, for the second type of polarization, to the square of the electric vector (parallel to the surface) in the first type of polarization, is $|\mathbf{n}^4|$ just at the surface of the metal, where $\mathbf{n}$ is the complex refractive index of the metal.[10] In the visible region, this ratio is of the order of 100 for Pt, and of the order of 5 for K. This factor is not sufficient to explain the difference between the effects of the two types of polarized light for the highly efficient surfaces with K as a base. The model which we use must itself differentiate between electric fields normal and parallel to the surface. In our model the potential is constant along the surface, so that electrons in the outer trough behave as if free with respect to electric fields parallel to the surface.

The thesis of this letter was developed by the writer while at the H. H. Wills Physics Laboratory, Bristol, England. He wishes to express his thanks to its director, Professor A. Tyndall, for his generous hospitality.

[6] R. H. Fowler, *Statistical Mechanics* (Cambridge), p. 268, 1929.
[7] C. Zener, Nature **132**, 968 (1933).
[8] Reference 5, p. 143.
[9] H. E. Ives, Phys. Rev. **38**, 1209 (1931).
[10] M. Born, *Optik* (Berlin), p. 260, 1933.

Transmutations of Sodium by Deutons

ERNEST O. LAWRENCE, *Radiation Laboratory, Department of Physics, University of California*

(Received October 27, 1934)

Under deuton bombardment sodium emits protons, neutrons and alpha-particles, and becomes radioactive. The radioactive substance, which was shown by chemical tests to be radio-sodium, decays with a half-life of 15.5 hours, emitting electrons with energies up to 1.2 mv, and 5.5±0.5 mv gamma-rays. One microampere of 1.7 mv deutons bombarding a target of NaCl produces about 4×10^6 radio-sodium atoms per second. The rapid increase in yield with voltage predicted by the Gamow formula has been found, and with the higher current and voltage that soon will be available, the already large yield of radio-sodium just stated should be increased more than 100-fold. Doubtless radio-sodium will find many uses in the physical and biological sciences. The number of emitted protons equals, within experimental uncertainty, the number of radio-sodium atoms created; this supports the view that Na^{24} is the radioactive isotope formed. The protons are distributed in ranges up to 49±2 cm (air at 20°C, 760 mm) with a rather pronounced group in the neighborhood of 17 cm. The number of neutrons, emitted presumably in a reaction in which Mg^{24} is formed, is of the same order of magnitude as the number of protons. The alpha-particles have a range of 6.5±0.3 cm and are emitted in a less frequent reaction in which presumably Ne^{21} is formed. Balance of energy in the reactions leads to the following atomic masses:

Na^{23}, 22.992±0.001; Na^{24}, 24.000±0.003;
Mg^{24}, 23.993±0.003.

INTRODUCTION

IN experiments[1] of the character of a preliminary survey, it was observed that some substances under deuton bombardment emit most of the known nuclear radiations—protons, alpha-particles, electrons, positrons, neutrons, gamma-rays—and in addition, become radioactive. These preliminary experiments and the more detailed work of other laboratories[2] made it clear that nuclear reactions induced by deutons are of considerable complexity, and require extensive and detailed study. The present paper is a report of an experimental investigation of some of the reactions of deutons with sodium.

RADIOACTIVITY

The experiments[3] were begun with an investigation of radioactivity induced in sodium by deuton bombardment. For this purpose a beam of high speed deutons from the larger[4] of our instruments for the acceleration of light ions was brought out through an aluminum window into the air. This arrangement has some convenient advantages for studying induced radioactivity. Throughout the experiments a beam of 2.15 mv deutons impinging on the window was used. The range of the deutons in the air outside was observed, by the blue glow throughout their paths, to be 4.7 cm (air at 20°C, 760 mm). By placing a piece of platinum in the path of the beam and observing the range of the scattered deutons with a linear amplifier, it was found that in addition to the main and quite homogeneous group indicated by the glow, there was a relatively small number of considerably greater range, extending to nearly 9 cm. However, the number of these more energetic deutons was so small that they undoubtedly played no important part in the effects here reported.

The procedure was to place sodium 5 mm from the aluminum window in the deuton beam for a given period of time and then to remove the sodium (or sodium-containing material) and place it near an electroscope where the radiations emitted by the radioactive substance in the sodium could be studied.

Although a target having a freshly prepared surface of sodium metal was exposed to the

[1] G. N. Lewis, M. S. Livingston and E. O. Lawrence, Phys. Rev. **44**, 55 (1933); E. O. Lawrence, M. S. Livingston and G. N. Lewis, Phys. Rev. **44**, 56 (1933); E. O. Lawrence and M. S. Livingston, Phys. Rev. **45**, 220 (1934); M. C. Henderson, M. S. Livingston and E. O. Lawrence, Phys. Rev. **45**, 428 (1934).

[2] M. L. E. Oliphant, P. Harteck and Lord Rutherford, Proc. Roy. Soc. **A144**, 692 (1934); J. D. Cockcroft and E. T. S. Walton, Proc. Roy. Soc. **A144**, 704 (1934); H. R. Crane and C. C. Lauritsen, Phys. Rev. **45**, 497 (1934); M. A. Tuve and L. R. Hafstad, Phys. Rev. **45**, 651 (1934).

[3] A preliminary account of some of the results of the experiments on radio-sodium is contained in a letter to the editor, E. O. Lawrence, Phys. Rev. **46**, 746 (1934).

[4] E. O. Lawrence and M. S. Livingston, Phys. Rev. **45**, 608 (1934).

deuton beam in order to provide an additional confirmation that sodium atoms were responsible for the activity observed, in most of the experiments a target of sodium chloride, in the form of a crystal of rocksalt, was used. In the first experiments it was found that exposure of the rocksalt to a microampere of deutons for a half hour produced a very large activity. The irradiated crystal, placed near the thin aluminum window of an ionization chamber of 300 cc volume (air at atmospheric pressure), produced an amount of ionization in the chamber, as indicated by the rate of deflection of the fiber of a Lauritsen type electroscope, of the order of magnitude of 10^8 ions per second. In the first few minutes after exposure to the deuton beam, this activity decreased considerably, but after an hour or so the decrease of activity was very much less rapid, and after several hours the activity decayed exponentially with a half-life of about 15 hours. From previous experience[5] it was apparent that the initial short period activity was due to radio-oxygen driven onto the target from the bombarded nitrogen of the surrounding air. In order to eliminate this spurious effect, observations of the sodium activity were taken always many hours after irradiation of the rocksalt, that is, after such a long period of time that the short period activity was reduced to a negligible amount.

Decay Period

In Fig. 1 is shown the variation with time of the radioactivity beginning 20 hours after a one hour exposure of the rocksalt crystal to a beam of 1 microampere of 1.7 mv deutons. The activity is plotted logarithmically, and from the slope of the straight line a half-life of 15.5 ± 0.5 hours is obtained. The precision of the measurements seemingly would warrant setting a smaller limit of error than 0.5 hour. However, it was found that temperature changes appreciably affected the calibration of the electroscope, and since the observations extended over many hours during which no great precautions were taken to keep the temperature constant, this rather large limit of error has been assigned.

The Disintegration Electrons

From the amount of ionization produced in the ionization chamber, the sensitivity of the electroscope, and the geometry of the arrangement, it was possible to estimate approximately the number of beta-particles emitted from the activated rocksalt through the course of time. Thus in Fig. 1 the ordinates represent a logarithmic plot of the absolute number of disintegration electrons emitted per second throughout the whole solid angle 4π resulting from an exposure of 1 hour to 1 microampere of 1.7 mv deutons. Extrapolating back to the time when the salt was exposed to the deuton beam, one obtains an initial yield of 1.6×10^5 disintegration electrons per second. From this value the saturation activity, that is, the activity produced by exposure to the deuton beam for an infinite time, can be calculated. This turns out to be 3.7×10^6 beta-particles per second, and is the rate at which radioactive atoms are formed in the sodium chloride by 1 microampere of 1.7 mv deutons. In other words, one radioactive atom is formed per 1.7×10^6 deutons.

Measurements of the energy of the beta-rays were made by interposing various thicknesses of aluminum sheets between the activated sodium chloride and the ionization chamber. The activated salt was about 3 cm from the ionization

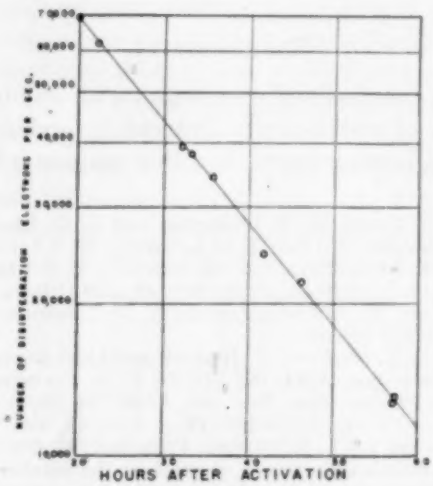

Fig. 1. Radio-sodium decay curve.

[5] M. S. Livingston and E. McMillan (Phys. Rev. **46**, 437 (1934)) have shown that even a platinum target becomes radioactive when exposed to deutons in air in the manner of these experiments, and that the effect is due to radio-oxygen, O^{15}, produced by bombardment of nitrogen.

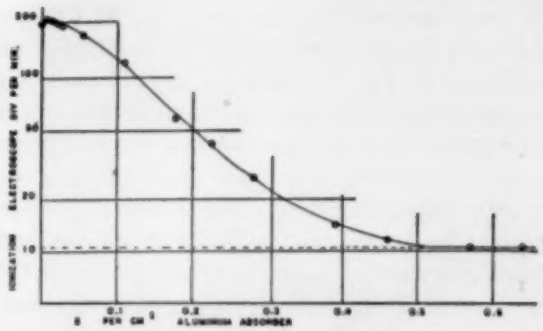

FIG. 2. Beta-ray absorption curve. The dotted line indicates the gamma-ray ionization.

chamber, whose linear dimensions were approximately 10 cm so that the solid angle subtended by the ionization chamber was quite large.

The results are shown in Fig. 2 where the ionization is plotted in essentially arbitrary units, namely rates of deflection of the electroscope fiber in divisions per second, on a logarithmic scale against the thickness of aluminum absorber in grams per sq. cm. The ionization falls off with increase in aluminum absorber to a constant value of about 1/20 of the initial value. Clearly the ionization is produced by both beta and gamma-rays and an indication of the maximum energy of the beta-rays is obtained by noting the thickness of aluminum at which the ionization becomes approximately independent of the amount of aluminum absorber. Thus the estimated maximum range of the beta-particles is about 0.51 gram per sq. cm.

Using Feather's[6] empirical formula for the relation between the maximum energy of beta-particles and their maximum range

$$E=(R+0.091)/0.511,$$

where R is in grams per sq. cm of aluminum, and the energy E is expressed in millions of electron volts, the observed range of the beta-particles indicates that their maximum energy is about 1.2 mv. In making an estimate of the maximum energy of beta-particles in this way, the tendency would of course be to estimate too low a value for the endpoint of the range, and therefore too low a value for the maximum energy. It remains for further and more extensive measurements, probably by magnetic deflections, to determine the endpoint with greater precision. However, the upper limit to the energy of the disintegration electrons is here determined with enough precision to show that the Sargent[7] relation holds. This beta-disintegration fits on the Sargent curve for Ra E and Th C.

[6] N. Feather, Phys. Rev. **35**, 1559 (1930).

RADIOACTIVE GAMMA-RAYS

From the relative amount of beta and gamma-ionization, the relative number of beta and gamma-rays can be estimated as follows. Using the same electroscope and ionization chamber, McMillan[8] has studied the annihilation radiation produced in activated carbon. He found that this 0.5 mv radiation gave rise to about 1/40 of the ionization produced by the positive electrons from the activated carbon. In the case of activated carbon (radio-nitrogen) it is to be expected, as indeed has been demonstrated approximately by Lauritsen and Crane,[9] that there should be twice as many gamma-quanta as positive electrons. In the present experiments several measurements of the ratio of gamma to beta-ionization gave values ranging from 1/33 to 1/20. If the radioactive sodium radiation were of the same energy as the annihilation radiation from N^{13}, one would conclude then that in this case more than two quanta accompany each beta disintegration. However, as will be seen below, gamma-rays from activated sodium have much higher energy (5.5 mv), and give more ionization per quantum passing through the ionization chamber. In view of this, the observations indicate that, within the uncertainty of the experiments, equal numbers of beta and gamma-rays are given off from radio-sodium. In other words, one gamma-ray accompanies each radioactive disintegration.

In order to determine the energy of the gamma-ray, absorption measurements were made in aluminum, copper and lead. For this purpose there was used another ionization chamber built especially for such absorption measurements and employed by McMillan[8] in his experiments on gamma-rays from various substances. The essential geometry of the arrangement is shown in

[7] B. W. Sargent, Proc. Roy. Soc. **A139**, 659 (1933).
[8] E. McMillan, Phys. Rev. **46**, 868 (1934).
[9] H. R. Crane and C. C. Lauritsen, Phys. Rev. **45**, 430 (1934).

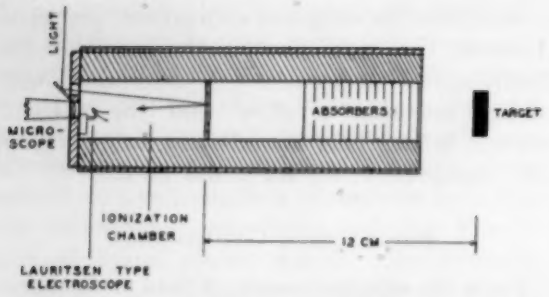

FIG. 3. Arrangement of ionization chamber and absorbers. The electroscope consists of a sputtered quartz fiber supported at one end on a light wire frame. A short cross-hair attached to the free end of the fiber is observed against a scale in the microscope eyepiece.

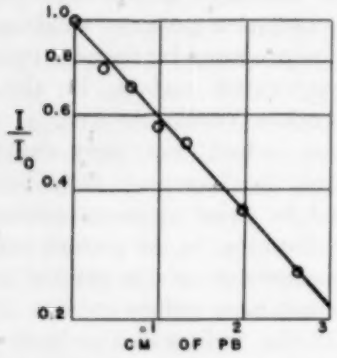

FIG. 4. Absorption in Pb of gamma-rays from radio-sodium.

Fig. 3. The cylindrical lead-lined ionization chamber was 2.5 cm in diameter and 5.7 cm long. The absorbers consisted of disks of various thicknesses, placed relative to the ionization chamber and to the source of gamma-rays, as shown in the diagram. The distance from the ionization chamber to the activated sodium was 12 cm.

The results of the absorption measurements in lead are shown in Fig. 4 where the relative ionization produced by the gamma-rays is plotted logarithmically as a function of the thickness of the lead absorber. Within experimental uncertainty the absorption is exponential, indicating that the radiation is monochromatic, with an apparent absorption coefficient of 0.51 cm^{-1}.

According to the theory of pair production (materialization of radiation) of Oppenheimer and Plesset[10] and of Bethe and Heitler,[11] which has been verified experimentally by McMillan[8] and by Lauritsen and Crane,[12] the absorption coefficient of the gamma-rays in lead does not uniquely determine the quantum energy, and it is necessary to make observations of absorption in lighter elements where pair production is not so important. Accordingly the apparent absorption coefficients of the radiation in copper and aluminum were observed, and the values 0.275 cm^{-1} and 0.066 cm^{-1}, respectively, were obtained.

Forward scattering of the radiation in the absorber influences the observed absorption coefficients, and it is a difficult matter to make proper corrections. Dr. McMillan calibrated the ionization chamber arrangement with highly filtered gamma-radiation from radium and found that the observed absorption coefficient was 6 percent less than the accepted value. For elements of low atomic number where pair production is not important, this correction is greater for more energetic gamma-radiation because the scattered radiation becomes greater in the forward direction. This increase in the scattering correction can be calculated from the geometry of source, absorber and ionization chamber on the basis of the Klein-Nishina formula. For elements of high atomic number and for radiation of five million volts or more, pair production absorption accounts for more than half of the total absorption, so that the correction for scattering in the case of heavy elements is correspondingly reduced.

With these considerations in mind, corrections to the observed absorption coefficients in aluminum, copper and lead have been made of 6, 5 and 3 percent, respectively. These corrected values,[13] given in terms of absorption per electron, are plotted in Fig. 5 against the atomic number of the absorber. A consideration of various sources of uncertainty in the measurements leads to the conclusion that these values are probably right to within 10 percent. The two straight lines represent respectively the

[10] J. R. Oppenheimer and M. S. Plesset, Phys. Rev. **44**, 53 (1933).

[11] Bethe and Heitler, Proc. Roy. Soc. **A146**, 83 (1934).

[12] H. R. Crane and C. C. Lauritsen, Int. Conf. Phys., London, Oct., 1934.

[13] According to a theoretical calculation by Hall (H. Hall, Phys. Rev. **45**, 216 (1934); H. Hall and W. Rarita, Phys. Rev. **46**, 143 (1934)) photoelectric absorption of 5 mv radiation is negligible in Al and Cu but in Pb it amounts to 4.3 percent of the total. A correction of this amount has accordingly been made in the plot of Fig. 5.

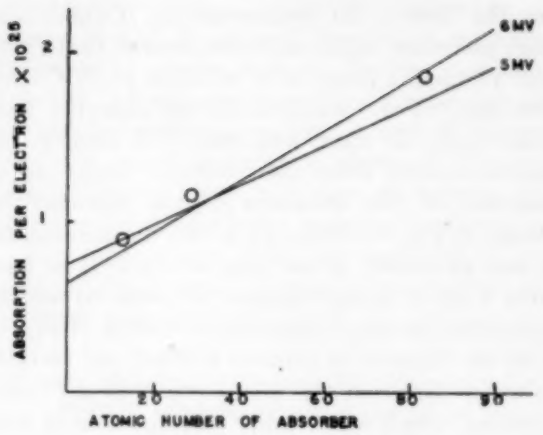

FIG. 5. The variation with atomic number of the absorption per electron of the radio-sodium gamma-rays.

variation with atomic number for 5 and 6 mv radiation of the total absorption, i.e., Klein-Nishina plus pair production, according to calculations supplied the writer some time ago by Professor Oppenheimer.[14] The observations show clearly that the absorption per electron in lead is more than twice as great as that in aluminum, and that therefore the radiation is of high energy. But on the basis of the absorption measurements alone, it is not possible to estimate with precision the quantum energy of the radiation. The extrapolated value for the absorption at zero atomic number indicates that the radiation is in the neighborhood of 5 mv, whereas the rate of increase of absorption with atomic number suggests radiation of about 6 mv. The best estimate from the absorption data has therefore been taken as 5.5 ± 0.5 mv.

Presumably the gamma-ray is emitted following the beta-disintegration, that is to say, from ${}_{12}Mg^{24}$ (see below) in an excited state. It is noteworthy that gamma-rays of about this energy have also been observed[15] from C^{12} and O^{16}. These three nuclei are of the same type in the sense that they can be regarded as made up of alpha-particles alone, and in view of this, it perhaps is not surprising that they should exhibit similar excitation levels.

[14] The writer is much indebted to Professor Oppenheimer for this information.

[15] H. Becker and W. Bothe, Zeits. f. Physik **76**, 421 (1932). E. McMillan, reference 8.

CHEMICAL TESTS

The atomic number of the radioactive element, which manifestly could not be far removed from that of sodium was determined by the following chemical tests. An activated sample of sodium metal together with some aluminum and magnesium was dissolved in concentrated sulfuric acid and then evaporated to dryness. The activity remained in the residue, indicating that the radioactive substance was certainly not fluorine or neon. The precipitate was next dissolved in water with the addition of a little ammonia. Phosphate was then added, which precipitated the magnesium and the aluminum. The activity was found to remain in the solution, showing that almost certainly the active substance was sodium. Fermi[16] observed radioactivity of 15 hours half-life induced in aluminum by neutrons, and he also came to the conclusion from chemical tests that the radioactive substance is a sodium isotope. In view of the identity of the observed half-lives, there can be little doubt that in both cases the same radioactive isotope was formed.

This chemical proof that radio-sodium is formed by the reaction of deutons with ordinary sodium suggests at once the following nuclear reaction:

$$ {}_{11}Na^{23} + {}_{1}D^{2} \rightarrow {}_{11}Na^{24} + {}_{1}H^{1}. \qquad (1) $$

THE PROTONS

The protons[17] which, according to the above reaction, accompany the production of radio-sodium, have been observed and studied in some detail as follows.

A carefully cleaned crystal of rocksalt was mounted in vacuum and bombarded with a few hundredths of a microampere of 2.15 mv deutons. Protons in a solid angle of $4\pi/200$ at right angles

[16] E. Fermi, E. Amaldi, O. D'Agostino, F. Rosetti and E. Segrè, Proc. Roy. Soc. **A146**, 483 (1934).

[17] Evidence of these protons was already at hand in the early experiments of Lawrence, Livingston and Lewis (reference 1). They found that several groups of protons, including one of 35 cm range, were emitted from a target of sodium phosphate bombarded by 1.3 mv deutons. At that time it was not established whether the groups were due to sodium or phosphorus or both (oxygen was excluded by experiments with other targets), but it seemed likely that at least one of the groups was due to sodium. In the present experiments it is evident that the 35 cm group was in fact due to this element.

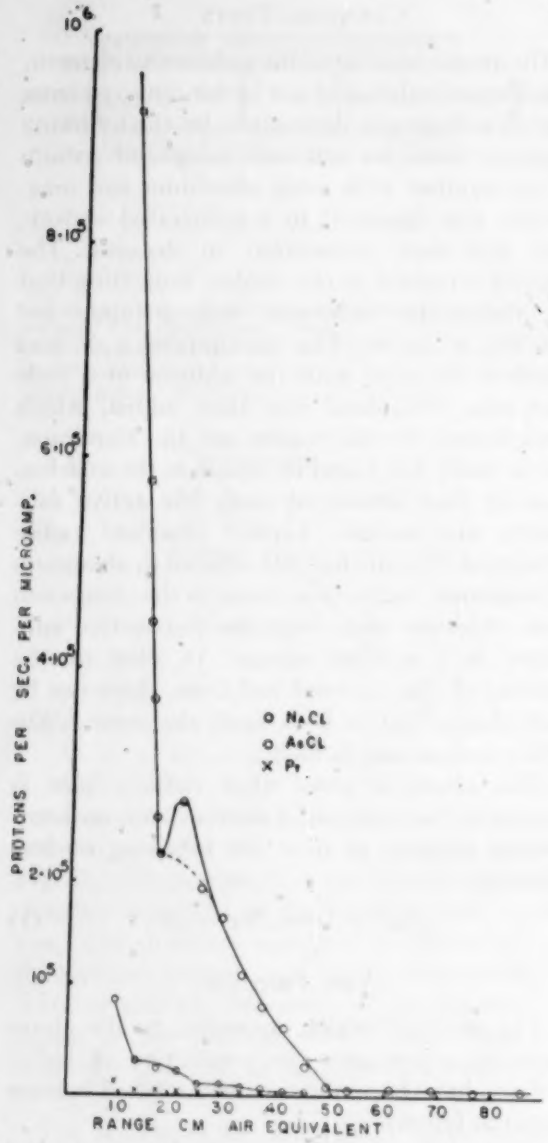

FIG. 6. Range distribution of protons emitted from Na under deuton bombardment.

to the deuton beam, passed through a mica window and through various absorbers into an ionization chamber 1 cm deep, where the ionization pulses produced by the protons were counted by a linear amplifier-thyratron-scale-of-8 arrangement. The bias voltage on the thyratrons was such that only those protons were counted that were near the end of their range when in the ionization chamber. For the most part, aluminum foils of 0.001 inch thickness were used for the absorption measurements. Calibration with polonium alpha-particles showed that they had a stopping power of 4 cm of air at 20°C and 760 mm.[18] For variations of the absorber less than 4 cm, air itself was used. The number of proton counts from the rocksalt target as a function of the thickness of the absorber is shown in Fig. 6. Although in the measurements it was necessary to use deuton currents of less than 1/10 of a microampere in order to record individual proton counts, the ordinates of Fig. 6 give the number of protons emitted per second in every direction per microampere of 2.15 mv deutons, which was readily calculated from the observational data.

Although considerable care was exercised with regard to the cleanliness of the targets, there existed a likelihood that an appreciable part of the observed proton emission from NaCl was due to contamination, particularly as the rocksalt was exposed to air before being placed in position in the vacuum chamber. Oxygen and nitrogen especially were suspects. The probable presence of a thin film of carbonaceous material from the vapor of the oil diffusion pumps was also recognized. However, a large amount of carbon contamination could be excluded on the basis of the range of the protons. From the observations that under deuton bombardment carbon emits protons having a range of 14 ± 1 cm at 0.5 mv[19] and 18 ± 1 cm at 1.2 mv,[20] it is to be expected that at 2.15 mv their range would be 24 cm. The peak in the proton range curve at 21 cm is close to this value and might conceivably be due to a slight amount of carbon contaminant. This possibility is noted in the figure by the dotted line.

In order to examine the constituents of air (particularly oxygen and nitrogen) as possible contaminants, observations were made of the proton emission from the sodium chloride target when bombarded with 1.2 mv deutons in air; following which the sodium chloride target was removed from the deuton beam and the proton emission from the air alone was observed. From

[18] All range measurements in this paper refer to air at 20°C, 760 mm.

[19] J. D. Cockcroft and E. T. S. Walton, Proc. Roy. Soc. **A144**, 704 (1934).

[20] E. O. Lawrence, M. S. Livingston and G. N. Lewis, Phys. Rev. **44**, 56 (1933).

the air two proton groups were observed, of ranges 86 and 26 cm, and in addition a copious emission of alpha-particles having ranges of 7.6 and 13.4 cm, respectively. By replacing the air atmosphere with oxygen, it was established that the great majority of these protons and alpha-particles were not due to oxygen and therefore, in all likelihood, were due to nitrogen.[21]

But quite apart from the question of the origin of the several groups of particles from air, a proton group having a range of 38 ± 2 cm was found to be present only when the sodium chloride target was bombarded. When account was taken of the lower deuton energy in the air experiments, this 38 cm group corresponded well with the 49 ± 2 cm group (see Fig. 6) observed in the vacuum experiments. Therefore the evidence strongly indicated that the 49 cm group was due to sodium chloride. The 17 ± 1 cm group observed in vacuum could only tentatively be ascribed to sodium chloride, inasmuch as these particles would have had a range in the air experiments of only 12 cm, and for this reason it would have been difficult to distinguish them in the presence of the large alpha-particle emission.

In order to distinguish between chlorine and sodium, a target of silver chloride was bombarded in vacuum, with 2.15 mv deutons, with the results also shown in Fig. 6. From this target three definite proton groups of ranges approximately 13, 23 and 38 cm, respectively, were observed. These are probably to be ascribed to chlorine, but require further investigation. However, since the protons emitted from the sodium chloride target were very much greater in number, they are certainly not to be ascribed to chlorine. Finally, in order to expose a possible unsuspected contaminant under the conditions of the experiment, the NaCl target was replaced by a platinum target in vacuum, and proton counts were made with the same deuton current. The very small number of counts shown in Fig. 6 was accounted for as due either to scattered deutons or to the general neutron background. The evidence therefore strongly indicates that the observed emission of protons from the sodium chloride target is to be ascribed to sodium.

It should be emphasized that the data of Fig. 6 represent a range distribution rather than an integrated range curve, inasmuch as only those protons were counted that were very near the end of their range. In order to estimate the total yield of disintegration protons, it was necessary therefore to determine how near to the end of its range a proton had to be in order to be counted. This was accomplished in the following manner. Protons emitted at right angles to the deuton beam in air were collimated by slits 3 mm wide and 3 cm apart, so that protons that passed through the two slits came from an air target less than 4 mm thick. In this manner a fairly homogeneous group of long range protons was obtained to test the performance of the amplifier. On the assumption that the spread in energy of the nitrogen protons was equal to that of the bombarding deutons over the thickness of the air target, it was calculated that the spread in ranges of these nitrogen disintegration protons was about 2 cm, while it was found that the linear amplifier counted the majority over a range interval of 4 cm. Hence it was concluded that in order for a proton to be counted, it had to pass through the linear amplifier within 2 cm of the end of its range. Thus the ordinates of the curves shown in Fig. 6 represent the number per second of disintegration protons in a range interval of 2 cm emitted in all directions per microampere.

If the protons are produced in the nuclear reaction in which radio-sodium is formed, it follows that the number of protons emitted per second should equal the number of radioactive atoms formed per second. This may be checked by numerically integrating the proton counts of Fig. 6, assuming that the linear amplifier counts effectively over a range interval of 2 cm. The rate of emission of protons with ranges greater than 9 cm is estimated in that way to be 5×10^6 protons per second per microampere. Scattered deutons prevented determination of the proton range distribution below 9 cm and extrapolation of the curve is necessarily uncertain. However, a reasonable extrapolation gives a total proton yield of 15×10^6 protons per sec. This is to be compared to the estimated rate of production of

[21] We expect to submit for publication in the not distant future an account of these experiments on the disintegration of nitrogen by deutons.

radioactive sodium atoms (i.e., the saturation beta-activity), which is 3.7×10^6 per second. The protons were produced by 2.15 mv deutons, while the estimate for the saturation radioactivity is for 1.7 mv deutons, and from the transmutation function, it is expected that the yield in the former case should be about five times that in the latter. Thus within experimental uncertainty the observations indicate that the yield of protons equals the yield of radio-sodium atoms, in support of the assumed reaction.

Finally, mention should be made of two aspects of the observed distribution of the emitted protons. First, the fact that at least two proton groups of ranges about 17 cm (3.4 mv) and 49 cm (6.2 mv), respectively, seem to be emitted from sodium, suggests that a gamma-ray is often emitted in the nuclear reaction with an energy corresponding to the difference in energy of the two groups which is, taking account of the energy of recoil of Mg, 3.9 mv. Second, the range distribution of the groups seems to be greater than is to be accounted for by the thick target effect, and it is not impossible that this wide energy distribution is related to the energy distribution of the disintegration electrons. These are matters that remain to be examined more closely later on.[22]

Differential Transmutation Function

In order to study the amount of the induced activity as a function of the energy of the bombarding deutons, a target consisting of several thin mica foils (each having a stopping power of about 1 cm air equivalent) was exposed to the deuton beam. Mica contains, among other things, sodium, and the variation of the sodium activity with energy of the bombarding deutons was determined by observing the amount of the

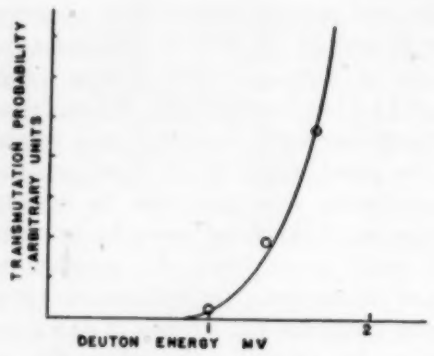

FIG. 7. The variation with deuton energy of the sodium radioactivity produced in a thin target.

15 hour activity produced in the several mica foils. The foil nearest the aluminum window exhibited the largest activity because the deutons had the greatest average velocity in passing through it. Thus the amount of the activity was observed to decrease rapidly with succeeding foils, and the observations yielded what might be termed a differential transmutation function, or thin target transmutation function. This manner of measuring the transmutation function has the advantage that it is unnecessary to take account of the magnitude of the current of bombarding deutons or of the time of exposure, as the integrated exposures of all the thin targets are automatically the same.

The activity decreased so rapidly with energy of the deutons that an appreciable effect was observed in only the first three mica foils. These results are plotted in Fig. 7. The ordinates represent the activity, necessarily on an arbitrary scale, and are proportional to the probability of activation of the sodium by the deutons for various energies in millions of volt-electrons as given by the abscissas.

The curve is a plot of the Gamow function

$$N=K(1/v)e^{-4\pi^2Ze^2/hv}.$$

N is the relative probability that a deuton of velocity v will penetrate the potential barrier of a nucleus of atomic number Z. The arbitrary constant K has been adjusted to the best fit with the experimental data.

Thus, as can be seen from this plot, the variation with deuton energy of the induced activity is accounted for on the assumption that

[22] Dr. McMillan and I have been studying the reactions of deutons with aluminum, and among other things find that aluminum[28] is formed with the emission of protons in a quite analogous manner to the sodium reaction here discussed. The range distribution of the protons from aluminum is quite similar to that of sodium. However, in the case of aluminum, we have been able to obtain a high resolving power by using thin targets and narrow collimating slits, and find that the apparent continuous range distribution in fact consists of a super-position of many proton groups. It therefore appears not unlikely that the wide distribution in ranges of the protons from sodium is due to many proton groups.

the all-important factor is the ability of the deuton to penetrate the barrier of the sodium nucleus. We have found this to be true also in the case of aluminum. Indeed, in every case so far examined carefully in our laboratory, the Gamow theory accounts for the variation of the probability of a nuclear reaction with the energy of the bombarding particle.

Utility of Radio-Sodium

Radio-sodium will doubtless find many uses because it has a conveniently long life, and can be produced in large amounts. In the present experiments with 1 microampere of 2.15 mv deutons, an amount of radio-sodium was produced which gave an activity of more than 10^7 beta-particles per second. The yield of radio-sodium increases very rapidly with the voltage and with currents and voltages that will soon be available, it will be possible to produce quantities of radio-sodium more than a hundred times greater than here reported.

The very energetic gamma-radiation, which is presumably monochromatic makes radio-sodium an ideal gamma-ray source for certain experimental studies. Already a more precise experimental investigation of the absorption of the radiation in various elements has been undertaken in our laboratory, the results of which should have important bearing on the theory of the Klein-Nishina and pair production absorption. Additional experiments using the Wilson chamber are planned, from which it is hoped it will be possible to gain more detailed information about the processes of both beta and gamma-absorption.

Radio-sodium is particularly suited for many biological uses because if injected into biological material it would leave after a few days activity an innocuous non-radioactive residue.

Neutrons

Since the end products of the reaction involving radio-sodium are Mg^{24}, H^1 and an electron, it seemed likely that an alternative reaction occurs in which sodium is converted directly into Mg^{24} with the emission of a neutron, *viz.*:

$$_{11}Na^{23}+{}_1D^2\rightarrow{}_{12}Mg^{24}+{}_0n^1. \qquad (2)$$

Neutron observations were made difficult by the rather high neutron background produced by deutons striking various parts of the apparatus other than the target under investigation. However, by making observations with the deutons electrostatically deflected alternately on and off the target, the background could be allowed for in qualitative fashion. In addition, a piece of Be mounted on a ground joint could be moved into the deuton beam directly in front of the target so that the neutron emission from the target could be compared with the emission from Be.

For the neutron observations a block of paraffin was placed directly in front of the ionization chamber and the recoil protons ejected by the neutrons were counted. The ionization chamber in these experiments subtended a solid angle at the target of about $4\pi/100$. Using a current of deutons of 0.04 microampere, the proton counts per minute were Be, 750; NaCl, 96; and the background, 48. Similar observations with a AgCl target using 0.1 microampere gave the following counts per minute: Be, 1840; AgCl, 112; and the background, 128. Neutron emission was thus definitely measurable above the background in the case of NaCl, but not in the case of AgCl. A third experiment with a platinum target gave, as expected, no effect above the background.

Thus, the experiments showed that under deuton bombardment Na emits neutrons. A rough estimate of the neutron yield may be made on the assumption that 1 recoil proton was recorded on the average for every 1000 neutrons passing through the ionization chamber. On this assumption, which is certainly correct in order of magnitude, it is calculated from the experimental data that the neutron yield from a NaCl target bombarded by 2.15 mv deutons is about 3 per 10^7 deutons. This nuclear reaction therefore has a probability of the same order of magnitude as the one in which radio-sodium is formed.

The Alpha-Particles

Observations of the ionization pulses with a cathode-ray oscillograph showed that in addition to the protons and neutrons, a considerable number of alpha-particles were emitted from

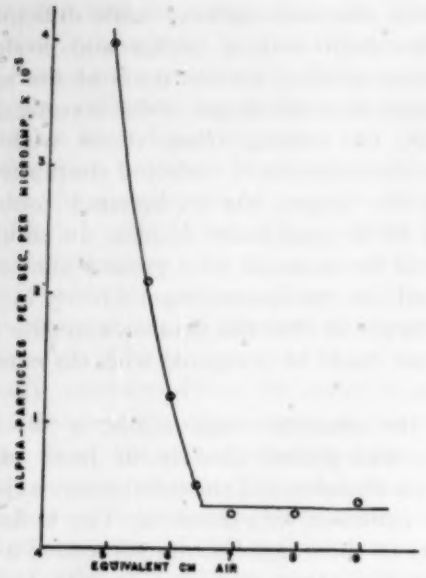

FIG. 8. Range distribution of alpha-particles from Na under deuton bombardment.

sodium chloride. From silver chloride, however, the alpha-particle emission was of a smaller order of magnitude, and it therefore was concluded that the alpha-particle emission in the former case was ascribable to sodium. In making range measurements, the alpha-particles were distinguished from the protons by increasing threefold the bias voltage on the thyratron counter. Throughout these measurements care was taken to keep the bombarding currents within a magnitude such that there was no appreciable piling up of proton pulses, which would give spurious counts. The results, reduced to the total yield per microampere of 2.15 mv deutons, are plotted in Fig. 8. The particles have a range of 6.5 ± 0.3 cm. The counts recorded in the case of a greater thickness of absorber were due to the neutrons both from the sodium and the general background radiation.

The reaction here concerned presumably is:

$$_{11}Na^{23}+{}_1D^2\rightarrow{}_{10}Ne^{21}+{}_2He^4.$$

The total yield of alpha-particles per second from sodium chloride bombarded by 2.15 mv deutons was calculated from the data to be 1 per 10^7 deutons. Thus the probability of this third reaction is smaller than that of either of the first two. According to the Gamow theory, this result is quite reasonable, since the probability that a nuclear reaction of this type will occur depends not only on the probability that a bombarding particle will get in, but also on the probability that a nuclear particle will get out. Because the nuclear barrier for the alpha-particle is greater than that for the proton, it follows that one would expect a greater probability for the proton reaction.

Energy Balance and Atomic Masses

By balancing energy in the reactions, the masses of Na^{23}, Na^{24} and Mg^{24} may be determined from the experimental data and known mass values as follows. If no gamma-radiation is given off in the alpha-particle reaction, we have

$$_{11}Na^{23}+{}_1D^2+(\text{k.e. of }{}_1D^2)={}_{10}Ne^{21}+{}_2He^4+(\text{k.e. of }{}_2He^4)+(\text{k.e. of }{}_{10}Ne^{21}).$$

The kinetic energy of the deutons was 2.15 mv ($=0.0023$ mass unit) and the alpha-particles had a range of 6.5 cm corresponding to 7.3 mv ($=0.0078$ mass unit), and it follows from conservation of momentum that the recoil kinetic energy of the Ne^{21} was 0.0017 mass unit. Taking Aston's value for He, 4.0022, and Bainbridge's value for H^2, 2.0136, and Bainbridge's provisional value[23] for Ne^{21}, 20.996 ± 0.001, we have accordingly

$$Na^{23}=20.996\pm0.001+4.0022+0.0078+0.0017-2.0136-0.0023$$
$$=22.9918^{22}\pm0.001.$$

This value for the mass of Na^{23} is not in satisfactory agreement with that derived from its chemical atomic weight,[24] i.e., 22.999 ± 0.003. In view of the possibility that gamma-rays are given off in the above reaction, the chemical value is more trustworthy.

Likewise, if it is assumed that no gamma-radiation is given off in the reaction in which radio-sodium is formed, we have

[23] The writer is much indebted to Dr. Bainbridge for this information.

[24] I am indebted to Professor Birge for calling my attention to the recent determinations by C. R. Johnson (J. Phys. Chem. **37**, 923 (1933) and Baxter and Hale (J. Am. Chem. Soc. **56**, 615 (1934), which indicate that sodium has a chemical atomic weight of 22.994 ± 0.002, which when reduced to the $O^{16}=16$ scale becomes 22.999 ± 0.003.

$$_{11}Na^{23}+{}_1D^2+(\text{k.e. of } D^2)$$
$$=Na^{24}+H^1+(\text{k.e. of } H^1)+(\text{k.e. of } Na^{24}).$$

Using the chemical value for Na^{23}, and the observed maximum proton energy, 6.2 mv (=0.0067 mass unit), we obtain

$$_{11}Na^{24}=22.999\pm0.003+2.0136+0.0023$$
$$-1.0078-0.0067-0.0006$$
$$=24.000\pm0.003.$$

Finally if the difference in mass between Na^{24} and Mg^{24} is represented by the sum of the maximum energy of the beta-rays (1.2 mv) and the energy of the gamma-rays, 5.5 ± 0.5 mv, we have

$$Mg^{24}=24.000\pm0.003-0.0013-0.0059$$
$$=23.993\pm0.003.$$

It should be noted that the assumed relation between the maximum energy of the beta-particles and the mass change in the beta-disintegration has not heretofore been established by experiment or justified by theory. The fact that the value for the mass of Mg^{24} obtained in this way fits satisfactorily on Aston's mass defect curve therefore may be interpreted as experimental evidence favoring the validity of this fundamental assumption.

I am much indebted to Doctors Edwin McMillan and Malcolm C. Henderson for valuable assistance. I wish also to acknowledge grants-in-aid from the Research Corporation, the Chemical Foundation and the Josiah Macy, Jr., Foundation.

JANUARY 1, 1935 PHYSICAL REVIEW VOLUME 47

Comparison of the Spectra of CaH and CaD

WILLIAM W. WATSON, *Yale University*

(Received October 29, 1934)

The spectrum of calcium deuteride has been photographed at high dispersion with a Ca arc in an atmosphere of heavy hydrogen as a source. Quantum analyses of the B and C systems are presented, and the rotational energy constants and spin doubling of the two states of the B bands are compared with those for CaH. The ratio B_e^i/B_e for the ground state is 0.51337 whereas the ratio of the reduced masses is 0.51276. This represents a decrease of 0.059 percent for the equilibrium internuclear distance in CaD. The spin doubling in the $B\,^2\Sigma$ state of CaD does not show the irregular variation with K found in CaH, and is of magnitude almost exactly in the ratio ρ^5 with that of the Λ-doubling in the $A\,^2\Pi$ state of CaH. Multiple large perturbations occurring in the $C\,^2\Sigma$ state of CaD are described.

INTRODUCTION

IN the several band systems of the CaH molecule are to be found striking examples of the phenomena of l-uncoupling, Λ-doubling, predissociation and perturbations.[1] The magnitudes of all of these effects depend upon the rotational constants B_v and the relative spacing of the rotational energy levels in the interacting states. Substitution of deuterium for hydrogen in this molecule therefore produces, because of the relatively large change in the reduced mass, interesting variations in these phenomena. In addition, the study of the hydrogen isotope effect in these bands provides an example for the prediction by Kronig[2] that in certain cases the potential energy function for the vibration of the non-rotating molecule is not identical for the two isotopes, the equilibrium distance being slightly smaller for the heavier isotope.

EXPERIMENTAL PROCEDURE

The light source was a d.c. arc carrying 2.5 amperes between a water-cooled copper anode and a hollow copper cathode filled with metallic

[1] For references cf. W. Jevons, *Report on Band-Spectra of Diatomic Molecules*.

[2] R. de L. Kronig, Physica **1**, 617 (1934).

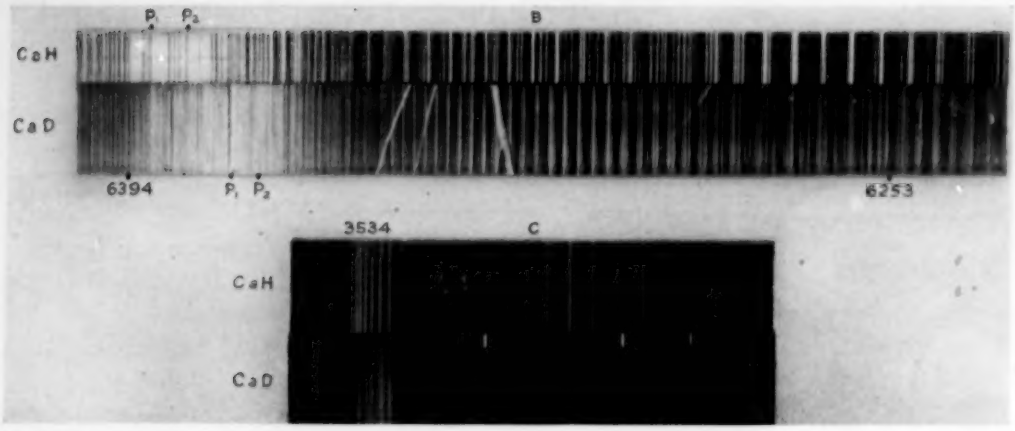

FIG. 1. Spectrograms of the *B* and *C* bands of CaH and CaD. Both of the CaD spectra have the CaH bands present with low intensity, and the spectrogram of the CaH *C* band shows some of the CaD lines. Note the marked difference between the *C* bands of the two isotopes.

calcium in an atmosphere of heavy hydrogen at about 4 cm of Hg pressure. The heavy hydrogen was obtained from a gram of 98 percent heavy water by interaction with calcium metal in a vacuum. Only half of the deuterium in the heavy water was liberated, of course, but the CaOD formed in the reaction was desired as a target containing deutons for a nuclear disintegration experiment in this laboratory. From the storage flask of about one liter capacity, heavy hydrogen was admitted occasionally during an exposure to the arc chamber, which had a volume of about two liters, in order to replenish the gas consumed in the manufacture of CaD_2.

Spectrograms of the *A*, *B* and *C* band systems of CaD were obtained in the second order of a 21-foot concave grating in a stigmatic mounting, the dispersion being about 2.2A/mm. Eastman Hypersensitive Panchromatic, I–S and Eastman 40 plates were used for the *B*, *A* and *C* band regions, respectively. That the light source was intense may be judged from the fact that the exposure times were in all cases about 15 minutes. On all the spectrograms CaH spectra are present, ordinary hydrogen having come from the walls and the hot electrodes, but the band lines due to CaD are several times more intense than the corresponding CaH lines.

Since there is but slight difference in the vibrational frequencies of the CaH molecule in the two states involved in each of these band systems, the $\Delta v=0$ sequence is very much stronger than the other sequences. Therefore according to the simple theory of the vibrational isotope effect the corresponding $\Delta v=0$ sequences of the CaD bands should be but little displaced from those of CaH. The resulting overlapping and interlacing of the rotational structure of the bands of the two isotopic molecules is troublesome, but the relative simplicity of the *B* and *C* bands (both $^2\Sigma\rightarrow{}^2\Sigma$) together with the greater intensity of the CaD lines makes the quantum analysis possible. The structure of the *A* band ($^2\Pi\rightarrow{}^2\Sigma$) of CaD at 7000A, however, is so complicated by the numerous fusions of lines with those of the weaker CaH bands as to defy accurate quantum analysis. At this time therefore a discussion only of the *B* and *C* band systems of CaD is presented. In Fig. 1 are displayed reproductions of typical spectrograms of these bands.

THE *B* BANDS OF CaD

The $\Delta v=0$ sequence of this system lies mostly in the region 6200 to 6400A, the origin of the 0,0 band falling within a few wave numbers of that of the corresponding CaH band. Since the reduced mass of CaD is almost twice that for CaH, the rotational energy levels of the former will have but half the spacing of the CaH levels. There will thus be roughly twice as many lines

TABLE I. *Assignment of frequencies in the "B" $^2\Sigma \rightarrow {}^2\Sigma$ 0,0 and 1,1 bands of CaD. cm^{-1} units.*

	0,0				1,1			
$J''+\frac{1}{2}$	P_1	R_1	P_2	R_2	P_1	R_1	P_2	R_2
1				15758.62		15739.40		15744.53
2	15744.52	15757.47	15740.73	63.71	15730.98	43.88	15727.48	49.32
3	40.09	62.20	37.05	68.96	26.55	48.25	23.39	54.21
4	35.86	67.11	33.40	74.35	22.42	52.74	19.53	59.31
5	31.80	72.12	29.82	79.92	18.31	57.33	15.85	64.57
6	27.94	77.17	26.59	85.58	14.28	62.33	12.61	69.95
7	24.17	82.50	23.43	91.50	10.38	67.14	09.01	75.47
8	20.56	87.90	20.56	97.43	06.70	72.31	06.00	81.15
9	17.35	93.52	17.74	803.56	02.95	77.64	03.05	86.99
10	14.15	99.16	15.12	09.92	699.56	83.30	00.21	92.85
11	11.05	805.12	12.61	16.32	96.48	88.76	697.78	99.10
12	08.24	11.16	10.35	22.88	93.72	94.25	95.47	805.10
13	05.56	17.29	08.24	29.63	91.24	99.90	93.03	11.47
14	02.92	23.64	06.29	36.56	87.97	805.88	90.79	18.09
15	00.28	30.02	04.51	43.20	85.22	11.94	88.76	24.39
16	698.53	36.56	02.92	50.48	83.07	18.09	87.07	31.21
17	96.49	43.20	01.46	57.69	81.15	24.39	85.22	37.98
18	94.58	50.10	00.28	64.99	78.69	30.69	83.87	44.89
19	92.92	57.06	699.00	72.45	76.93	37.25	82.65	51.85
20	91.42	64.09	98.07	79.98	75.29	43.86	81.22	58.90
21	90.10	71.15	97.21	87.62	73.53	50.56	80.51	66.13
22	88.80	78.52	96.49	95.38	72.39	57.27	79.66	73.34
23	87.69	85.85	96.13	903.16	71.19	64.18	78.69	80.69
24	86.82	93.32	95.76	11.11	69.70	71.23	78.23	88.12
25	86.20	900.81	95.54	19.15	69.01	78.18	77.64	95.47
26	85.64	08.51	95.54	27.18	68.30	85.25	77.39	903.14
27	85.15	16.16	95.76	35.34		92.43	76.93	10.65
28	84.93	23.96	96.13	43.53		99.69		18.36
29	84.76	32.01	96.49	51.83		906.97		26.03
30	84.76	39.74	97.00	60.13		14.26		33.76
31	85.15	47.72	97.74	68.50		21.67		41.51
32	85.64	55.75	98.53	76.98		29.05		49.31
33	86.20	63.80	99.46	85.18		36.49		57.02
34	86.74	71.91	700.62	93.86		43.96		64.92
35	87.61	80.02	02.03	16002.41		51.37		72.70
36	88.68	88.26	03.41	10.89		58.88		80.50
37	89.60	96.36	05.06	19.35		66.38		88.24
38	90.78	16004.58	06.70	27.94		73.82		96.05
39	91.93	12.82	08.24	36.51		81.29		16003.85
40	93.62	21.02	09.98	44.96		88.72		11.58
41	94.96	29.22		53.53		96.05		19.34
42	96.53	37.56		61.92		16003.43		26.81

in a given energy range in a branch of the deutride band. For example, the line R_1 ($55\frac{1}{2}$) of the CaD is close to R_1 ($30\frac{1}{2}$) of CaH. In the P-branches which form heads at about $K=26$ this closer spacing of the lines results in more fusions of lines at and near the heads, with resulting lessened accuracy of measurement. Table I contains the quantum assignments of frequencies in the 0,0 and 1,1 CaD bands, while in Table II are given the usual R–P combination differences from which the rotational energy constants are computed.

From the $\Delta_2F(K)$ values of Table II the constants B_v and D_v of the expression for the rotational energy of the molecule may be computed in the usual manner. Knowing B_0 and B_1, the quantities α and B_e of the relation $B_v=B_e-\alpha(v+\frac{1}{2})$ are obtained. B_e is the value of this rotational constant when the nuclei are at their equilibrium distance apart, and it is the ratio of these B_e constants for the same electronic state of the two isotopic molecules which should equal, according to the simple theory of the isotope effect in band spectra, the ratio of their reduced masses. It is important to note that the B_v values so calculated are really B_v^* values,[3] differing considerably from the real B_v values for a state such as this upper $^2\Sigma$ state which interacts strongly with a near-lying $^2\Pi$ state. We return to this point below. In Table III are collected the results of these calculations, including revised and more accurate values for the corresponding constants of the CaH states.

For comparison of these constants for the two isotopes one needs the ratio ρ^2 of their reduced masses. Taking the mass-spectrograph determinations of 1.00778 and 2.01363 atomic weight units for hydrogen and deuterium,[4] respectively, and with $m_{Ca}=39.97$, $\rho^2=\mu_{CaH}/\mu_{CaD}=0.51276$. Any possible departure of the mass of Ca from this value 39.97 affects ρ^2 inappreciably. From this value of ρ^2 it follows that $\rho=0.716066$, $\rho^3=0.367168$ and $\rho^4=0.262918$.

[3] R. S. Mulliken and A. Christy, Phys. Rev. **38**, 87 (1931).
[4] K. T. Bainbridge, Phys. Rev. **41**, 115 (1932).

TABLE II. *Combination differences for the "B" $^2\Sigma \rightarrow {}^2\Sigma$ CaD band. The $\Delta_2F(K)$ values are the average of the R_1-P_1 and R_2-P_2 differences in each case.*

	Lower state combinations					*Upper state combinations*				
	0,0				1,1	0,0				1,1
$J''+\frac{1}{2}$	$R_1(J-1)$ $-P_1(J+1)$	$R_2(J-1)$ $-P_2(J+1)$	K''	$\Delta_2F''(K)$	$\Delta_2F''(K)$	$R_1(J)$ $-P_1(J)$	$R_2(J)$ $-P_2(J)$	K'	$\Delta_2F'(K)$	$\Delta_2F'(K)$
2		21.57					22.98			
3	21.61	30.31	2	21.59	21.30	22.11	31.91	2	22.54	21.77
4	30.40	39.14	3	30.36	29.87	31.25	40.95	3	31.58	30.57
5	39.17	47.76	4	39.15	38.41	40.32	50.10	4	40.63	39.40
6	47.95	56.49	5	47.86	46.83	49.23	58.99	5	49.66	48.38
7	56.61	65.02	6	56.55	55.59	58.33	68.07	6	58.66	57.04
8	65.15	73.76	7	65.09	64.07	67.34	76.87	7	67.70	66.03
9	73.75	82.31	8	73.76	72.58	76.17	85.82	8	76.52	74.92
10	82.47	90.95	9	82.39	81.05	85.01	94.80	9	85.42	83.84
11	90.92	99.57	10	90.94	89.39	94.07	103.71	10	94.43	92.46
12	99.56	108.08	11	99.57	97.45	102.92	112.53	11	103.32	100.93
13	108.24	116.59	12	108.16	106.17	111.73	121.39	12	112.13	109.15
14	117.01	125.12	13	116.80	114.49	120.72	130.27	13	121.05	118.17
15	125.11	133.64	14	125.11	122.76	129.74	138.69	14	130.00	127.01
16	133.53	141.74	15	133.58	130.91	138.03	147.56	15	138.36	135.32
17	141.98	150.20	16	141.85	139.28	146.71	156.23	16	147.13	143.69
18	150.28	158.69	17	150.24	147.40	155.52	164.71	17	155.87	152.38
19	158.68	166.92	18	158.68	155.37	164.14	173.45	18	164.42	160.67
20	166.96	175.24	19	166.94	163.69	172.67	181.91	19	173.06	168.88
21	175.29	183.49	20	175.26	171.40	181.05	190.41	20	181.48	177.35
22	183.46	191.49	21	183.47	179.31	189.72	198.89	21	190.07	185.25
23	191.70	199.62	22	191.59	187.50	198.16	207.03	22	198.52	193.33
24	199.65	207.62	23	199.63	195.14	206.50	215.35	23	206.76	201.76
25	207.68	215.57	24	207.65	202.99	214.61	223.61	24	214.98	209.53
26	215.66	223.39	25	215.61		222.87	231.64	25	223.24	217.39
27	223.58	231.05	26	223.48		231.01	239.58	26	231.33	
28	231.40	238.85	27	231.22		239.03	247.40	27	239.30	
29	239.20	246.53	28	239.02		247.25	255.34	28	247.31	
30	246.86	254.09	29	246.70		254.98	263.13	29	255.16	
31	254.10	261.60	30	254.09		262.57	270.76	30	262.85	
32	261.52	269.04	31	261.56		270.11	278.45	31	270.43	
33	269.01	276.36	32	269.02		277.60	285.72	32	278.02	
34	276.19	283.15	33	276.27		285.17	293.24	33	285.44	
35	283.23	290.45	34	283.19		292.41	300.38	34	292.82	
36	290.42	297.35	35	290.43		299.58	307.48	35	299.98	
37	297.48	304.19	36	297.41		306.76	314.29	36	307.12	
38	304.43	311.11	37	304.31		313.80	321.24	37	314.05	
39	310.96	317.96	38	311.03		320.89	328.27	38	321.06	
40	317.86		39	317.91		327.40	334.98	39	327.83	

It is known from the fact that the spin doubling in this lower state is very small that there is but slight interaction with any other electronic state of the molecule. We may consider therefore that the B_e'' values computed in the usual fashion are correct. The ratio of the two B_e'' values, which with the usual assumption of the equality of the potential energy function for the two isotopic molecules should equal ρ^2, is 0.51337. This means a decrease in the equilibrium distance between the two nuclei in CaD of 0.059 percent. Holst and Hulthén[5] have reported about the same decrease, 0.056 percent, in the distance between the two nuclei for AlD as compared to AlH in their lowest $^1\Sigma$ state.

Now Kronig has recently shown[2] that the correct treatment of the wave equations for the diatomic molecule leads to the conclusion that the potential energy curves for two isotopic molecules need not be identical provided that the "united atom" (a concept valid only for hydrides) has an $L>0$ and has other near-lying perturbing electronic states. Since the united atoms for both AlH and CaH have $L=2$ (the lowest ^2D level of Sc for CaH) and have other perturbing levels within a range of one or two volts, both molecules might be expected to show sizable and about equal decreases in equilibrium distance for their deutrides.

That the ordinary rotational energy term formula applied to the excited state of these bands does not yield correct B_v values is shown by the fact that the B_e values so obtained ($B_e'=4.4918$ for CaH and 2.2813 for CaD) have a ratio 0.50788. The explanation of this large departure in the wrong direction from the reduced mass ratio lies in the fact that the analysis of the data always gives B^* values,[3] differing from the true B_v values by terms arising from the interaction with certain other states of the molecule. If the interaction of this $^2\Sigma$ state is solely with a neighboring $^2\Pi$ state, then it may be shown that

$$B^*-B_v=-2B_v^2l(l+1)/\nu(\Pi,\Sigma).$$

[5] W. Holst and E. Hulthén, Nature **133**, 496 (1934).

The interaction for this $^2\Sigma$ state of CaH being largely with the $A\ ^2\Pi$ state lying but 1320 cm^{-1} ($=\nu(\Pi, \Sigma)$) below it, this correction to B_0^* for CaH is about -0.067, while for CaD the correction is but -0.017 because of the B_v^2 factor. Inclusion of these corrections gives an indicated B_e ratio considerably nearer[6] the value ρ^2. But since interacting electronic states such as these never stand exactly in the relation of "pure precession" to each other, these corrections to obtain true B_v and B_e values can never be made with great accuracy.

The α constants for the ground state listed in Table III have a ratio almost exactly ρ^3, as they

TABLE III. *Rotational constants of the "B" $^2\Sigma \rightarrow {}^2\Sigma$ CaD and CaH bands.*

	CaD	CaH		CaD	CaH
B_0''	2.1777	4.2296	$B_0'^*$	2.2600	4.4338
B_1''	2.143	4.1333	$B_1'^*$	2.215	4.318
α''	0.035	0.096	α'	0.045	0.116
B_e''	2.196	4.2776	D_0'	-5.4×10^{-6}	-2.36×10^{-4}
D_0''	-4.8×10^{-6}	-1.84×10^{-4}	D_1'	-6.5×10^{-6}	-2.44×10^{-4}
D_1''	-6.1×10^{-6}	-1.82×10^{-4}	γ'	-0.364	-0.945 or -0.543
γ''	0.032	0.045			

should have according to the theory of the isotope effect. Comparison of the spin doubling $\Delta\nu_{12}(K)$ in the $B\ ^2\Sigma$ state of the two isotopes is also of some interest. The variation of this doubling with K is presented in Fig. 2. Now according to theory this variation should be strictly proportional to $(K+\frac{1}{2})$, and the factor of proportionality γ should equal, if strong interaction exists between the two states, the slope p of the Λ-doubling curve for the near $^2\Pi_d$ levels. There should be a ratio B_0 between these constants for the two isotopic molecules. The expected linear spin-doubling relation does hold for CaD, the slope of the line in Fig. 2 being -0.364. Division of this by ρ^2 gives -0.709 which is nearly the value -0.704 of p for the

[6] It follows from the definition of q on p. 89 and of B^* in Eq. (16) of reference 3 that $B^*-B_v=-q$, not $+q$ as stated by Mulliken and Christy after their Eq. (19). Since q is in this case negative, for CaH $B_0'=4.4338-0.067=4.367$, while for CaD $B_0'=2.260-0.017=2.243$. Addition of $\frac{1}{2}\alpha$ to these quantities (using the α' values from Table IV) gives $B_e'=4.425$ and 2.265 for CaH and CaD, respectively. The ratio of these is 0.511865, fairly close to the value for ρ^2. However, the only significance to be attached to this calculation is that it forms an approximate check on these theoretical relations between B^* and B_v values.

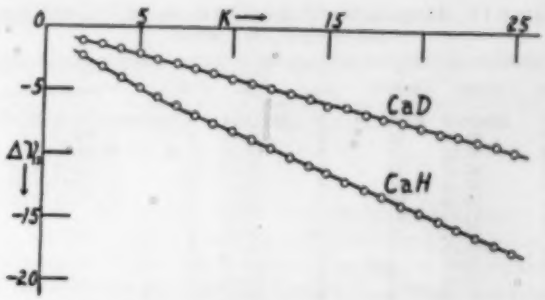

FIG. 2. Comparison of the spin doubling in the $B\ ^2\Sigma$ state of the CaD and CaH molecules.

$^2\Pi$ state of CaH. The spin-doubling curve for the CaH state shown in Fig. 2 has an initial slope of -0.945, changing for the higher rotational levels to -0.543. This change of slope is probably due to a perturbation by other near-lying rotational levels, the absence of it for CaD being attributed to the different spacing of the rotational levels. The conclusion from this comparison of B_e, B_v^* and α values, as well as the spin- and Λ-doublings, in corresponding states of these two molecules is, then, that the variation of the theoretical relations as a function of the mass of the molecule is entirely verified.

THE *C* BANDS OF CaD

In contrast to the lack of the CaH perturbation in the $B\ ^2\Sigma$ state as mentioned above, the C band of CaD at 3534A displays violent perturbations

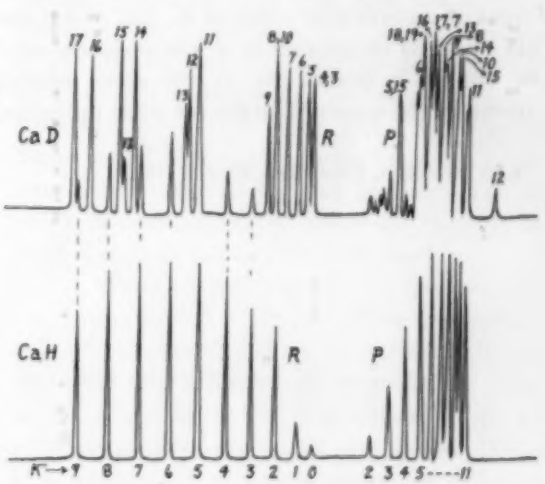

FIG. 3. Microphotometer traces of the C bands of CaD and CaH. The numbers on the CaD lines are the assigned values of K''.

TABLE IV. *Assignment of frequencies in the "C" $^2\Sigma \rightarrow {}^2\Sigma$ 0,0 band of CaD. cm^{-1} units.*

Int.	ν obs.	$R(K'')$	Int.	ν obs.	$P(K'')$	Unassigned
7	28469.62	$R(17)$	5	28321.73	5,15	28334.74(1) $R(1)$?
7	61.89	16	6	12.91	6	31.94(1)
8	48.66	15	9	11.28	18,19	30.40(1)
2	46.65	13	8	08.62	16	29.14(1) $R(0)$?
8	42.13	14	10	06.67	17,7	16.33(1b) $P(2)$?
4	19.18	13	7	04.68	13	14.12(5) $P(3)$?
6	17.41	12	7	02.30	8	
7	12.92	11	6b	00.89	14	
5	381.28	9	9	298.73	9	
8	77.61	8,10	7	95.45	10	
7	72.44	7	7	94.04	15	
7	67.33	6	6	90.53	11	
6	63.05	5	2	78.17	12	
6	60.81	4,3				

in its upper state which do not occur in the corresponding CaH levels. Comparison of the structure of this band for the two molecules in the reproduction in Fig. 1 and in the microphotometer traces in Fig. 3 indicates these perturbations at once. The intensities, frequencies and quantum assignments of the lines in this 0,0 C band of CaD are given in Table IV. These assignments are made with the necessary condition that there should be the same lower state $R(J-1)-P(J+1)$ combination differences as found in the B band of CaD. For these two systems have a common ground state, and no perturbations are found in this B band. Without this condition as a guide it would be quite impossible to make the quantum analysis, for every line in the band is perturbed, the resulting confusion in the P-branch being particularly bad.

A prominent feature is the sudden cessation of lines at a particular value of K, just as for the CaH band as developed in a low pressure arc.[7] The cut-off is practically at the same energy content in the upper $^2\Sigma$ state for each molecule, since the band origins lie within a few cm^{-1} of each other. An explanation of this sudden drop of the intensity to zero in the two branches as due to predissociation into the continuum of the D state of CaH has been given by Grundström and Hulthén.[8]

As usual in the phenomenon of perturbations, two lines having the same K values sometimes appear at a perturbation point. This occurs definitely at $K=14$. Also these perturbations are multiple, with centers at about $K=3$, 10, 13, and >17. This would indicate the presence in this energy range of CaD levels of more than one other state with levels spaced similarly and having all of the properties necessary for perturbing the $C\ ^2\Sigma$ levels. The $D\ ^2\Sigma$ state may be one of these, but of other states in this interval nothing is known. The displacements in these perturbations are evidently of the usual "anomalous dispersion curve" type, but it is difficult to calculate the exact magnitudes of the shifts because of the fact that there are no unperturbed lines from which the normal course of the levels may be computed. From an attempt at such a calculation, by using predicted constants from the isotope effect theory, it is evident that, as for the C state of CaH, a sizable term linear in K is present and with a coefficient about in the ratio ρ^2 to the 2.22 value[8] for CaH. Finally, it should be mentioned that the 0,1 band of this CaD system is also present on our spectrograms, but with rather low intensity. Inspection shows that large perturbations similar to those of the 0,0 band occur in its branches. The same perturbations should be found in the two bands, of course, because of their common upper state.

[7] R. S. Mulliken, Phys. Rev. **25**, 509 (1925).

[8] Cf. B. Grundström, Zeits. f. Physik **69**, 235 (1931).

A Spectroscopic Determination of e/m

C. D. SHANE, *Department of Astronomy, University of California, Berkeley*
AND
FRANK H. SPEDDING, *Department of Chemistry, University of California, Berkeley*

(Received November 5, 1934)

A determination of e/m was made by accurately measuring the difference in wave number between the Hα lines of ordinary and heavy hydrogen. The observations were made with a Fabry and Perot etalon used in conjunction with a spectrograph of sufficient resolving power to separate the interference patterns of the two Hα lines. The effects of the weak fine structure components were eliminated and values of e/m were derived from the two main components. The final mean gives $e/m = 1.7579 \pm 0.0003 \times 10^7$. From this determination the ratio of the mass of the hydrogen atom to the mass of the electron is found to be $1835.6 \pm 0.2_5$. There is no indication of systematic errors in the work so that the probable errors may be fairly taken as representing the actual uncertainties in the results.

INTRODUCTION

IT was pointed out by Birge[1] in 1929 that the mean value of e/m determined from the acceleration of free electrons was $(1.769 \pm 0.002) \times 10^7$ whereas spectroscopic methods gave $(1.761 \pm 0.001) \times 10^7$. That the difference between these values might be real was suggested by the small size of the probable errors. This led to the possible interpretation that the value of e/m for free electrons was not the same as for electrons within the atom. In view of the importance of this question considerable work has been done recently in determining e/m by both methods. The more important results are listed in Table I. Evidently the discrepancy shows a tendency to disappear with later and more refined experimental methods.

TABLE I.

Date	Observer	e/m (spectroscopic)	e/m (acceleration)
1930	Perry and Chaffee[2]		1.761 ± 0.001
1931	Campbell and Houston[3]	1.7579 ± 0.0025	
1932	Kirchner[4]		1.7587 ± 0.0009
1933	Dunnington[5]		1.757 ± 0.0015
1933	Spedding, Shane and Grace[6]	1.758	
1934	Gibbs and Williams[7]	1.757 ± 0.001	
1934	Kinsler and Houston[8]	1.7570 ± 0.0010	

[1] Raymond T. Birge, Rev. Mod. Phys. **1**, 1 (1929).
[2] C. T. Perry and E. L. Chaffee, Phys. Rev. **36**, 904 (1930).
[3] J. S. Campbell and W. V. Houston, Phys. Rev. **38**, 581 (1931).
[4] F. Kirchner, Ann. d. Physik **12**, 503 (1932).
[5] F. G. Dunnington, Phys. Rev. **42**, 739 (1932).
[6] F. H. Spedding, C. D. Shane and Norman S. Grace, Phys. Rev. **44**, 58 (1933).
[7] R. C. Gibbs and R. C. Williams, Phys. Rev. **44**, 1029 (1933).
[8] L. E. Kinsler and W. V. Houston, Phys. Rev. **45**, 104 (1934).

Of the various spectroscopic methods the one that is probably most accurate consists in determining the difference in the Rydberg constant corresponding to two different hydrogen-like atoms. Observationally this resolves itself into the measurement of the difference in wave number of corresponding lines in the spectra of two such substances. This method was applied by Houston[9] using ordinary hydrogen and ionized helium. In application the principal defect lies in the different fine structure of the lines to be measured. When through the work of Professor G. N. Lewis, experimental amounts of water containing high concentrations of the heavy hydrogen isotope were available, it became possible to make determinations by the above method relatively free from this difficulty. The fine structure is the same for corresponding lines of H^1 and H^2 and only affects the results to a small extent through the difference in temperature widening. The value given by Spedding, Shane and Grace in the above table is a preliminary result derived by this method. The only other determination in which H^1 and H^2 were used is that of Gibbs and Williams.[7]

The present paper reports the final results of our investigation. The procedure possesses, we believe, three points of advantage over that used by Gibbs and Williams. First, sufficient spectroscopic resolving power was employed to yield separate interference fringe systems for $H^1\alpha$ and $H^2\alpha$ whereas in the experiments of Gibbs and Williams the two systems overlapped. The

[9] W. V. Houston, Phys. Rev. **30**, 608 (1927).

spectroscopic separation of the fringe systems resulted in greater accuracy of photometric measurement. Second, in view of the resulting simplicity of the fringe systems, a more complete analysis of the effects due to the faint unresolved components of the lines was possible. Finally, through the method of cooling the discharge tube, the lines obtained showed improved sharpness.

The determination of e/m was intimately bound up with a study of the fine structure of $H\alpha$ and a measurement of the fine structure constant, $1/\alpha$, of which the results are published in the succeeding article.

Experimental Procedure

The source of illumination was a modified Wood's tube operated from a 15,000-volt transformer and completely immersed in liquid air. An image of the source was focused between the plates of an etalon interferometer whose separation of 0.782 cm was chosen so as to give a relative displacement of half a fringe between the two main components of the $H\alpha$ lines. The interference fringes were focused on the slit of a large grating spectrograph by a lens of 32 inches focal length. The dispersion of this spectrograph in the first order was sufficient to give separate images of $H^1\alpha$ and $H^2\alpha$.[10] A typical spectrogram is illustrated in Fig. 1.

Photometry and Measurement of Plates

Each plate was standardized by photographing on it light of approximately the wavelength of $H\alpha$, passed through an optical wedge of known transmission. Microphotometer tracings were then made of these standards as well as of $H^1\alpha$ and $H^2\alpha$ with the Zeiss microphotometer belonging to the Physics Department.

The tracings were accurately measured in both coordinates. The ordinates were reduced to relative intensities by means of the reduction curves derived from the tracings of the standards. Owing to the slightly non-uniform intensity in the illumination of the slit, it was necessary to use the relative intensities of the successive fringe maxima and minima to derive a curve of correction factors by which all measured intensities were multiplied to reduce them to the case of uniform illumination. The intensities thus reduced were ready for plotting.

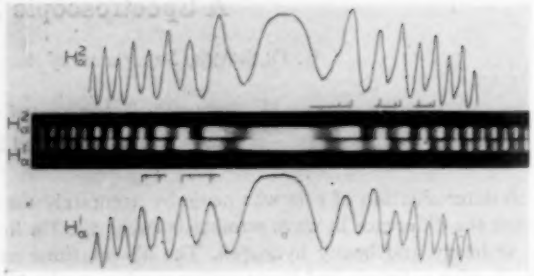

Fig. 1. Spectrograms and microphotometer curves of $H^2\alpha$ and $H^1\alpha$.

It was necessary to alter the scale of abscissae in such a way as to give a uniform scale in terms of orders of interference. Theoretically the linear distance of a point from the center of the fringe system is very nearly proportional to the square root of the difference between the order of interference at the point and the order at the center of the fringe system. Thus if the distances of points from the center be squared and the resulting numbers be taken as abscissae, one should get a scale proportional to the order of interference. When the intensities were plotted against these abscissae, it was found that the fringe maxima corresponding to a given component were nearly but not quite equally spaced. These departures from equal spacing were due to errors in selecting the center of the fringes and to small distortions in the optical system. In no case were the second differences as much as 4 percent of the first differences. The spacings of the maxima were then differenced, and from the first and second differences the scale of abscissae was corrected so that the separations of adjacent maxima due to a given component were all equal to unity. It was found that the first and second differences changed slightly in passing from one side of the fringe center to the other due to distortions, but as we might expect, these quantities remained the same for $H^1\alpha$ and $H^2\alpha$. Therefore mean values were used for these two lines but for each side of the fringe center the appropriate mean values were taken. The arbitrary zero values from which the reduced abscissae were calculated were chosen the

[10] A more detailed description of the apparatus is given in the following article.

FIG. 2. Typical intensity curves.

same for $H^1\alpha$ and $H^2\alpha$ so that the curves for these two lines would have a relative displacement corresponding to the decimal part of their difference in order of interference. The whole number in this case was 6.

With this final scale of abscissae the intensity curves were plotted over a range of one order, the successive orders being superposed on the same diagram. A typical example is shown in Fig. 2 where the three orders used on one side of the center are plotted in juxtaposition. When the fringes on both sides of the center had been plotted in this manner, the means of the ordinates for equal values of the abscissae were determined and used to plot a single curve known as the master curve for the line. In the case of plates, Nos. 31, 33 and 34, three fringes on each side of the center were used while for the remaining plates three fringes on one side of the center and two on the other were plotted. The omission of one fringe was due to a distortion in the optical system that affected the spacings of the outer fringes on one side of the center in such a way that it was impossible to bring them into accurate juxtaposition with the others by the use of second differences only. The master curves derived in this manner served as a basis for all succeeding measurements and calculations.

REDUCTIONS AND OBSERVATIONS

Theoretically the $H\alpha$ line consists of five components whose calculated intensities are 9.00, 7.08, 1.13, 1.00 and 0.20.[11] These are shown in Fig. 1 of the succeeding article. For convenience of reference these components will be called 1, 2, 3, 4, 5, in order of decreasing theoretical intensity. The purpose of the present work was to determine the difference in wave number between the corresponding main components of $H^1\alpha$ and $H^2\alpha$. To evaluate accurately these differences in wave number, it was necessary to subtract from the master curve the three small components. The observations indicate that the theoretical intensities of these components are not to be closely relied upon. The selection of the intensities which were used for this purpose is discussed in the following paper. As the observations indicated no definite difference in relative intensity for the components of $H^1\alpha$ and $H^2\alpha$, mean values for these two lines were determined and used in the reductions.

If we assume that the intensities to be subtracted are known, there remain to be found the positions and forms of the curves corresponding to these components. Since the small components through blending affect the positions of the main components by at most about two percent of an order of interference, small errors in placing them are not important. They were, therefore, inserted in their theoretical positions as calculated from an assumed fine structure constant $1/\alpha=138$, referred to components 1 and 2 after these had been freed by estimation from blends with the small components.

The calculation of the forms of the curves to be subtracted was more complicated. The procedure was as follows. Assuming a given component to be monochromatic, the intensity curve for its fringe system is

$$J'(\theta)=j'(1+2r\cos\theta+\cdots+2r^n\cos n\theta+\cdots),$$

where $\theta=2\pi$ times the order of interference; r=geometrical mean reflecting power of the interferometer plates; j'=a constant depending on the intensity of the source; $J'(\theta)$=intensity at order $\theta/2\pi$. The components were not monochromatic, but were widened due to a number of causes of which the Doppler widening due to temperature was predominant. We are, therefore, justified in assuming to a sufficient approximation that the intensity distribution in a component is given by the expression e^{-u^2/a^2} where u is measured in the same units as θ.

The resulting intensity distribution $J(\theta)$ is given by

$$J(\theta)=\int_{-\infty}^{+\infty} e^{-u^2/a^2}J'(\theta-u)du$$

[11] W. V. Houston and Y. M. Hsieh, Phys. Rev. **45**, 263 (1934).

or

$$J(\theta)=j(1+2rb\cos\theta+\cdots+2r^nb^{n^2}\cos n\theta+\cdots),$$

where $j=a(\pi)^{\frac{1}{2}}j'$ and $b=e^{-\alpha^2/4}$.

For the spectrograms under consideration r was found to be 0.69 while b was determined separately for $H^1\alpha$ and $H^2\alpha$ on each spectrogram. The method of determining b consisted in finding from the master curve the ratio of the maximum intensity of each of the two components to the intensity at a point one-tenth of an order from the maximum, care being taken to work on the side of the maximum least affected by the fainter components. Then by successive trials a value of b was found for which the ratios of the computed and observed values of $J(\theta)$ agreed. With this value of b, a table was calculated giving a typical fringe corresponding to the reflecting power of the interferometer and the line widening of the spectrogram.

With the typical fringe determined, it was possible for any given intensities of the faint components (1) to multiply the ordinates by a suitable factor, (2) to shift the abscissae by amounts corresponding to the theoretical positions of these components and (3) to subtract the resultant curves successively from the master curve. The result yielded a curve showing the two main components unaffected by the lesser ones to the extent that the assigned intensities were correct.

With the two main components freed from the effect of the fainter ones, the next step was to locate the positions of their centers in terms of fractional orders of interference measured from the assigned zero positions common to both $H^1\alpha$ and $H^2\alpha$. A single determination consisted in selecting an ordinate and taking the mean of the two corresponding abscissae. Seven such determinations were made for each component choosing equally spaced ordinates falling on the steep part of the curve. The mean of these seven values was taken as the center of the component. Then the separation between $H^1\alpha$ and $H^2\alpha$ in orders of interference could be found from either of the two strong components, the whole number being supplied from previous knowledge that with the interferometer spacing used it should be approximately 6.5. For the first three plates the interferometer separation was 0.78190 cm while for the last three it was 0.78179 cm. These values were used in calculating the difference in wave number between $H^1\alpha$ and $H^2\alpha$. For the calculation of e/m the following modification of Birge's formula was used:

$$e/m=\frac{FR_{H^1}(H^2-H^1)}{(R_{H^2}-R_{H^1})H^2(H^1-m)}.$$

The following values of the constants were used:

$H^1=1.007775$,[12] $\quad R_{H^1}=109{,}677.759$,[13]
$H^2=2.01363$,[12] $\quad F=9651.1\pm0.8$.

The value of F given by Birge, 9648.9 ± 0.7, was increased by 2.2 ± 0.4 to effect the reduction to the Aston scale of atomic masses.[14]

Results

The collected results are contained in Table II. The values derived from plate 34 have been rejected from the means. This plate was obtained with the gas in the tube at unusually low pressure, in fact, the discharge ceased immediately after the exposure had been made. The low pressure in the tube may account for the abnormally high intensity of the third component. With this high intensity there still remained distortions in the residual curve for the main components of $H^2\alpha$ that could be removed only by increasing the third as well as the fourth and fifth components to such an extent that the residual curve would have had little value. In $H^1\alpha$ this difficulty did not appear but owing to the greater temperature broadening in this case it might well be concealed. These factors together with the strongly discrepant value of the separation derived from the second component were considered sufficient reason for excluding this plate from the final averages.

The results which we accept as most probable are contained in the last section of Table II. The intensities of the faint components recorded in this section are based on the discussion of intensities given in the succeeding paper.

[12] Kenneth T. Bainbridge, Phys. Rev. **44**, 57 (1933).
[13] W. V. Houston, Phys. Rev. **30**, 608 (1927).
[14] I am indebted to Professor Birge for suggesting this correction to the value of the Faraday.

TABLE II. *Spectroscopic data and values of e/m.*

	Plate number	31	33	34	40	41	42	Mean
	Intensity of 3rd	1.28	1.51	2.33	1.48	1.44	1.24	
	Separation, from 1st	6.481	6.487	6.487	6.485	6.487	6.485	
4th=0	e/m	1.7593	1.7576	1.7576	1.7580	1.7574	1.7580	1.7581±2
5th=0								
	Separation, from 2nd	6.484	6.484	6.475	6.481	6.487	6.485	
	e/m	1.7585	1.7585	1.7609	1.7590	1.7574	1.7580	1.7583±2
	Intensity of 3rd	1.44	1.75	2.57	2.00	2.04	1.78	
	Separation, from 1st	6.481	6.486	6.487	6.488	6.490	6.486	
4th=1	e/m	1.7593	1.7579	1.7576	1.7571	1.7566	1.7577	1.7577±3
5th=1								
	Separation, from 2nd	6.484	6.483	6.475	6.482	6.488	6.485	
	e/m	1.7585	1.7588	1.7609	1.7589	1.7571	1.7580	1.7582±2
	Intensity of 3rd	1.42	1.72	2.56	1.92	2.00	1.73	
	Intensity of 4th	0.58	0.69	0.60	0.82	0.88	0.84	
	Separation, from 1st	6.481	6.486	6.487	6.487	6.490	6.486	
5th=1	e/m	1.7593	1.7579	1.7576	1.7574	1.7566	1.7577	1.7578±3
	Separation, from 2nd	6.484	6.484	6.475	6.482	6.489	6.487	
	e/m	1.7585	1.7585	1.7609	1.7588	1.7569	1.7574	1.7580±3

In calculating the probable error of the definitive result, we must take account of the uncertainty in the intensities of components 4 and 5. Lacking definite information we have assumed rather arbitrarily that the probable errors of these were in each case one-half the intensities themselves. A comparison of the means from the first and second sections of the table reveals a difference of 3 in the last place, corresponding to a difference in the strengths of components 4 and 5 equal to their theoretical values. In treating the fourth and fifth components together in this manner it might be suspected that there is some compensation between the effects of the two taken separately. Since their actual intensities need not differ from the theoretical values in the same ratio, this combined treatment might lead to a too optimistic view of the probable error. To test this, all the calculations were made omitting the fifth entirely and including the fourth. The result showed that the fifth alone did not change the separation by as much as one in the last place. Thus there is no appreciable compensating effect of the type mentioned. We may, therefore, take 1.5 in the last place to be the probable error arising from the assumption of theoretical intensity. This combined with the accidental probable error and the probable error of the Faraday, which is one part in 12,000, gives the resultant probable error of 2.7 in the last place.

Therefore, the definitive value is

$$e/m = 1.7579 \pm 0.0003 \times 10^7.$$

Dividing e/m by $e/M_H(9576.7 \pm 0.8)$ we obtain

$$M_H/m = 1835.6 \pm 0.2_5.$$

It should be noted in this last result that as the Faraday has been removed, it is no longer necessary to include its probable error.

An inspection of the table shows that the results derived separately from the first and second components agree within the limits of accidental error. This gives some encouragement to the belief that the values derived are fairly free from systematic error. When in addition it is considered that the plates were taken under a variety of conditions of temperature and pressure with resulting strong variations in the intensities and sharpness of the various components and that no appreciable dependence of the results on these conditions is evident, we feel justified in thinking that the calculated probable errors describe closely the actual uncertainties in the results.

The assistance of Dr. Norman S. Grace who collaborated during the early stages of the work is gratefully acknowledged.

The Fine Structure of Hα

FRANK H. SPEDDING,* C. D. SHANE,† AND NORMAN S. GRACE,‡ *University of California, Berkeley*

(Received November 5, 1934)

The fine structure of Hα was investigated using Fabry and Perot interference patterns produced in the light of ordinary and heavy hydrogen. The auxiliary spectroscopic dispersion was sufficient to separate the patterns of $H^1\alpha$ and $H^2\alpha$. Accurate photometric methods were used in interpreting the spectrograms and a new method of analyzing the observed patterns was developed. Following are the principal results: (1) Three components of each line are directly observable, while the two remaining components predicted by theory could not be resolved. (2) The observational evidence indicates definitely the same relative intensities of the components for $H^1\alpha$ and $H^2\alpha$. (3) The relative intensities insofar as they are determined depart markedly from the theoretical values. These departures are consistent with the hypothesis of a diminished population of atoms in the $3D$ energy states. (4) The fine structure constant was determined yielding $1/\alpha = 137.4 \pm 0.2$. There is some evidence of systematic dependence of this result on conditions of excitation in the source so that the probable error overestimates the accuracy of the result. The correct value probably lies between 137 and 138.

INTRODUCTION

IN a note published in the Physical Review[1] of July 1, 1933, we reported preliminary results on the fine structure separation of the Hα doublet derived from a study of the lines of ordinary and of heavy hydrogen. After eliminating as far as possible the effects of the fainter components, the separation was found to be 0.324 cm^{-1}, leading to a value for the reciprocal of the fine structure constant $1/\alpha = 138$. The spectrograms on which this report was based were secured with rather low pressure in the discharge tube, and it was felt that there might be some dependence of the results on this condition. Accordingly for a more complete study, spectrograms were taken with varying conditions of pressure. An improved optical arrangement was used to give more extended interference fringe systems, and finally the method of analyzing the photometric curves was considerably refined. The present paper reports the final results of this investigation.

Since the publication of our preliminary results, important papers on the subject by Houston and Hsieh[2] and by Williams and Gibbs[3] have appeared. From an analysis of the lines Hβ to Hε in ordinary hydrogen Houston and Hsieh find a value of $1/\alpha = 139.9$. They conclude that the theory of fine structure requires correction to reconcile their observations with the latest value given by Birge,[4] namely, 137.4. Williams and Gibbs, from a study of $H^1\alpha$ and $H^2\alpha$, find doublet separations corresponding to values of $1/\alpha = 141.7$ and 138.8, respectively. The results derived in the present paper are in close accord with Birge's latest value. We feel that the difference between our results and those of the observers mentioned above may be largely explained on the basis of the more detailed method of analyzing the observations which we used.

DESCRIPTION OF APPARATUS

The source of illumination was a modified form of Wood's tube with a length of 150 cm between electrodes and an internal diameter of 1 cm. The entire length of the tube including the electrodes was immersed in liquid air. The light to be photographed was taken longitudinally from the central 50 cm of the tube, and emerged through an extension projecting out of the liquid air. The source of hydrogen consisted of a few drops of water containing approximately equal parts of H^1 and H^2 furnished through the kindness of Professor G. N. Lewis. This water was contained in a small side tube which could be opened into the discharge tube by means of a

* Department of Chemistry.
† Department of Astronomy.
‡ Department of Physics.

[1] Frank H. Spedding, C. D. Shane and Norman S. Grace, Phys. Rev. **44**, 58 (1933).

[2] W. V. Houston and Y. M. Hsieh, Phys. Rev. **45**, 263 (1934).

[3] R. C. Williams and R. C. Gibbs, Phys. Rev. **45**, 475 (1934).

[4] Raymond T. Birge, Science **79**, 438 (1934).

stopcock. In preparing the discharge tube for operation it was pumped with the discharge running for about a day. Toward the end it was flushed out several times by admitting small amounts of the water vapor. Just before starting a run water vapor was admitted, the tube was immersed in liquid air, and the discharge was started. It would run for about one second and then stop due to absorption of the hydrogen by the cold aluminum electrodes. The tube was then removed and the discharge turned on while the tube warmed up. Another charge of water vapor was admitted and the process was repeated. At each stage the discharge at liquid air temperature would persist several times longer than at the preceding stage. After repeating the process a suitable number of times the discharge would continue for several hours.

In all cases it was possible to regulate the relative intensities of $H^1\alpha$ and $H^2\alpha$ by admitting small amounts of the nearly pure gases[5] from bulbs sealed on the apparatus for the purpose. On the other hand, considerable difficulty was encountered in maintaining the pressure at a value sufficient to give the two strong components of the lines with the theoretical relative intensities. When a fresh charge of gas was admitted to the tube during its operation the strong components would have nearly theoretical relative intensities but this persisted for only a few seconds. Probably this condition could have been maintained if a continuous flow of gas through the tube had been provided, but this was impossible owing to the small amount of heavy hydrogen available. Following Houston's procedure the last three plates were taken with a certain amount of helium in the tube in order to maintain sufficient pressure. This gave more nearly correct relative intensities for the strong components.

Attempts were made to increase the sharpness of the lines by reducing the current and by an intermittent discharge on $\frac{1}{4}$ of a second and off $1\frac{3}{4}$ seconds. This resulted in no improvement. Finally the tube was run while immersed in liquid hydrogen. This was unsatisfactory because it was very difficult to maintain the discharge, and no increased sharpness in the lines resulted.

The tube was operated from a 15,000-volt transformer. At various times the current was measured and found to range between 25 and 30 milliamperes with very little dependence on pressure. The difference in potential between the electrodes was, of course, much smaller than 15,000 volts except at such times as the discharge was on the point of ceasing due to low pressure.

An image of the source was focused between the plates of a Fabry and Perot etalon by a system of lenses arranged to give a fairly uniform illumination over a spectrograph slit length of $1\frac{1}{2}$ inches. The reflecting power of the silvered surfaces of the plates was 0.69. A lens of 32 inches focal length formed an image of the fringe system given by the interferometer on the slit of the spectrograph. This spectrograph is of the Littrow type possessing a plane grating of 6 inches aperture and a lens of 30 feet focal length. The first order was used and the dispersion was such that $H^1\alpha$ and $H^2\alpha$ were separated on the photographs by 1 mm. Thus a slit width of practically this amount could be used without overlapping of the two lines. The photographs with this apparatus showed the two lines $H^1\alpha$ and $H^2\alpha$ as sections taken across the centers of their interference ring systems. The spacing of the interferometer plates, 0.782 cm, was chosen to give for each line the fringes of one of the two main components almost exactly midway between pairs of adjoining fringes of the other main component.

Intensities of the Components

Six plates were selected for measurement and discussion. Of these, Nos. 31, 33 and 34 were taken with no helium in the discharge tube while for Nos. 40, 41 and 42 helium was introduced with a resulting higher total pressure. Determinations of the temperature of the source for each plate were afforded by the quantities b, referred to in the preceding paper, which measure the sharpness of the main components of the Hα line. If it be assumed that all widening is due to temperature, a simple calculation yields a result which may be taken as an upper limit to the temperature. The results ranged between 160°

[5] We are greatly indebted to Professor G. N. Lewis who prepared some highly concentrated H^2 gas for this purpose.

TABLE I. *Master curves.*

Decimal of order of interference	31		33		34		40		41		42	
	$H^1\alpha$	$H^2\alpha$	$H^1\alpha$	$H^2\alpha$	$H^1\alpha$	$H^2\alpha$	$H^1\alpha$	$H^2\alpha$	$H^1\alpha$	$H^2\alpha$	$H^1\alpha$	$H^2\alpha$
0.725		20.7	22.0		30.0			23.5		20.8		
.750	20.4	22.2	20.8	21.8	30.6	17.4	34.1	23.4	31.8	21.2	33.0	23.0
.775	20.0	24.0	20.6	23.3	32.0	18.0	31.6	24.4	32.4	22.6	33.2	23.7
.800	20.2	25.8	21.0	25.1	33.9	19.1	35.8	26.1	33.7	24.5	33.9	25.2
.825	21.6	27.4	22.5	26.6	35.8	20.8	37.1	28.7	35.4	27.3	35.2	27.6
.850	23.3	29.1	24.5	28.4	37.8	23.4	38.9	32.1	37.4	30.7	36.9	31.0
.875	25.8	31.3	27.4	31.3	40.2	26.6	40.9	35.5	39.6	34.9	39.1	35.2
.900	28.8	34.9	31.2	35.1	42.5	30.1	43.3	40.2	41.7	39.7	41.4	39.5
.925	32.1	39.8	35.3	40.3	45.1	33.6	45.3	44.2	44.0	44.3	43.4	43.7
.950	35.2	44.8	39.5	44.9	47.3	36.5	46.8	47.3	46.0	47.9	45.2	47.1
.975	37.6	48.8	42.4	48.2	49.0	38.7	48.1	49.3	47.3	50.4	46.5	49.2
.000	38.9	51.2	44.2	49.9	50.0	39.8	48.9	50.0	48.1	51.1	47.2	50.0
.025	39.6	49.7	44.6	49.0	49.8	39.1	48.8	48.7	47.5	49.8	47.0	49.1
.050	39.0	45.2	43.7	45.4	48.2	37.1	47.6	46.0	46.0	46.8	46.0	46.4
.075	36.8	39.2	41.6	39.8	46.0	34.3	45.7	42.7	43.9	42.5	44.5	43.0
.100	34.0	32.8	38.6	33.1	43.2	31.0	43.4	39.1	40.9	37.8	42.2	39.1
.125	31.1	27.2	34.8	26.8	39.8	27.5	40.9	35.6	37.8	33.5	39.3	35.3
.150	28.7	22.8	31.2	22.0	35.8	24.6	37.7	32.6	34.8	29.8	36.3	32.2
175	26.8	19.4	28.4	19.0	32.1	23.3	34.7	30.5	31.9	27.5	33.7	29.6
.200	25.6	17.4	26.4	17.1	28.4	23.5	32.1	29.6	29.8	26.3	31.5	28.5
.225	24.8	16.3	25.5	16.0	25.6	25.4	30.2	29.8	28.6	26.3	29.9	28.2
.250	25.1	16.0	25.4	15.8	23.8	27.8	29.1	30.7	28.1	27.2	29.1	28.7
.275	26.2	16.4	25.8	16.2	23.2	30.2	29.4	31.8	28.5	28.4	29.3	29.7
.300	27.5	17.4	26.8	16.8	23.8	32.0	30.7	33.1	29.9	30.1	30.4	31.0
.325	29.3	19.1	28.6	18.4	25.6	33.6	32.7	34.7	32.0	31.8	32.4	32.5
.350	31.5	21.3	31.1	20.5	27.9	35.4	35.0	36.6	34.8	33.8	34.8	34.4
.375	33.9	24.7	34.4	24.0	30.4	37.2	38.0	39.0	37.9	36.2	37.8	36.8
.400	36.8	28.4	37.8	28.9	33.2	39.8	41.3	41.8	41.2	39.0	40.0	39.5
.425	40.3	32.7	41.4	35.1	35.8	43.1	44.3	44.4	44.2	41.1	43.8	42.0
.450	43.3	36.8	45.5	41.0	37.8	46.3	46.5	46.7	46.9	43.8	46.2	44.4
.475	45.8	39.8	48.4	45.5	39.2	48.7	48.1	48.8	48.9	45.9	47.9	46.2
.500	47.5	41.3	50.0	48.1	40.0	49.6	49.2	49.0	49.8	46.2	49.0	46.3
.525	47.6	40.1	50.0	46.4	40.4	48.5	49.4	47.8	49.8	44.8	49.1	45.2
.550	45.9	36.4	48.4	43.4	39.9	45.6	48.8	45.2	48.7	42.3	48.1	43.1
.575	43.0	32.6	45.4	38.0	38.9	41.0	47.3	41.6	46.7	38.7	46.6	40.3
.600	39.0	28.5	41.2	31.9	37.2	35.6	45.3	37.8	44.0	34.7	44.8	37.1
.625	34.5	24.8	36.2	26.3	35.4	30.5	42.9	34.0	41.3	30.5	42.6	33.6
.650	30.8	22.1	31.0	22.5	33.2	25.6	40.6	31.0	38.6	26.8	40.4	30.0
.675	27.2	20.8	27.0	20.6	31.5	21.7	38.7	28.0	36.1	24.1	37.8	27.2
.700	24.4	20.4	24.0	20.3	30.6	19.4	36.9	26.0	34.4	22.5	35.6	25.4
.725	22.5	21.2	22.0	20.5	30.4	18.1	35.8	25.4	33.2	21.7	34.4	24.3
.750	21.2			21.8		17.8	35.1		32.5		33.8	24.1

and 322°, the low pressure plates yielding the lower temperatures. This is what might be expected from the superior conductivity of gas at the lowest pressure used.

The preceding paper describes the photometry and reductions of these plates up to the point of finding the master curves. Table I gives the coordinates of points on the master curves used in this investigation. The method of removing from the master curves the effects of the three faint components for any assigned intensities has also been explained. It remains here to discuss in some detail the assignment of the intensities to be subtracted.

Fig. 1[6] shows a typical master curve for $H^2\alpha$. If the three faint components did not exist, we should expect the fringes of each of the two strong components to possess symmetry about the vertical line passing through their maxima, while the two minima should have equal ordinates. The imposition of these three conditions on the residual curve formed by subtracting the three faint components should provide a means of finding the intensities to be subtracted. In practice it was found that the conditions were insensitive to components four and five in the sense that all three requirements could be

[6] Dr. Harvey E. White kindly furnished this figure.

satisfied within observational error by assigning any reasonable intensities to these components and calculating the intensity of component three by least squares. It was also found that for this purpose the conditions of symmetry for component one had negligible weight compared with the other conditions. These considerations led to the following method of treatment.

Data derived from the master curve were used to calculate a typical fringe as explained in the preceding paper. The scale of ordinates was chosen to give an intensity 1/7.08 times the intensity of the second component. This latter intensity was derived by freeing the master curve by estimation from the effect of the third component which was the only important one for the purpose. Theoretically the five components have intensities 9.00, 7.08, 1.13, 1.00 and 0.20. Thus the typical fringe had an intensity 1.00 based on the theoretical value for the second component. The ordinates of the typical fringe were multiplied by 1.69 thus giving 1.5 times the third component, the abscissae were displaced so as to bring the maximum to the theoretical position of this component and the resulting curve was subtracted from the master curve. This gave the first residual curve. 2.5 times the third component was then subtracted from the master curve, giving the second residual curve. One times the fourth component subtracted from the first residual curve gave the third residual curve, and two times the fifth component subtracted from the third residual curve gave the fourth residual curve.

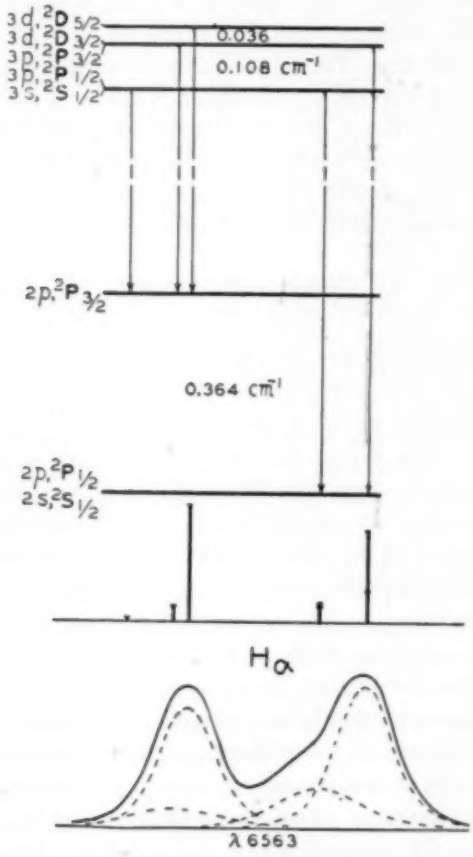

FIG. 1. Fine structure of Hα.

Data were now taken from each residual curve as follows. The vertical distance between one of the two maxima and the *highest* minimum was divided into twelve equal parts. At each point of division the mean of the two abscissae on that fringe was calculated, thus giving eleven points each representing the center of the fringe for a particular ordinate. These points were plotted on a new chart and the resulting curve was known as a line of centers. The process was repeated for the other fringe of the master curve. If the three faint components had been properly removed the two lines of centers should be vertical and the reciprocals of their slopes should be zero. In each case the average slope reciprocals, hereafter called "slopes" for the sake of brevity, were determined omitting the upper one and lower two points which were of small weight. From these data for the four residual curves it was then possible to derive coefficients giving the change in slope for a standard change of intensity for each of the faint components. Using these coefficients and the slope of the line of centers for any one of the residual curves, a linear equation could be formed involving corrections to the three intensities used in the residual curve necessary to make the line of centers vertical. The fringe due to the first component was very insensitive to the faint components as regards slope of the line of centers and was therefore not used. The remaining condition, that the two minima should be equal, was imposed in much the same way, namely by the determination of coefficients and the derivation of an equation. Thus there were available

two equations involving corrections to the assigned intensities of the three faint components. After much experimenting it was found that components four and five were indeterminate within the errors of observation, so that solutions were made only for component three based on hypotheses concerning the other two. This was done by least squares from the two equations, on the basis of different hypotheses concerning the fourth and fifth components. In this work the approximation of linear relationships between the intensities of the faint components and the various observed quantities was made. This while not strictly true, was found by tests to be correct in the applications within the observational errors. The solutions obtained in this manner gave the most probable values for the third component on the basis of the adopted assumptions regarding the fourth and fifth. All intensities were calculated in units of the theoretical intensity using the second component as a standard. The intensities of the third component are recorded in the first line of each section in Table II. An inspection of the values given in the first two sections reveals no differences between $H^1\alpha$ and $H^2\alpha$ exceeding the possible errors of determination. It was therefore decided to form the mean intensity for $H^1\alpha$ and $H^2\alpha$ in each case and to use these values in calculating the results listed in the remaining portions of the table.

The intensities of the first component on the different plates were calculated on the assumption of theoretical intensity for the fourth and fifth and the corresponding measured intensities for the third. This was accomplished by subtracting from the master curve the faint components with these assigned intensities and measuring the heights of the maxima of the residual curve. Account was taken of the fact that the minimum of the fringe for each component added something to the maximum of the other component and must, therefore, be subtracted. The resulting intensities of the first component measured in terms of its theoretical value are included in the fourth section of Table II. Again the differences between the results for $H^1\alpha$ and $H^2\alpha$ do not exceed the observational errors. We conclude, therefore, that the components have the same relative intensities in $H^1\alpha$ and $H^2\alpha$.

It is clear that all plates agree in giving intensities too low for the first component and too high for the third. This can be explained qualitatively if we assume a population of the $3D$ energy levels less than would occur in thermodynamic equilibrium. The upper level for the first component is a $3D$ state while the second originates partly in a D state and partly in a P state (see Fig. 1). Thus, in accordance with the hypothesis, both components should be weakened but the first should be affected more than the second. This would give in the adopted scale of intensities a relatively faint first component. On the other hand the third component originates from P and S states for its upper level and should, therefore, not be weakened but, relative to the second, it should be strengthened. This is in accord with the observations. The fourth originates from a D state only, since the corresponding line from the P state is forbidden by the selection rules, and it should be weakened like the first. The fifth comes from the S state and should be strengthened relatively to the second. Briefly, the hypothesis of a diminished D population explains the weakened first and the strengthened third components and predicts weakened fourth and strengthened fifth components.

When we examine the changes in intensity from plate to plate it is apparent that the weakening of the first component is accentuated on the low pressure spectrograms whereas no systematic effect is noted for the third component. The errors of observation may be large enough to mask the effect in the latter case, or there may be departures from the equilibrium populations of the P and S states capable of explaining this observation if we assume it to be correct.

If the hypothesis of a diminished population in the $3D$ energy levels is correct, the fourth component should be affected in the same ratio as the first. We therefore assigned intensities to the fourth component on each plate bearing the same ratio to their theoretical values as were found for the first. These were used as a basis for the results which we regard as most probable.

TABLE II.

		Interferometer separation = 0.78190 cm						Interferometer separation = 0.78179 cm							
		31		33		34		40		41		42		Mean	
	Plate number	$H^1\alpha$	$H^2\alpha$	$H^1\alpha$	$H^2\alpha$	$H^1\alpha$	$H^2\alpha$	$H^1\alpha$	$H^2\alpha$	$H^1\alpha$	$H^2\alpha$	$H^1\alpha$	$H^2\alpha$	$H^1\alpha$	$H^2\alpha$
	Intensity of 3rd	1.31	1.25	1.46	1.56	2.39	2.27	1.72	1.23	1.11	1.77	1.39	1.10		
4th = 0	Center of 1st	0.017	0.498	0.017	0.504	0.511	−0.001	0.504	−0.009	0.504	−0.009	0.508	−0.006		
5th = 0	Center of 2nd	0.527	1.010	0.527	1.012	1.042	0.515	1.033	0.506	1.016	0.512	1.028	0.509		
	Separation cm^{-1}	0.326	0.327	0.326	0.325	0.339	0.330	0.338	0.329	0.327	0.333	0.333	0.329	0.3300 ± 18	0.3286 ± 9
	Intensity of 3rd	1.54	1.35	1.76	1.74	2.78	2.36	2.29	1.70	1.90	2.18	1.91	1.64		
4th = 1	Center of 1st	0.027	0.509	0.025	0.512	0.523	0.010	0.508	−0.001	0.517	−0.004	0.513	0.001		
5th = 1	Center of 2nd	0.529	1.010	0.530	1.013	1.046	0.517	1.037	0.510	1.022	0.515	1.033	0.513		
	Separation cm^{-1}	0.321	0.320	0.323	0.320	0.334	0.324	0.338	0.327	0.323	0.332	0.333	0.327	0.3276 ± 22	0.3252 ± 14
	Intensity of 3rd	1.28		1.51		2.33		1.48		1.44		1.24			
4th = 0	Center of 1st	0.017	0.498	0.017	0.504	0.512	−0.001	0.506	−0.009	0.502	−0.009	0.509	−0.006		
5th = 0	Center of 2nd	0.526	1.010	0.528	1.012	1.041	0.516	1.028	0.509	1.021	0.508	1.026	0.511		
	Separation cm^{-1}	0.326	0.328	0.327	0.325	0.338	0.330	0.334	0.331	0.332	0.331	0.331	0.331	0.3300 ± 10	0.3296 ± 9
	Intensity of 3rd	1.44		1.75		2.57		2.00		2.04		1.78			
	Intensity of 1st	0.59	0.57	0.67	0.71	0.61	0.59	0.81	0.82	0.86	0.91	0.83	0.85		
4th = 1	Center of 1st	0.028	0.509	0.026	0.512	0.523	0.010	0.510	−0.002	0.508	−0.002	0.515	0.001		
5th = 1	Center of 2nd	0.527	1.011	0.530	1.013	1.042	0.517	1.031	0.513	1.025	0.513	1.030	0.515		
	Separation cm^{-1}	0.319	0.321	0.322	0.320	0.332	0.324	0.333	0.329	0.331	0.329	0.329	0.329	0.3268 ± 18	0.3262 ± 13
	Intensity of 3rd	1.42		1.72		2.56		1.92		2.00		1.73			
	Intensity of 4th	0.58		0.69		0.60		0.82		0.88		0.84			
5th = 1	Center of 1st	0.024	0.505	0.024	0.510	0.519	0.006	0.510	−0.003	0.507	−0.003	0.514	0.000		
	Center of 2nd	0.527	1.011	0.529	1.013	1.042	0.517	1.031	0.513	1.024	0.513	1.028	0.515		
	Separation cm^{-1}	0.322	0.324	0.323	0.322	0.334	0.327	0.333	0.330	0.331	0.330	0.329	0.329	0.3276 ± 15	0.3270 ± 11

POSITIONS OF MAIN COMPONENTS

With given values of the intensities for the faint components it was possible to find the positions of components one and two by using the lines of centers. The means of the abscissae in each of these lines were formed omitting the upper one and the lower three points. This gave the center of the corresponding fringe. By comparing results from the different residual curves, coefficients were found relating changes in these centers to changes in the intensities of the faint components. A center found from a given residual curve combined with these coefficients furnished a linear equation from which the center could be calculated for any intensities of the first component. In this manner the centers of components one and two were determined on the basis of the adopted intensities.

The lines headed "center of 1st" and "center of 2nd" in each section of Table II give the positions of the fringe centers determined in this way on the basis of the various hypotheses concerning the faint components. The differences between fringe centers for the first and second components when divided by twice the interferometer spacing yields the separation in wave numbers for the two strong components. These values are given in the last line of each section. For the reasons given in the preceding article the data derived from plate 34 have not been included in the means.

DISCUSSION OF RESULTS

It is clear from the results quoted in the table that there is no appreciable difference in doublet separation for $H^1\alpha$ and $H^2\alpha$. This is in disagreement with the results of Williams and Gibbs who find 0.308 and 0.321 for $H^1\alpha$ and $H^2\alpha$, respectively. We feel, however, that our treatment possesses certain advantages over theirs, particularly with reference to our spectrographic separation of $H^1\alpha$ and $H^2\alpha$ and to our more detailed analysis of the intensity curves of the fringe systems.

We regard as the most probable value of the separation the weighted mean of the values for $H^1\alpha$ and $H^2\alpha$ taken from the last section of Table II, the weights being 1 and 2, respectively. From the formula[7]

$$\alpha^2 = (1296/73)(\Delta\nu/R)$$

we find $1/\alpha = 137.4 \pm 0.2$. The probable errors quoted are calculated values based solely on the accordance of the observations and understate the uncertainty of the results. There appears to

[7] See Ruark and Urey, *Atoms, Molecules and Quanta*, p. 135 for the term values used in deriving this equation.

be a distinct systematic difference between the separations depending on the pressure used in the source. It is conceivable that this is real. On the other hand it may be due to wide variation in intensities of the unresolved components. If we assume that the fourth and fifth components have zero intensities on the low pressure plates and theoretical intensities on the high pressure plates, the systematic difference is greatly reduced. The only conclusion to be drawn at present from this difference is that the uncertainty of the separation must be much greater than is indicated by the calculated probable errors. Our best estimate of this uncertainty may be expressed by saying that $1/\alpha$ probably lies between 137 and 138.

JANUARY 1, 1935 PHYSICAL REVIEW VOLUME 47

Are the Formulae for the Absorption of High Energy Radiations Valid?

J. R. OPPENHEIMER, *University of California, Berkeley*

(Received November 12, 1934)

In this paper we consider the discrepancies between theoretical prediction and experiment for the absorption of cosmic-ray electrons and gamma-rays. By applying a strict criterion for the validity of classical electron theory, it is possible to derive new formulae for impact and radiative energy losses of high energy electrons, which may be regarded as theoretical lower limits for these quantities, and which are in far better agreement with experiment than the formulae given by an uncritical application of quantum mechanics to these problems. These limitations on classical electron theory are consistent with those given by possible unitary classical field theories, but are more incisive than those given by the unitary theory of Born.

1. THE THEORETICAL FORMULAE

THE question of the validity of the theoretical formulae for the absorption of high energy radiations has been brought to a new prominence by recent experimental and theoretical researches. On the one hand the observation of the cloud chamber tracks of cosmic rays has made it possible to extend our knowledge of the specific ionization and energy loss of electrons from particles of a few million volts on up to a few billion.[1] On the other hand two mechanisms of absorption, increasingly important at high energies, have been carefully investigated theoretically:[2] the pair production by gamma-rays, and the radiative energy losses of electrons. The question of whether the formulae derived for the probability of these processes, and the more familiar formulae for the ionization and impact energy losses of fast electrons, should hold for the very high cosmic-ray energies, has often been discussed, and has been explicitly studied by v. Weizsaecker[3] and by Williams.[4] The conclusion to which these researches have led is that the formulae should remain valid. The experiments, however, do not speak for this. We want here to reconsider the question in the light of this discrepancy.

The predictions of the theory are these: (1) The specific primary ionization of an electron (or positron) should pass through a minimum as the energy of the electron increases, and should increase slowly with the energy throughout the entire range of cosmic-ray energies. If the velocity of the electron be $v=\beta c$, then the specific ionization should vary[5] with v according to

$$(1/\beta^2)[\ln \epsilon\beta+\ln (k/\alpha)-\tfrac{1}{2}\beta^2]$$

$$\text{with} \qquad \epsilon=(1-\beta^2)^{-\frac{1}{2}}; \quad \alpha=e^2/\hbar c. \qquad (1)$$

Here k is a constant of the order of 10, depending on the f-values of the atomic electrons of the matter through which the ray is passing. According to this formula one has to expect an

[1] C. D. Anderson and S. H. Neddermeyer, International Conference on Physics, London, 1934.

[2] H. Bethe and W. Heitler, Proc. Roy. Soc. **A146**, 83 (1934).

[3] v. Weizsaecker, Zeits. f. Physik **88**, 612 (1934).

[4] E. J. Williams, Phys. Rev. **45**, 729 (1934).

[5] e.g., H. Bethe, *Handbuch der Physik*, XXIV, 1, 2nd edition, 1932.

increase of the ionization in air, which amounts to seventy percent when the energy of the electron rises from three million to a billion volts.

Often it is not the primary ionization which is observed, but the "probable" ionization:[6] the total ionization produced by the primary and by secondaries with energies less than $\epsilon' mc^2$ (in practice $\epsilon' \gg \alpha^{-2}$, $\epsilon' < 1$). This probable ionization is measured roughly by the total energy loss to secondaries of energy $< \epsilon' mc^2$, and increases with ϵ less rapidly than the primary ionization, since the increase in ionization comes chiefly from secondaries of very low energy. For the probable ionization we have instead of (1)

$$(1/\beta^2)\{\ln(\beta\epsilon) + \ln(k_1\sqrt{\epsilon'}/\alpha^2) - \tfrac{1}{2}\beta^2\}, \quad (1a)$$

with $k_1 \sim 2.5$ for hydrogen.

(2) An electron passing through matter will be accelerated by the nuclear fields, and will radiate. If σ_ν is the differential cross section of a nucleus for radiation of a quantum of energy $h\nu$, one may define a cross section for energy loss

$$\sigma = (1/\nu_0)\int_0^{\nu_0} \sigma_\nu d\nu; \quad \nu_0 = \epsilon mc^2/h.$$

This has been computed by Heitler and Sauter[7] for a model in which the nuclear field is taken to be the Coulomb field of a charge Ze:

$$\sigma = 4\alpha Z^2 \rho^2 (\ln 2\epsilon - \tfrac{1}{3}), \text{ with } \rho = e^2/mc^2, \quad (2)$$

a result valid for $\epsilon \gg 1$. These calculations have been extended by Bethe and Heitler to the case of a nuclear field screened externally by the statistical charge distribution of the atomic electrons. With this model σ does not increase indefinitely, but approaches, for $\epsilon \to \infty$, an asymptotic value

$$4\alpha Z^2 \rho^2 [\ln(183/Z^{\frac{1}{3}}) + 1/18]. \quad (3)$$

For energies above 10^8 volts σ does not differ seriously from its limiting value (3). Essentially these same results have been derived by v. Weizsaecker by a method which we shall have to consider in detail.

(3) Gamma-rays of high energy will produce pairs in nuclear fields. Bethe and Heitler have carried through the calculations of the cross section for pair production in the fields of unscreened and screened nuclei, and find

$$\sigma = 4\alpha Z^2 \rho^2 [7/9 \ln 2\epsilon - 109/54], \quad (4)$$

$$\sigma = 4\alpha Z^2 \rho^2 [7/9 \ln(183/Z^{\frac{1}{3}}) - 1/54]. \quad (5)$$

All of these calculations are approximate, for the effect of the nuclear field is treated as small, and the formulae obtained are to be regarded as the first terms in a series of powers of αZ. Complete calculations which do not involve this approximation have not been made; but by using the wave functions of Furry[8] it is at least possible to see that the error involved does not become progressive as the energy increases, that, for example, no terms of the form $\alpha Z\epsilon$ occur; and this conclusion, as Williams has observed, follows also from the argument of v. Weizsaecker. The formulae (4) and (5) have thus to be regarded as legitimate approximations for small Z, no matter how great the energy. In the case of pair production σ is known to be quite accurately proportional to Z^2 for gamma-rays of energy 2.6 and 5.4 million volts;[9] and it appears from this that one may expect (5) to hold without serious error even for heavy elements.

2. The Experimental Evidence[10]

According to (3), a beam of high energy electrons should have a good part of its energy converted into gamma-radiation in a centimeter of lead; in an equal distance this gamma-ray will be largely reconverted into pairs. The two mechanisms together therefore furnish a very rapid mechanism for the degradation and absorption of electrons, positrons or gamma-rays, an absorption which deviates strongly from a mass absorption law. It is therefore possible to do justice to the great penetration of the cosmic rays only by admitting that the formulae are wrong, or by postulating some other and less absorbable component of the rays to account for their penetration.

Other arguments lead to this same alternative. Thus it is possible to observe the ionization of

[6] E. J. Williams, Proc. Roy. Soc. **A135**, 108 (1932).
[7] Reference 2.
[8] W. H. Furry, Phys. Rev. **46**, 391 (1934).
[9] E. McMillan, Phys. Rev. **46**, 868 (1934).
[10] Such clarity as there is in this account of the experimental situation I owe entirely to Dr. Anderson and Mr. Neddermeyer, who have with great patience explained to me just what the evidence is, what it indicates, and how little it proves.

cosmic-ray tracks in cloud chambers. This has been done by Anderson and Neddermeyer and by Kunze,[11] who fail to find evidence for the increase in ionization with ϵ predicted by (1). According to Dr. Anderson, estimates of two kinds have been made:

(a) Estimates of the density of thin tracks, which should give the *primary* ionization, for which (1) holds. Although a seventy percent difference in density for low energy β-particles could be detected, no difference could be detected for tracks varying from a few million to a few billion volts.

(b) Actual counts on diffuse tracks. Here it is the total ionization produced by primary for secondaries of energy below some value $\bar{E}$ which is measured. $\bar{E}$ is determined by the fact that when an energetic secondary is curled up in the magnetic field, it makes the separate counting of the drops impossible. $\bar{E}$ probably lies between 10^8 and 10^9 volts. For this "probable" ionization we have instead of (1) to use (1a). Here again there is no large increase in ionization with ϵ. A small increase might still escape detection.

It would thus seem necessary to say, either that the increase of ionization predicted by (1) or (1a) does not occur, or that all of the high energy tracks by Anderson are made by protons. This second alternative, which has been seriously advocated by Williams,[4] meets with the difficulty that there are tracks (with an $H\rho$ corresponding to a 5×10^8 volt electron, for instance) for which one would expect an ionization observably greater than the minimum, whether they are made by electrons or protons. But the uncertainties in the ionization observations do not make it possible to exclude the possibility of protons completely.

Anderson and Neddermeyer[1] have made studies of the energy losses in lead plates. For tracks of not too high energy ($\sim3\times10^8$ volts), the energy loss can be directly measured. There is good evidence for large energy losses, which are almost certainly radiative. The losses are smaller than one would expect from (3). But the number of tracks is small; large fluctuations are to be expected; and it is not certain, though it is probable, that the formula (3) gives too high a result.

With higher energy tracks, where energy losses are not directly measurable, one can still conclude that, if the tracks are made by electrons (and positrons) both (3) and (5) cannot be right, since one does not observe at all that multiplication of tracks by gamma-radiation and pair production which (3) and (5) would predict.

Against the hypothesis that these high energy tracks are made by protons, positive and negative, there are two further arguments. In the energy range where one can unambiguously distinguish between electronic and protonic mass, protons are an extreme rarity, and although positive and negative curvatures occur with about equal frequency for the high energy tracks, no definitely recognizable negative protonic tracks have been seen. The second argument concerns the production of high energy secondary electrons. The number and distribution of these corresponds to what we should expect for primaries of electronic mass, and can hardly have been produced by protons of the observed distribution in $H\rho$. It does not seem likely that protons are important in the energetic part of the cosmic radiation.

Little evidence exists for the validity of the theoretical formulae for pair production by gamma-rays of very high energy. The theoretical formulae hold quite well up to energies of 10^7 volts, but beyond that there are no definite tests of the formulae. Gilbert[12] has, however, measured the absorption coefficient of the shower producing components of the cosmic rays. This absorption follows the Z^2 law; and the radiation is probably a gamma-radiation. The total absorption found by Gilbert is, however, only one-fourth of that to be expected from (5) for single pair production alone.

It is with this experimental evidence in mind that we wish to reexamine the question of the validity of the theoretical formulae. We shall see that when we restrict ourselves to those contributions to the formulae where the applicability of theory cannot be held in doubt, we obtain results to be regarded as theoretical lower limits for the probability of the processes in question—which in every case differ radically from the corresponding formulae of Section 1. For radia-

[11] P. Kunze, Zeits. f. Physik **83**, 1 (1933).

[12] C. W. Gilbert, Proc. Roy. Soc. **A144**, 559 (1934).

tive losses, for the probable total ionization, for pair production by gamma-rays, the modifications in the formulae appear to resolve satisfactorily the discrepancies with experiments. This is probably not true in the case of primary ionization, for which the modified formulae still call for a detectable increase in the range of cosmic-ray energies.

3. The Limitations of Classical Electron Theory

The origin of the critique of the theoretical formulae lies in classical electron theory. The domain of applicability of this theory is limited to problems in which an unambiguous separation of the field of the electron itself and the external field acting on it is possible: in which, that is, the effect of the proper field is with good approximation given by the inertia of the electron, and in which the radiative reaction of the electron may be treated as a small correction. Thus we may consider the expansion given by Lorentz[13] for the proper force of an electron, taken momentarily at rest, and considered as a distribution of charge, spherically symmetric, and limited to a region of order of magnitude $\rho=e^2/mc^2$:

$$F=m\ddot{x}+2e^2\dddot{x}/3c^3+O(e^2\rho\ddddot{x}/c^4). \qquad (6)$$

The condition that the terms in this series decrease rapidly is then that

$$\dddot{x}\rho/\ddot{x}c\ll 1; \quad \ddddot{x}\rho/\dddot{x}c\ll 1, \cdots$$

etc. The frequencies of the motion of the electron must therefore be small compared to $\bar{\nu}=mc^3/e^2$. When the external forces are in this sense slowly varying, classical electron theory can be unambiguously applied.

This condition: that the radiative reaction be small compared to the inertial reaction—and thus the external ponderomotive force—does not depend on the choice of reference system; in fact the usual method of computing the radiative forces in a system in which the electron is not at rest is to transform $2e^2/3c^3\dddot{x}$ by a Lorentz transformation, under which all terms of (6) transform similarly. But only in a coordinate system in which the electron is substantially at rest $(1-\beta^2\sim 1)$ can the criterion for the applicability of electron theory be put simply as the condition that the fields acting on the electron shall not vary much in a time $\bar{\tau}=1/\bar{\nu}$.

Since the formalism of the Dirac electron theory and the quantum theory of the field may be regarded as a natural quantum theoretic generalization of the dualistic classical electron theory, one may expect that this formalism too will fail in the same region as its classical counterpart. The fact that a relativistic quantum theory is possible at all depends then essentially upon the smallness of α, which gives the relative magnitude of successive terms in (6) for the frequencies $\sim mc^2/h$ characteristic of relativistic electron theory. Since, in the problem of the energy losses and radiation of very high energy electrons, energies corresponding to frequencies $\geq\bar{\nu}$ necessarily occur, the question of the validity of the theoretical formulae requires investigation.

4. Application to the Classical Theory of Energy Loss[14]

One may treat the ionization and energy loss of a fast electron by computing the probability of transition induced in the atomic systems by the field, calculated classically, of the (undeflected) primary; for all impacts in which the momentum transfer is small compared to the primary momentum this treatment is fully justified; and it is the probability of these impacts which can be observed by studying the primary and 'probable' ionization of the electron tracks. The components of the primary field responsible for this ionization are low frequency components, for which $\nu\ll\bar{\nu}$; the secondary electron, in these impacts, never attains velocities very close to that of light, and if only these low frequency components acted on the electron, there could be no question

[13] H. A. Lorentz, *Theory of Electrons*, p. 252.

[14] The question of the energy losses of very energetic electrons has been much considered by Swann, who has also emphasized that with increasing ϵ the radiative forces may increase enormously. The present treatment differs from Swann's in two essential points: (a) Swann concludes that when the radiation computed classically would be equal to the energy transferred, no transfer at all will occur, whereas we argue that the magnitude of the radiation reaction merely makes classical electron theory inapplicable. (b) Swann assumes that for large ϵ the radiative reactions are large for all impacts, whereas we find this true only for impacts with parameter $p<\bar{p}=\rho\epsilon$. This is why we find a finite constant lower limit for the energy loss, instead of concluding, as does Swann, that it should vanish as $\epsilon\to\infty$. We do not believe that the *vanishing* of the energy loss can be justified by any electrodynamics.

of the validity of the theoretical formulae. It is substantially this argument which has so often led to the conclusion that the formulae should hold.[15] The cogency of this argument can, however, be questioned. The argument may be formulated in this way: *Assume* the validity of theory to describe the reaction of the electron to all components, high as well as low, to the field, then we can show that the high frequency components contribute nothing to the probability of the processes—small energy transfers—in which we are interested. Then for the low frequency components alone there is no question of the validity of theory. But to establish this it is necessary to assume the validity of the theory also for the high frequency components, and this assumption cannot be justified. The condition for the rapid convergence of (6) is a condition on the total motion of the electron, and thus on the whole external field acting on it, and we must be prepared to find that the ponderomotive force acting on the electron cannot, when rapidly varying fields are involved, be taken simply as the sum of the forces exerted by the separate Fourier components. It is in this point that we differ from v. Weizsaecker and from Williams; and it is only by insisting on this that we can understand at all why the theoretical formulae can fail.

We are here making a distinction, which in the domain of classical electron theory does not need to be made, between the external field strengths computed by classical theory, and the ponderomotive force, which is of the same general character as that developed by Born[16] in his modified unitary electrodynamics. Such a distinction is possible only in a theory in which the field equations are not linear, since for a linear theory it would follow from the conservation laws that the ponderomotive force of the sum of two fields is the sum of the ponderomotive forces of the separate fields. The existence of such nonlinearities seems, however, inevitable in any theory which would account for the specific stability of the electron; and it may be remarked that the theory of the positron, even in its present incomplete form, involves such nonlinearities for the field equations.

In the following discussion we shall then suppose—in distinction to v. Weizsaecker and Williams—that whenever high frequency components are present in the external field with an amplitude comparable to that of the low frequency components, the application of electron theory becomes dubious. To the question of the application of Born's electrodynamics to these problems we shall return in Section 7.

The normal component of the electric intensity in the field of the primary which is responsible for the greater part of the ionization, is given by the Fourier resolution:

$$\mathcal{E}^{\perp}=\int e^{i\nu t}\mathcal{E}_{\nu}^{\perp}d\nu, \quad \text{with}$$

$$\mathcal{E}_{\nu}^{\perp}=\frac{\pi i e\nu}{2\epsilon v^2}H_1^{(1)}(\nu p i/\epsilon v)\cdot e^{-i\nu z/v}. \quad (7)$$

Here p, the impact parameter, is the distance from the track, z is measured along the track and $=0$ for $t=0$, and again $\epsilon=(1-\beta^2)^{-\frac{1}{2}}$, and v is the primary velocity. The components of frequency $\nu\geq\bar{\nu}$ are large near the track, and begin to fall off rapidly as $p>\bar{p}=\epsilon v/\nu\sim\epsilon\rho$. $\mathcal{E}^{\perp}{}_{\text{maximum}}$ at $\bar{p}$ is $m^2c^5/e^3\epsilon v$, and thus for $\epsilon\gg 1$, the field is always weak. We may, however, expect that for impacts in which the field within $\bar{p}$ is of importance the theoretical calculations can give totally wrong results. In a purely classical calculation of the energy loss, the *omission* of such impacts has the effect of introducing a lower limit $\bar{p}$ for the impact parameter, and thus gives an energy loss which does not increase with ϵ; instead of the classical formula of Bohr: energy losses $<mc^2$

$$\sim(4\pi e^4/mv^2)\ln(\epsilon mv^3/e^2\omega), \quad (8)$$

(ω the resonance frequency of the atomic electrons), we obtain

$$\sim(4\pi e^4/mv^2)\ln(mv^3/e^2\omega). \quad (9)$$

The increase in energy loss which comes from the equatorial flattening of the field, and the consequent increase in the upper limit of the impact parameter ($p_{\max.}\sim v\epsilon/\omega$), is compensated by the decrease in close impacts. The impacts which are excluded by taking $\bar{p}$ as a lower limit for the impact parameter involve relatively large energy transfers; but for $\epsilon\sim 100$ transfers of

[15] Reference 6; J. F. Carlson and J. R. Oppenheimer, Phys. Rev. **41**, 763 (1932).

[16] M. Born, Proc. Roy. Soc. **A143**, 410 (1934); M. Born and L. Infeld, Proc. Roy. Soc. **A144**, 425 (1934).

energy of the order of 20 volts are being excluded. We might therefore suppose that for primary energies $>5\times10^7$ volts, the observed ionization will no longer increase with energy. To the difficulties in extending these considerations to a quantum theoretic calculation of ionization we shall return later. In the problem of radiative losses these complications do not arise.

5. Application to Radiative Losses

In the treatment of radiative losses one considers the probability of radiation of an electron (or positron) when it is accelerated in the screened field of a nucleus—a field given (very roughly) by the potential

$$V=Ze\{1/r-1/r_0\} \quad \text{for} \quad r<r_0$$
$$=0 \quad \text{for} \quad r>r_0$$

with $\quad r_0=\hbar^2/me^2Z^{\frac{1}{3}}$.

The frequencies of the radiated energy are of the order $\epsilon mc^2/h$; the velocity of the electron is large, and here again it is not at once clear whether classical electron theory should be applicable. To simplify the consideration of this question, v. Weizsaecker has considered the problem in another coordinate system: that in which the impinging electron is at rest. This electron is now accelerated by the field of the passing nucleus, and will radiate. One needs, however, in this coordinate system to consider frequencies for the emitted radiation which are of the order of mc^2/h; and in this system, for such radiative processes, the electron never attains an energy very large compared to mc^2. The situation is thus quite analogous to that in the problem of ionization: the components of the field of the passing nucleus which one needs to consider are $\ll\bar{\nu}$, and this in a coordinate system where the electron does not attain a velocity very close to c. Here again, in the classical treatment of the problem, there are impacts for which the field acting on the electron varies rapidly in a time $\bar{\tau}=1/\bar{\nu}$, and for which therefore we must call in question the validity of the electron theoretic treatment.

v. Weizsaecker has in fact shown that one may give a semi-classical treatment of the problem, for $\epsilon\to\infty$, which leads to (2) and (3). In this treatment one introduces again an impact parameter p, considers the radiation for an electron initially at p, and integrates over p. This treatment can be justified for such values of p that the field of the nucleus is there varying little over a wave packet which is large enough to permit a fair definition of the momentum change of the electron during this impact; such wave packets are large compared to $\hbar/mc$; and one thus concludes that for values of $p\gg\hbar/mc$ the method may be used. For $p<\hbar/mc$ the field varies rapidly; and v. Weizsaecker shows that for such impacts we may expect little radiation. Thus $\hbar/mc$ is roughly the lower limit of the impact parameter. For an unscreened nucleus the percentage error introduced by the necessary vagueness of $p_{\min.}$ vanishes with $\epsilon\to\infty$; for a screened nucleus it does not, but remains of the order $\hbar/mcr_0$. This is because, for an unscreened nucleus, the outer limit of the impact parameter, determined by the condition that the impact time be not too long compared to $\hbar/mc^2$, increases with ϵ; whereas for the screened nucleus it remains $=r_0$.

For $\epsilon\gg1$, $p>\hbar/mc$, the field of the nucleus can now be represented with good approximation as the superposition of plane electromagnetic waves traveling parallel to the nucleus; the amplitude of these waves is given, from (7), by

$$\mathcal{E}_\nu\sim(\pi ivZe/2\epsilon c^2)H_1^{(1)}(ivp/\epsilon c).$$

The radiative losses can thus be regarded as arising from the scattering of these waves; and for the treatment of this v. Weizsaecker uses the formula of Klein-Nishina—the result is

$$\sigma\sim4\alpha Z^2\rho^2[\ln p_{\max.}-\ln p_{\min.}]$$
$$\sim4\alpha Z^2\rho^2\ln\epsilon \qquad \text{for no screening} \quad (3a)$$
$$\sim4\alpha Z^2\rho^2\ln(1/\alpha Z^{\frac{1}{3}}) \qquad \text{screening.} \quad (4a)$$

The justification for regarding these formulae as valid for large ϵ v. Weizsaecker finds in the circumstance that only components of the nuclear field and the radiation field for which $\nu\ll\bar{\nu}$ play a part in these results.

We have, however, to remember that for impacts for which $p<\bar{p}=\epsilon\rho$, the impact time is short compared to $\bar{\tau}$, and frequencies $>\bar{\nu}$ appear in the field acting on the electron. They do not contribute *directly* to the probability of radiative losses, but their presence makes the application

of electron theory and the use of the superposition principle for the force on the electron questionable. If we omit altogether the contribution of these impacts, we have again to introduce a new lower limit for p, $\bar{p}=\epsilon\rho$. For $\epsilon>137$, $\bar{p}>\hbar/mc$, and we find smaller radiative losses than those given by (3a) and (4a):

$$\sigma\sim 4\alpha Z^2\rho^2 \ln(1/\alpha) \quad \text{no screening,} \tag{3b}$$

$$\left.\begin{aligned}&\sim 4\alpha Z^2\rho^2 \ln(1/\alpha^2 Z^{\frac{1}{3}}\epsilon)\\ &\sim 0 \quad \text{for} \quad \epsilon>\sim\alpha^{-2}Z^{-\frac{1}{3}}\end{aligned}\right\}\text{screening.} \tag{4b}$$

6. Discussion: Application to Primary Ionization

Formula (9) for the ionization energy losses, and (4b) for radiative losses (and presumably γ-ray pair production), have been derived by neglecting all contributions from those impacts to which classical electron theory may not certainly be applied; they thus give us lower limits for the effects to be expected in fact, since it is possible (and for some problems certain) that *some* contribution will come from these 'fast' impacts which cannot at present be rigorously treated.

These lower limits (4b) and (9) differ significantly from (4a), (8), the theoretical formulae obtained by applying present theory to all impacts. For in (9) there is no increase with ϵ of the low energy ionization energy losses. According to (4b), moreover, the probability of radiative losses (and pair production by γ-rays) begins to *decrease* for $\epsilon>137$, and vanishes altogether for $\epsilon\sim(137)^2Z^{-\frac{1}{3}}$, or 10^9–10^{10} v. In spite of the rough nature of these conclusions, and the tentativeness of the experimental results, we may thus say that the discrepancies between theory and experiment which appear to exist when we use the theoretical formulae of Section 1 disappear when we leave out of consideration those processes where the application of present theory is dubious.

In the classical calculation of energy transfer, we have seen that the limitation on the impact parameter $p>\bar{p}$ leaves out all impacts in which large energies are transferred to the secondary. The number and distribution of the secondaries with energies $E'\gg mc^2$, $E'\ll\epsilon mc^2$, has been studied by Anderson and Neddermeyer.[1] They find good agreement with the classical formula for the probability of production of such secondaries:

$$\sigma dE'=(\pi e^4/mc^2)(dE'/E'^2). \tag{10}$$

(In the range investigated the interchange terms by which the quantum theoretical formulae differ from (10) are negligible.) The number of secondaries is small, and the observed energy has to be corrected for energy loss; nevertheless, these experiments give no evidence of a discrepancy here between theory and experiment, and show that high energy secondaries are produced, and with frequency that can hardly be less than that predicted by a factor of two. These secondaries are produced in impacts to which we should not expect electron theory to apply; and the approximate validity of (10) cannot be justified from our point of view. What the experiments themselves seem to show is that the theoretical predictions for the number of high energy secondaries are not more seriously in error than those for low energy secondaries.

The classical treatment of small energy losses cannot be justified quantum theoretically. For one cannot make wave packets which at the same time define precisely enough the momentum of the electron ($\Delta P<\alpha mc$) and over which the field varies relatively little, except for values of the impact parameter $p>\hbar/mc\alpha$; and impacts for smaller p contribute essentially to this energy loss. One can, however, formally obtain the correct quantum theoretic answer for the energy by introducing as a lower limit for p not ρ but $\hbar/mc$.[17] If we do this but introduce $\bar{p}$ as a further lower limit, we find that the low energy losses ($E'<mc^2$) increase with ϵ till $\epsilon\sim137$, and then remain constant.

When $\epsilon\gg\alpha^{-2}$, $\bar{p}\gg\hbar/mc\alpha$, classical calculations can be made for all impacts for which $p>\bar{p}$, since in this region the problem of energy transfers can be treated as a pure dispersion problem. If now we again take $\bar{p}$ as a lower limit for the impact parameter, we find that the primary ionization approaches, for $\epsilon\to\infty$, a finite limit, and in place of (1) obtain:

$$\sim\ln(\alpha^{-3}) \quad \text{for} \quad \epsilon\gg\alpha^{-2}. \tag{11}$$

This gives a primary ionization about 70 percent greater than the minimum value of (1). The corresponding result, for $\epsilon\to\infty$, for the total energy loss $<mc^2$, is given essentially by (9).

[17] F. Bloch, Ann. d. Physik **16**, 285 (1933).

This limiting value is roughly equal to the minimum value of the classical expression for this energy loss, and is about 25 percent greater than the minimum of the corresponding quantum theoretic value. These results are again to be regarded as lower limits, for $\epsilon \to \infty$, since in their derivation impacts with $p < \bar{p}$ have been omitted altogether.

To find the course of this increase of ionization with ϵ, we should have to treat wave packets so large that in a part the field was rapidly varying, and in the rest slowly varying. A simple but hardly adequate way to do this is to set the field of the primary zero within $\bar{p}$; this procedure in the classical calculation leads of course to (9). If we do this we find that for $\epsilon \ll \alpha^{-2}$, formula (1) should hold.

These conclusions help somewhat to mitigate, but do not resolve, the discrepancies between theory and the cloud chamber observations of ionization. In spite of the qualitative character of (11), we think it certain, both that electrons of arbitrarily high energy will give a primary ionization measurably greater than the minimum value, and that for large ϵ the increase predicted by (1) cannot be regarded as theoretically established.

7. Relation to Classical Unitary Electron Theories

In Section 3 we have formulated a condition for the validity of electron theory: that the successive terms in the Lorentz expansion (6) should diminish rapidly, that in particular, the radiative reaction should be small compared to the inertial reaction. The ground for the necessity of this limitation is that the stability of the electron itself is not to be understood on the basis of Maxwellian electrodynamics: non-Maxwellian forces must be assumed to account for the stability; of their nature, apart from this, we know nothing; and it is therefore not possible to take the reaction of the electron to these forces into account in detail; we have to confine ourselves to those problems in which the effect of these forces is given essentially by the inertial reaction of the electron which must then for stability be equal to the external ponderomotive force. In any classical theory which accounts for the electron's stability, the limitations we have discussed could be removed.

Recently Born has proposed a modification of Maxwellian electrodynamics in which the electron itself appears as a possible (if not unique) singular solution of the field equations of finite energy $= mc^2$. When the electron is subjected to an external field, its motion can be deduced from the conservation laws for energy and momentum, which are to hold in spite of the fact that the field equations, from which they may in general be deduced, fail to hold along some world line—the electron's path. One has thus a consistent classical theory which gives a specific answer even where the earlier electron theory could not be applied. What does this theory give for the problems of ionization and radiative loss we are here considering?

When the fields acting on the electron are weak, $|F| \ll \bar{F} = m^2c^4/e^3$, and when they vary slowly (for the electron nearly at rest $\nu \ll \bar{\nu}$) then this motion agrees with that given by electron theory. When the electron (nearly at rest) is acted on by a disturbance whose frequency grows large compared to $\bar{\nu}$, then, as Born has shown, the reaction of the electron is in general much smaller than that computed from the Lorentz Force. And when the external fields are of the order $\bar{F}$, the treatment of these fields as small perturbations breaks down, and we may again expect deviations from electron theoretic formulas.

It is with the latter condition that we are concerned, since, as we have seen, the frequencies in the field which are directly involved in energy loss and radiation are low, and deviations from classical electron theory are to be expected only if the superposition principle for the ponderomotive force breaks down. The external fields become comparable to the proper field $\bar{F} = m^2c^4/e^3$ for impact parameter $p \sim \rho\epsilon^{\frac{1}{2}}$, for impact energy losses, and for $p \sim \rho(Z\epsilon)^{\frac{1}{2}}$ for radiative losses. The theory of Born thus does not give as strong a limitation on the validity of classical theory as we have used: $\bar{p} \sim \rho\epsilon$.

This situation is, however, not intrinsic to a classical unitary electron theory, and depends upon the fact that the Lagrangian of Born's theory involves the field strengths, but not their

derivatives. Consider for instance the Lagrangian $L=\frac{1}{2}\psi(1+\rho^2\varphi/\psi)^{-1}$ with $\psi=\frac{1}{2}F^{\mu\nu}F_{\mu\nu}$, and

$$\varphi=\tfrac{1}{2}(\partial F^{\mu\nu}/\partial x^{\alpha})g^{\alpha\beta}(\partial F_{\mu\nu}/\partial x^{\beta}).$$

The field equations of this Lagrangian are of the 3rd order—and nonlinear. They have a static spherically symmetric singular solution, of finite energy, which reduces for $r\gg\rho$ to a Coulomb field. For this Lagrangian the superposition principle breaks down for

$$p\sim\rho\epsilon^{\frac{1}{2}};\quad p\sim\rho Z^{\frac{1}{2}}\epsilon^{\frac{1}{2}},$$

for impact and radiative losses respectively. More generally, if L involves derivatives of the fields of order n, and gives an electron of finite energy as a singular solution, then the superposition principle breaks down for

$$p_{\text{imp.}}\sim\rho\epsilon^{(n+1)/(n+2)},\quad p_{\text{rad.}}\sim\rho Z^{1/n+2}\epsilon^{(n+1)/(n+2)}.$$

The $\bar{p}=\rho\epsilon$ which we have used as a limit for classical theory in this paper is thus given by a unitary field theory whose field equations are integral equations, for which $n\to\infty$.

We adduce these considerations, not because we believe that the solution to the problem of electronic stability lies in a theory of this type, but because they show that there is, even in classical theory, no inconsistency in the criteria we have used for the validity of electron theory. The discrepancies between theoretical prediction and the experiments can thus be understood on a purely classical basis.

JANUARY 1, 1935 PHYSICAL REVIEW VOLUME 47

The Disintegration of the Nuclei of Light Atoms by Neutrons

II. Neon, Fluorine and Carbon

WILLIAM D. HARKINS, DAVID M. GANS AND HENRY W. NEWSON, *Department of Chemistry, University of Chicago*

(Received November 8, 1934)

Neon and fluorine. Quantitative information is presented on the disintegration, by capture of a neutron, of 11 nuclei of neon and 13 of fluorine. The reactions are considered to be:

$$^{20}_{10}\text{Ne}_0+^{1}_{0}n_1\rightarrow{}^{17}_{8}\text{O}_1+{}^{4}_{2}\text{He}_0$$
$$^{19}_{9}\text{F}_1+^{1}_{0}n_1\rightarrow{}^{16}_{7}\text{N}_2+{}^{4}_{2}\text{He}_0$$

in which nitrogen 16 is a new isotope of nitrogen. As in the earlier work on nitrogen, it is found that: (1) Neutrons effective in disintegration appear both to come directly from the source and to be scattered by nuclear impact prior to the disintegration. (2) Kinetic energy disappears in the process, or is (rarely) conserved. This kinetic energy decrement may be transformed into mass, if mass increases in the reaction, or into γ-rays; it may also excite the heavier product nucleus and later give rise to an artificial radioactivity. (3) The maximum, minimum and average kinetic energy for the neutrons which in our experiments have been found to disintegrate fluorine, neon and nitrogen are listed below in the table.

Carbon. Mass values obtained in positive ray work give 6.9 m.e.v. as the mass increase in the reaction:

$$^{12}_{6}\text{C}_0+^{1}_{0}n_1\rightarrow{}^{9}_{4}\text{Be}_1+{}^{4}_{2}\text{He}_0.$$

If the mass values are extremely accurate only neutrons with kinetic energy greater than about 6.9 m.e.v. can therefore disintegrate carbon. Of 6 disintegrations found among 6400 pairs of photographs with ethylene, only 1 involves a neutron which approximates this energy. The other disintegrations may be those of oxygen or nitrogen from the water vapor and trace of air in the chamber. Carbon has therefore not yet been disintegrated with certainty by neutrons. It is of interest that about 20 percent of the neutrons found in this work have extremely high velocities, so that their kinetic energy is from 13.6 to 15.1 m.e.v., and that the energy transformed into γ-rays rises as high as 10 m.e.v.

	No. of disintegrations	Kinetic Energy in m.e.v. Min.	Ave.	Max.
Nitrogen	(28)	1.9	5.4	16.1
Fluorine	(13)	1.9	6.7	13.2
Neon	(11)	3.1	10.6	15.1

I. INTRODUCTION

THE first paper[1] of this series on the disintegration of light atoms by neutrons presented values related to the mechanics of the disintegration of twenty-eight nitrogen nuclei. Further experiments have since been carried out with deuterium, carbon, fluorine and neon. This paper gives the quantitative relations found for the disintegration of 11 neon and 13 fluorine nuclei.[2]

[1] Harkins, Gans and Newson, Phys. Rev. **44**, 529 (1933).

[2] For preliminary reports, see Harkins, Gans and Newson, Phys. Rev. **44**, 236, 945 (1933).

II. Experimental Details

Most of the photographs were obtained with the modified Wilson cloud chamber described in the first paper. Some of the work, however, was done with a chamber in which the closely fitted piston was sealed gas-tight to the cylinder with a sylphon bellows. For quantitative work, this arrangement appears to be superior to that in which the sylphon itself acts as the wall for the piston, for with a closely fitted piston the stroke required for a given expansion ratio is at a minimum, which lessens the highly undesirable surge in the gas during and after the expansion.

As in the earlier work, two views at an angle of about 73° are obtained for each disintegration, and are transformed by projection into a single photograph in the actual plane of the disintegration. In the photograph only two of the three tracks are visible.

III. Disintegration by Capture or by Non-Capture

The question as to whether the disintegration of N^{14} by neutrons occurs by capture or by non-capture, has been discussed in detail by Harkins and Gans[3] with the conclusion that while evidence for disintegration by capture is very good, there appears to be no evidence which supports disintegration without capture of the neutron.

In the present work, it is found that for about half of the events, the calculated path of the neutron passes through the source in a direction toward the nucleus which is hit. For the other half, the neutron is either scattered by a nuclear collision prior to the disintegrative capture, or is not captured. In the latter case, the details of the disintegration may be analyzed by the equations given by Harkins and Gans.[3] If, however, it is assumed, as is here done, that the reactions occur by capture, then the energies and velocities of the various particles may be calculated as outlined by Harkins, Gans and Newson.[1]

IV. The Disintegration of Neon Nuclei by Neutrons

About 4800 pairs of photographs with neon in the chamber have shown 11 pairs sufficiently good to give useful data concerning the disintegration. It is assumed that the reaction which takes place is

$$\begin{aligned} &{}^{20}_{10}\mathrm{Ne}_0 \qquad\qquad +{}^{1}_{0}n_1 \\ &(19.9967\pm0.0009)+(1.0067-E) \\ &\qquad \rightarrow {}^{17}_{8}\mathrm{O}_1 \\ &\qquad \rightarrow (17.0032\pm0.003-E') \\ &\qquad\qquad +{}^{4}_{2}\mathrm{He}_0 \\ &\qquad\qquad +(4.00216\pm0.0004). \end{aligned} \tag{1}$$

Here E represents the energy (in mass units) converted into a γ-ray in the formation of a neutron from boron, and E' is the similar value for O^{17} formed from N^{14} by capture of an α-particle. If E and E' are both zero, then 0.002 unit of mass or 1.9 m.e.v. (million electron-volts) would be required for this reaction. The actual amount to be supplied is probably greater than 2 m.e.v. since E is probably larger than E'. This calculation is subject to modification by the amount of the unknown error in the mass of the neutron.

The data related to the disintegrations of neon are collected in Table I. The lowest velocity for a neutron which disintegrated a nitrogen nucleus is 1.9×10^9 cm/sec., while for neon the corresponding velocity is 2.4×10^9. The minimum kinetic energy of the neutron is thus 1.9 m.e.v. for nitrogen and 3.1 m.e.v. for neon. For nitrogen, the maximum kinetic energy of the neutron is 16.1 m.e.v., while for neon it is 15.1 m.e.v. The average kinetic energy of the 28 neutrons which disintegrated nitrogen nuclei is 5.4 m.e.v., while that for 11 neon nuclei is 10.6 m.e.v.

As in all earlier work, the kinetic energy of the particles is found to be less after the disintegration, by an amount in the case of neon which varies from $(0.8-0.93\times10^3E')$ to $(11.0-0.93\times10^3E')$ m.e.v.

It is assumed that of the kinetic energy thus lost, the amount in excess of $(1.9-0.93\times10^3E')$ m.e.v. (which difference is the mass increment in the reaction, a value subject to the errors in the mass values) is converted into a γ-ray, or may appear as the energy of an artificial radioactivity. In the disintegration in which the minimum kinetic energy, 0.82 m.e.v., is lost, no γ-ray may be emitted, and the discrepancy between the 0.82 m.e.v. lost and the 1.9 m.e.v.

[3] Harkins and Gans, Phys. Rev. **46**, 397 (1934).

TABLE I.

Quality of photographs: A, Excellent; B, Good; C, Fair
Type of disintegration: D, Neutron direct from source;
S, Neutron scattered by nuclear collision prior to disintegrative impact
X = Heavy product nucleus, O^{17} for Ne; N^{16} for F.

No.	R_{He} (Mm, Dry air at 15°C, 1 Atm.)	R_X	ϕ	θ	v_{He} (cm/sec. $\times 10^{-9}$)	v_X	v_n	KE·He (ergs $\times 10^6$)	$KE \cdot X$	$KE \cdot n$	$-\Delta KE$	KE·He (electron-volts $\times 10^{-6}$)	$KE \cdot X$	$KE \cdot n$	$-\Delta KE$
							Neon								
101 AS	4.3	1.6	106.4	31.6	0.480	0.207	2.44	0.76	0.60	4.96	3.60	0.48	0.38	3.12	2.26
102 AD	11.8	2.9	81.5	68.3	0.980	0.345	2.74	3.20	1.69	6.19	1.30	2.01	1.06	3.89	0.82
103 AD	8.8	2.7	97.6	39.7	0.915	0.335	3.87	2.77	1.59	12.43	7.91	1.74	1.00	7.81	4.97
104 AS	12.4	2.4	81.0	42.5	1.01	0.296	4.40	3.31	1.21	16.07	11.55	2.08	0.76	10.1	7.26
105 AD	15.0	4.1	132.3	23.7	1.12	0.485	4.50	4.15	3.29	16.87	9.42	2.61	2.07	10.6	5.92
106 BS	6.0	3.2	111.5	22.5	0.630	0.360	4.57	1.32	1.81	17.34	14.21	0.83	1.14	10.9	8.93
107 AD	21.5	4.8	159.3	10.7	1.30	0.585	4.90	5.60	4.90	19.89	9.39	3.52	3.08	12.5	5.90
108 BD	23.9	4.7	129.1	26.9	1.36	0.565	5.10	6.11	4.49	21.64	11.03	3.84	2.82	13.6	6.93
109 AD	13.2	3.7	103.9	32.6	1.04	0.440	5.27	3.56	2.72	23.07	16.80	2.24	1.71	14.5	10.6
110 AS	9.9	4.1	136.0	17.9	0.880	0.485	5.27	2.56	3.29	23.23	17.34	1.61	2.07	14.6	10.9
111 BS	28.9	3.9	75.0	60.5	1.44	0.463	5.36	6.95	2.99	24.03	14.08	4.37	1.88	15.1	8.85
							Fluorine								
201 CD	11.2	2.0	76.3	76.7	1.00	0.25	1.90	3.31	0.83	3.04	− 1.11	2.08	0.52	1.91	− 0.70
202 AD	6.0	2.1	105.7	38.3	0.69	0.27	2.59	1.56	0.94	5.55	3.05	0.98	0.59	3.49	1.91
203 CD	5.9	2.5	126.5	27.5	0.69	0.30	2.59	1.56	1.19	5.55	2.80	0.98	0.75	3.49	1.76
204 BS	6.0	2.0	86.5	43.5	0.69	0.25	2.90	1.56	0.83	6.81	4.42	0.98	0.52	4.28	2.78
205 BD	9.0	2.5	90.8	45.2	0.88	0.31	3.42	2.56	1.27	9.67	5.98	1.61	0.80	6.08	3.76
206 AS	23.8	2.2	57.3	82.7	1.34	0.28	3.44	5.88	1.06	9.80	2.87	3.69	0.66	6.16	1.80
207 AD	14.1	4.1	160.0	11.0	1.08	0.48	3.51	3.85	3.09	10.25	3.32	2.42	1.94	6.44	2.08
208 AS	20.8	2.8	76.1	62.9	1.27	0.35	3.72	5.33	1.59	11.49	4.57	3.35	1.00	7.22	2.87
209 AS	15.6	3.6	110.1	38.4	1.13	0.43	3.77	4.21	2.40	11.81	5.20	2.65	1.51	7.42	3.27
210 AD	20.5	3.1	81.1	56.9	1.26	0.37	4.01	5.24	1.82	13.32	6.27	3.29	1.14	8.37	3.94
211 AS	11.2	2.2	69.2	53.8	0.98	0.28	4.04	3.15	1.06	13.52	9.31	1.98	0.66	8.50	5.85
212 BD	10.6	3.9	124.1	25.9	0.97	0.46	4.42	3.10	2.80	16.09	10.18	1.95	1.76	10.11	6.40
213 BD	11.2	2.5	66.7	45.3	1.00	0.31	5.04	3.31	1.27	21.00	16.42	2.08	0.80	13.20	10.32

required as mass may be due to the experimental error in the measurement of the individual disintegration, to errors in the masses used in the calculation, or to both.

A plot of the data to detect definite nuclear levels, such as those indicated by the corresponding data for nitrogen, would here involve too few events to be of value. To prove or to disprove the existence of such levels requires more extensive and more accurate work.

V. The Disintegration of Fluorine Nuclei by Neutrons

Out of 1600 pairs of photographs taken to detect the effects of fast neutrons in carbon tetrafluoride and 3200 pairs in difluor-dichlor-methane, both diluted with helium, 13 pairs were suitable for measurement. Only eleven pairs, however, were of a quality comparable with those obtained in nitrogen, neon, etc.

The reaction for the disintegration of fluorine by capture is:

$$^{19}_{9}F_1 + ^{1}_{0}n_1 \rightarrow ^{20}_{9}F_2 \rightarrow ^{16}_{7}N_2 + ^{4}_{2}He_0.$$

This reaction is remarkable in that a new isotope of nitrogen of mass 16 and isotopic number 2 appears. In the preliminary announcement of the discovery of this new isotope, the writers[4] considered that it would be likely to be unstable and to emit an electron to form oxygen 16. This has been verified by Fermi[5] who finds nitrogen 16 to be radioactive, and to change to oxygen 16, as was predicted. In disintegration 201, the kinetic energy is found to increase by 0.7 m.e.v. While this case represents the only known instance of an increase of kinetic energy, such an increase is not impossible, and can be accounted for by a decrease in rest mass during the reaction, with conversion of this mass into kinetic energy and possibly in part also into a γ-ray. Since the mass of the N^{16} formed is unknown, this supposition cannot be tested. In any case, however, this particular pair of photographs was rather poor, and the experimental error probably exceeds the 0.7 m.e.v. involved.

The maximum value for the kinetic energy which disappears is 10.3 m.e.v. as shown in

[4] Harkins, Gans and Newson, Phys. Rev. **44**, 945 (1933).
[5] Fermi, Amaldi, D'Agostino, Rasetti and Segrè, Proc. Roy. Soc. **A146**, 483 (1934).

Table I. The average value for the kinetic energy of the neutron at impact is 6.7 m.e.v.

The number of disintegrations obtained under similar conditions is much larger for fluorine than for neon nuclei, and is of the same order as for nitrogen nuclei.

VI. The Disintegration of Carbon Nuclei by Neutrons

If carbon 12 is disintegrated by capture:

$$^{12}_{6}C_0 + ^{1}_{0}n_1 \rightarrow ^{9}_{4}Be_1 + ^{4}_{2}He_0$$

the increase of mass in the reaction is equivalent to 6.9 m.e.v. If this energy, in addition to any γ-ray energy liberated in the reaction, is supplied by the decrement in the kinetic energy accompanying the process, it would require a neutron of velocity greater than 3.6×10^9 cm/sec. Since the average velocity of the neutrons which disintegrated nitrogen nuclei is less than this value, it is to be expected that carbon nuclei will be disintegrated much less frequently than nitrogen nuclei by the same source of neutrons.

Of 6400 pairs of photographs taken with ethylene (C_2H_4) in the chamber, 6 pairs showed good photographs of disintegrations. Most if not all of these may, however, be due to the disintegration of oxygen nuclei in the water vapor used to form the cloud tracks in the chamber or of nitrogen nuclei from any residual air in the chamber. Only one disintegration represented a decrease of kinetic energy sufficient to supply the mass increment in the disintegrative-synthesis for carbon. In this disintegration, which was by a neutron directly from the source,

$R_{He} = 13.8$ mm	$KE\cdot He = 2.24$ m.e.v.
$R_{Be} = 3.8$ mm	$KE\cdot Be = 1.68$ m.e.v.
$\phi = 97.6°$	$K\epsilon\cdot n = 10.19$ m.e.v.
$\theta = 22.4°$	$-\Delta KE = 6.27$ m.e.v.
$v_{He} = 1.04\times10^9$ cm/sec.	
$v_{Be} = 0.60\times10^9$ cm/sec.	
$v_n = 4.42\times10^9$ cm/sec.	

Possibly this event is also due either to oxygen or nitrogen. It is not yet certain, therefore, that carbon 12 has been disintegrated by neutron impact.

The average energies in millions of electron-volts which have been thus far found to disintegrate light nuclei are:

Element	N	F	O*	Ne	C
No. of disintegrations	28	13	4	11	1
Energy of neutron (m.e.v.)	5.4	6.7	7.0	10.6	High

An important source of error in this work is the uncertainty in the energy-range relations of the heavier nucleus, as has been pointed out by us[5] and by Feather.[6] Fortunately the energy of this nucleus is usually less than that of the lighter one.

The writers wish to thank Martin Kamen for assistance in the experimental work, and to acknowledge the help of a grant from the Alexander Dallas Bache Fund of the National Academy of Sciences, and a grant-in-aid of the National Research Council, which made this work possible.

* From the work of Feather, Nature **130**, 237 (1932).
[6] N. Feather, Proc. Roy. Soc. **A142**, 702 (1933).

Collisions of the Second Kind Between Magnesium and Neon

J. H. MANLEY AND O. S. DUFFENDACK, *University of Michigan*

(Received August 29, 1934)

The relative intensities of a group of lines in the spectrum of Mg II as excited by a low voltage arc in a mixture of magnesium vapor and neon have been measured at various pressures of neon. Marked effects due to collisions of the second kind between magnesium atoms and neon ions and metastable atoms are found. The ratio of intensities at 2.0 and at 0.017 mm of neon was taken as a measure of the enhancement or the relative collision cross section for the excitation of the initial level. The results show a decrease of cross section with increase of energy-discrepancy, a finite cross section for exact resonance, and a definite dependence on the L value of the term excited by the collision. Approximate calculation places the cross section at about 10^{-11} cm^2 for collisions between neon ions and magnesium atoms.

I. INTRODUCTION

SINCE the initial experiments of Franck and Cario on energy transfer in collisions of the second kind, many types of experiments have revealed this phenomenon and yielded ideas of the efficiency of the process. The present study is that of a particular type of collision, one in which a normal atom is both ionized and excited by a metastable atom or an ion. Considerations of lifetime and concentration eliminate all but these two forms of atoms as active agents. The process may be represented by the reaction

$$E_i+F_i\rightarrow E_f+F_f+\sigma, \qquad (1)$$

where E_i is the initial energy of one atom, F_i that of another, the subscripts f refer to the final energies, and σ is thus defined as the energy-discrepancy between the initial and final states of the system. By analogy the effects have been called those of "resonance," and consequently σ measures the exactness of resonance.

The efficiency of energy transfer in these collisions will be measured by the yield of the reaction, that is, the number of excited atoms N—energy E_f—per cubic centimeter per second, and this number, considered as the result of a collision between two types of atoms of concentration N_1 and N_2 moving with a relative velocity v and having a certain action cross section q, is given by

$$N=qN_1N_2v. \qquad (2)$$

If the probability of transfer $P(r)$ at a distance of approach r is used instead of the concept of a cross section (2) becomes

$$N=2\pi N_1N_2v\int_0^\infty P(r)dr. \qquad (3)$$

The past investigations of the problem, both experimental and theoretical, have been concerned with the functional dependence of cross section on energy-discrepancy, and it has been found in all cases that the cross section decreases with increasing σ. There is, however, a distinct difference in point of view between the theoretical and the experimental work. The theoretical work has shown a variation of the cross section for the excitation of *one* state with energy-discrepancy, which is not possible of observation except in the utilization of the magnetic quantum levels where the energy can be varied by the magnetic field as in the experiment of Hanle.[1] In all other cases the consideration has been to measure the cross section for the excitation of *different* states as a function of their unperturbed energy-discrepancy from resonance. The measurements of Duffendack and Thomson[2] indicate a general agreement of the two views—a monotonic decrease of cross section with increase of energy-discrepancy—but some anomalies point to a dependence of cross section on the particular term excited. The present work was undertaken in order to determine not only the cross section for the excitation of levels of various energies but also to investigate other factors influencing the action cross section in these collisions of the second kind.

II. EXPERIMENTAL METHOD

By the use of the methods of spectrographic photometry[3] it is possible to measure the relative

[1] Hanle, Zeits. f. Physik **85**, 548 (1933).
[2] Duffendack and Thomson, Phys. Rev. **43**, 106 (1933).
[3] Duffendack and Thomson, J. O. S. A. **23**, 101 (1933).

intensities of lines excited under conditions favorable for collisions of the second kind or under purely electronic impacts. The relative intensities in these two cases may be taken as a measure of the population of the initial state for a particular line, and that, in turn, as an indication of the relative efficiency of population by collisions of the second kind and by electron impact. The ratio thus obtained is designated as the enhancement of the line or of the level from which the line originates. It is, of course, essential that other effects be excluded. In general one may write the measured enhancement

$$E=\frac{J_r^n}{J_e^n}=\frac{N_e^n+N_r^n+f_\alpha(N_e^\alpha+N_r^\alpha)}{N_e^n+f_\alpha N_e^\alpha} \quad n<\alpha<\infty. \quad (4)$$

J_r^n = intensity of a line, initial state n, under conditions for excitation by collisions of the second kind.

J_e^n = intensity of a line, initial state n, electronically excited.

N_e^n population of the state n by electron impact.

N_r^n = population of state n by collisions of the second kind.

f_α = fraction of state α populating state n by transitions from above (Kaskadensprünge).

It is evident that only if Kaskadensprünge are small and resonance effects large compared with electronic excitation is the measured enhancement that which the term usually denotes, namely, N_r^n/N_e^n. It is generally not possible to determine the f_α's because they are essentially transition probabilities for lines in the infrared, but since the number of transitions is proportional to the cube of the frequency, which is small, the effect is in most cases negligible. It is necessary, however, to check each result for the possibility of such population from above. Knowing the enhancement of a particular level under the proper conditions, the relative cross section follows immediately, for the enhancement is given by

$$E \backsimeq N_r^n/N_e^n=q_r^n N_1 N_2 v_r/q_e^n N_e' N_2' v_e', \quad (5)$$

N_1 = concentration of metastable atoms or of ions,
N_2 = concentration of normal atoms,
N_e = electron concentration.

The case chosen as most favorable for study was the excitation of the magnesium spark spectrum by positive ions of neon. As is evident from Fig. 1, there is a large number of levels within a small range of energy-discrepancy, and so there is the possibility of determining the efficiency of excitation of terms of nearly the same energy-discrepancy. Furthermore, experimentally, the simplicity of the magnesium spectrum outweighs the difficulties due to the action of the vapor on glass, condensation on the electrodes, and the like.

The tube used to secure a low voltage arc in magnesium vapor and neon is illustrated in Fig. 2. A small quartz crucible *A* wound with a heater coil of 12 mil tungsten wire provided an easily controlled source of magnesium vapor. A nickel cylinder *B* surrounds the crucible to cut down radiation and convection losses. Electrons for the arc were supplied by a pancake filament *F* of Isovolt alloy located near the mouth of the crucible. In order to prevent excessive diffusion of magnesium vapor a cap *C* with a projecting observation tube *T* covers the crucible mouth and the filament. This cap was used as the anode of the arc. The observation tube was found to be very effective in cutting down diffusion of vapor to the quartz window of the large Pyrex bulb in which the whole electrode assembly was mounted. This particular arrangement for obtaining the spectrum of elements of moderate boiling points possesses the advantage of good temperature control, constancy of excitation, and ease of degassing and purification—important factors in intensity work. The low temperature emitter obviates continuous background which may be very troublesome. The tube and electrodes were thoroughly outgassed and the neon purified by continual circulation through charcoal and glass bead traps immersed in liquid air.

Although enhancement measurements have usually been made with a spark or an arc spectrum as the "normal" or electron-excited spectrum, this is not feasible in the case of magnesium because of the difficulty of securing the spectrum free from objectionable background. The intensities of the various lines were therefore measured at different neon pressures, the low pressure data thus approaching electronic excitation of the magnesium vapor. The ratio of intensities at high and low neon pressures may then be taken as a measurement of the enhancement

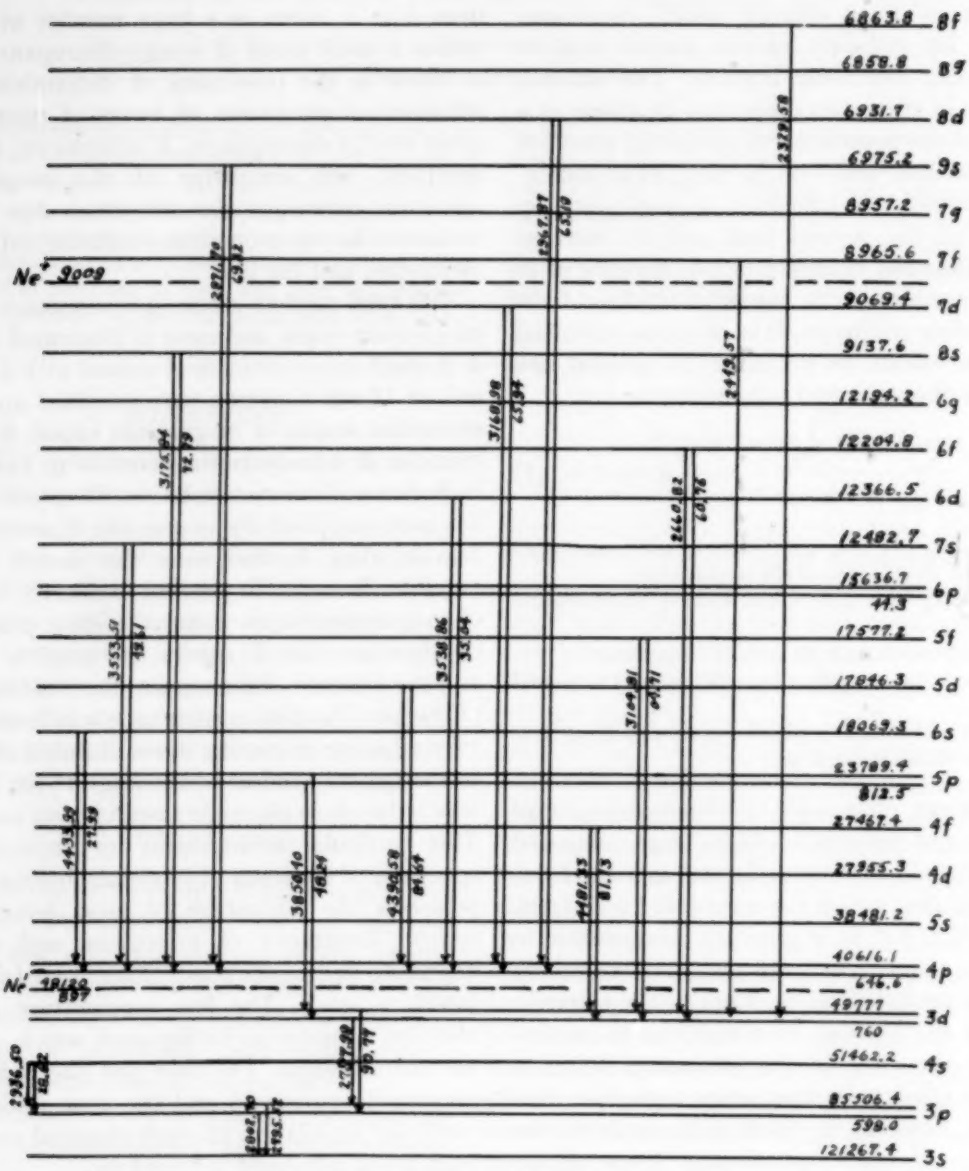

FIG. 1. Energy levels in magnesium.

due to neon ions. All intensity measurements were made relative to the intensity of the Mg I $4^3D \rightarrow 3^3P_2$, 3096 line. Such a choice of reference reduces the error from possible variation of direct electronic excitation of the Mg II terms. Although the final state of this line is the metastable $^3P_2$ and, therefore, is liable to a self-absorption varying with neon pressure as a result of the change of effectiveness of neon in creating or destroying $^3P_2$ atoms, it was found that the ratio of the 3093 ($^3D\,^3P_1$) line, from which the relatively strong 4571 line originates, to the 3096 line was the same at various neon pressures. It is quite probable that the neon plays no essential role in the distribution of atoms in the $^3P_0$, $^3P_1$, $^3P_2$ states because of their small separation in energy. Neon pressure may, however, affect the electronic excitation of the ^3D initial state, and in order to investigate this point, the ratios of the intensities of the Mg II lines to the 3096 line were measured as a function of arc voltage at constant pressure as equivalent in electronic

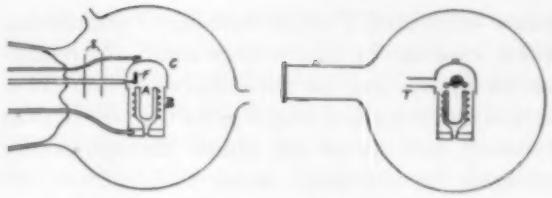

FIG. 2. Diagram of arc tube.

excitation to variable pressure at constant voltage.

Near constancy of the intensity of the desired lines relative to the 3096 line for voltages as large as 50 volts indicated that any change of electron velocities has negligible effect on the intensity of lines from spark levels. This also suggests that direct electronic excitation of these levels is very small. All subsequent measurements were made with an arc current of 40 m.a. at 25 volts.

The crucible temperature, about 500°C, was chosen to give sufficient magnesium vapor for visible excitation of the strong arc lines but kept low enough to prevent more than a negligible amount of ionization of magnesium atoms by electron impact. This latter condition is easily checked, for there is a critical magnesium pressure above which the arc voltage drops sharply due to the neutralization of space charge by the easily ionized magnesium atoms. At the same time the neon lines disappear and the complete arc spectrum of magnesium is excited. The crucible temperature was kept constant at all neon pressures by resistance measurement.

III. RESULTS

The results for the pressure dependence of the intensity of the Mg II lines are given in Fig. 3, in which the logarithm of the intensity relative to the 3096 arc line is plotted against the logarithm of the neon pressure. Because of the spread at 0.017 mm some of the points are not shown, but the curves are drawn toward these points. Compared to the reference line, the 3175–73, $8^2S \rightarrow 4^2P$, shows a rapid decrease of intensity with decrease of neon pressure below 0.8 mm; the 3104, $5^2F \rightarrow 3^2D$, a less rapid decrease; and the 2802–2795, $3^2P \rightarrow 3^2S$, scarcely any change. The conclusion follows that the excitation of the low terms is chiefly electronic whereas the terms near the energy of the neon ion owe

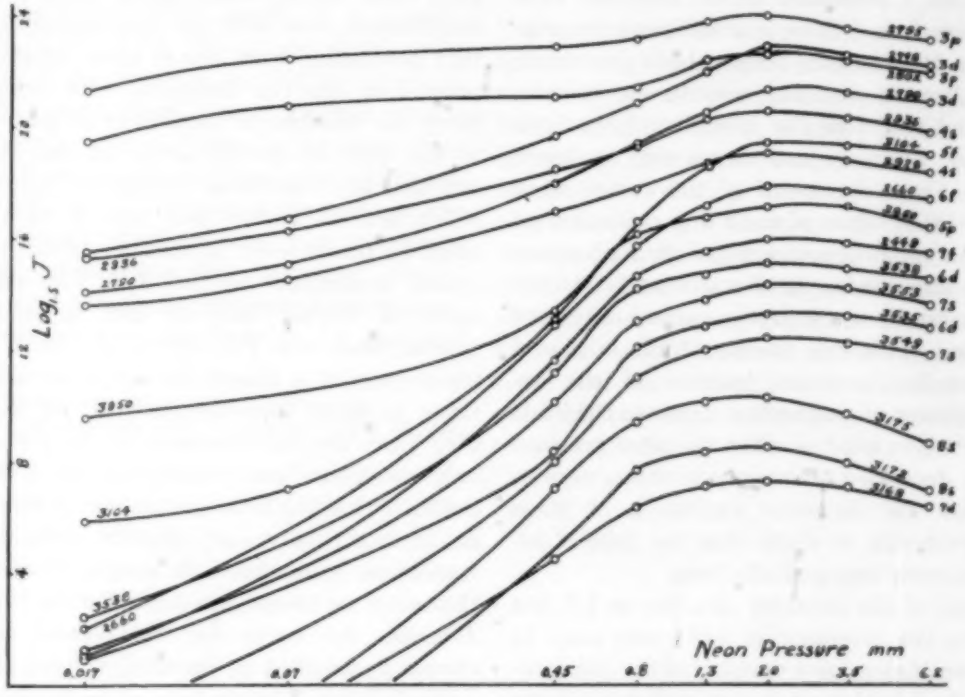

FIG. 3. Pressure dependence of intensities of Mg II lines.

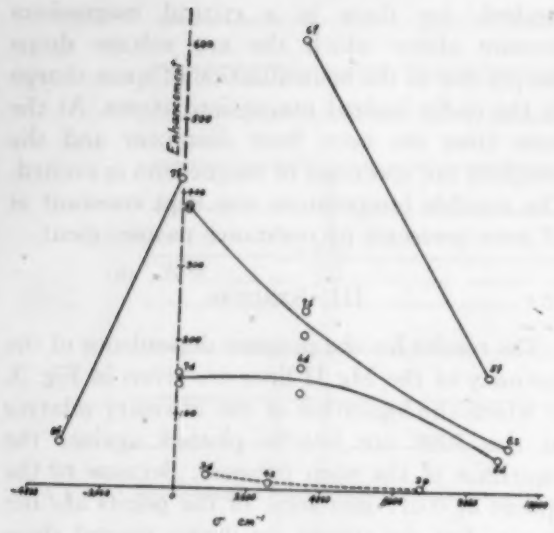

FIG. 4. Enhancement of lines for various energy-discrepancies (σ).

their excitation chiefly to collisions of the second kind. Since the arc is operated at constant current and a region of practically neutral space charge is photographed, the positive ion concentration should be independent of pressure and thus also the intensity of those lines excited by positive ions. Calculation shows, however, that at the current used there is insufficient gas concentration at pressures below about one millimeter to keep a constant positive ion concentration, and therefore the intensity of the lines excited by positive ions drops off at lower pressures. From the trend of the curves at a pressure of 0.017 mm of neon it is evident that positive ion excitation of some of the high terms is still considerable for the characteristic constant value attributed to electronic excitation is not yet reached. This low pressure limit is placed experimentally, however, because of the excessive diffusion of magnesium vapor to the leads and observation window when the neon pressure is further decreased. Not only is this a serious factor, but the electronic excitation of these levels is evidently so slight that the time of exposure becomes impractically long.

The ratio of the intensity of a line at 2.0 mm of neon to the intensity at 0.017 mm may be taken, nevertheless, as a measure of the enhancement of the initial level due to collisions of the second kind, and, if other methods of population of this level can be shown to be small, the results can be interpreted as the relative action cross section for excitation. Fig. 4 gives the points thus obtained, and curves are drawn through points belonging to the same series to illustrate the regularity. The 3^2D, 4^2S and 3^2P levels are placed with an energy-discrepancy (σ) measured from the neon level on the supposition that they are too far distant from the ion energy for enhancement, but that excitation by collisions of the second kind with neon metastable atoms is responsible for the enhancement.

IV. Discussion

As pointed out above, for enhancement measurements to have a definite meaning, it is necessary that electronic excitation be small compared to resonance excitation and population from above be negligible. The form of the intensity-pressure curves indicates that electronic excitation of high series members is practically negligible, so Kaskadensprünge remain as the only possible cause of ambiguity.

The small enhancement of the 3^2D level, even though it is a terminal state for several strong lines from higher levels which show large enhancements, can only be interpreted to mean that population from above is far smaller than population due to collisions with neon ions. Since the number of transitions is proportional to the cube of the frequency of the radiation emitted, any transitions among the higher terms which are all within one volt of each other, must be much fewer in number than the mentioned transitions to the 3^2D. The empirical result of Bleeker[4] may be used to calculate a typical case, the $7^2D \rightarrow 6^2F$ and the $7^2D \rightarrow 5^2F$ transitions. It is found that there should be six times as many transitions to the 5^2F as to the 6^2F. That the enhancement of the 5^2F level is only about one-fourth that of the 6^2F is therefore evidence that the total population of these levels is, at most, only very slightly influenced by transitions from above. It should be mentioned that since no transitions are observed from high P-terms, the curve for the s-series certainly cannot be falsified by population from above.

[4] Bleeker, Zeits. f. physik. Chemie **120**, 63 (1926).

The enhancement curves certainly indicate a finite cross section at $\sigma=0$ in accord with the work of Hanle[1] and the theory of Stueckelberg.[5] The finite cross section and the asymmetry of the curves negate the resonance interpretation of the older theory of Kallman and London[6] which gives an infinite cross section at $\sigma=0$ and a symmetry cut-off for negative values of σ by the temperature of the gas.

The variation of the enhancement with the nature of the term is a result to be expected theoretically but not heretofore observed experimentally. Since the cross section depends on the square of the matrix element of the interaction potential V, $|\int\psi_i V\psi_f d\tau|^2$, one might inquire why any regularity exists, since presumably both V and ψ_f will be characteristic of the state excited. The regularity is, therefore, necessarily interpreted as a similarity of interaction potentials and wave functions for states with the same L-value, and the difference between series as due to a variation of either or both of these quantities with azimuthal quantum number. The present status of the theory, particularly the lack of knowledge of the wave functions of these states and of the interaction fields, prevents more detailed conclusions.

From the experimental results it is possible to obtain, by use of Eq. (5), an idea of the order of magnitude of the cross section in these collisions. At a pressure of 2.0 mm we may assume that the positive ion and electron concentrations are equal in the region photographed and therefore the ratio N_1/N_e' becomes the ratio of the electron concentration at the two pressures. Since the current was kept constant $N_1/N_e' = N_e/N_e' = v_e'/v_e$ and this ratio may be calculated from the mobility of electrons at 2.0 mm and from the field acceleration at 0.017 mm for in the latter case the mean free path is several times the length of the arc space. This ratio is approximately 1 : 20. Due to the constant magnesium pressure, $N_2/N_2'=1$. For neon ions we may take a velocity slightly above that corresponding to the gas temperature, say 10^5 cm/sec., and in the low pressure case the electron velocity may be computed from the field and was about 2×10^8 cm/sec. Strictly, these velocities should be relative to the magnesium atoms, but from the geometry of the tube their motion is nearly at right angles to the current flow, and therefore the approximation of the magnesium atoms at rest should be correct in order of magnitude. Combining these factors with a measured enhancement of 400, for example, yields $q_r^n \backsimeq 2\times10^7 q_e^n$. It has been found that the electronic cross section for inelastic collisions is of the order of 3×10^{-18} cm^2, whence $q_r^n \backsimeq 6\times10^{-11}$ cm^2. This cross section, some 10^5 times the kinetic theory value is characteristic of collisions of the second kind where the energy-discrepancy is small. Stueckelberg has calculated cross sections of 2×10^{-13} cm^2 with an assumed interaction potential.

V. Conclusions

From intensities of the lines of the Mg II spectrum in the presence of neon the form of the cross section *vs.* energy-discrepancy curve has been found for the *s*, *d* and *f* series, and the following information concerning the cross section for collision between neon ions and magnesium atoms has been obtained: (a) The cross section has a maximum, finite value for $\sigma=0$. (b) There is a sharper decrease of cross section for increasing negative values of σ than for positive. (c) The cross section depends on the L-value of the state excited by collision. (d) The order of magnitude of the cross section in this case is 10^{-11} cm^2.

[5] Stueckelberg, Helv. Phys. Acta **5**, 370 (1932).
[6] Kallman and London, Zeits. f. physik. Chemie **B2**, 220 (1929).

A Radiofrequency High-Voltage Generator

DAVID H. SLOAN, *Radiation Laboratory, Department of Physics, University of California*

(Received October 24, 1934)

A large radio oscillator with unrectified alternating anode power-supply sends high-frequency power into a 50 meter wave-length antenna which is coiled up without insulation, and enclosed in a metal vacuum tank. Over 800,000 volts is generated inside of the tank exactly where it is to be used for x-rays or for accelerating ions. There is no insulation to become punctured. Single tuned-circuit resonance transformers are superior to coupled tuned-circuit Tesla coils. Resonance transformers, oscillator circuits, power tubes, power supply and coil construction are described. X-ray production, and ion acceleration are outlined.

THE insulation of vacuum tubes is a serious problem in their adaptation to extremely high voltage. A method is here described for generating a very high voltage entirely inside the vacuum tube in which it is to be used. Short-wave high-power radio technique makes possible a resonance transformer whose high-voltage secondary consists of only ten to fifteen turns of heavy copper pipe, entirely free from insulating material, and internally water-cooled. The surrounding copper wall inside the evacuated steel tank is the support for the grounded voltage-node of the coil, thus placing the free high-voltage end in the vacuum exactly where it is to be used. Failure of insulation is positively avoided by the completely metallic construction.

RESONANCE TRANSFORMERS

Radio oscillator tubes are used to generate the high voltage in a resonant circuit. Two general classes of circuits are possible. The first class consists of coupled separately-tuned resonant circuits, such as the Tesla coil. They are not satisfactory because of their low efficiency. The second and only practical class of circuits for this high voltage generator consists of single tuned resonant circuits, hereafter called resonance transformers. The term "resonance transformer" accurately characterizes the behavior of a single resonant circuit, insofar as the transfer of power from one section of the circuit to another is concerned, provided that the frequency is exactly the resonant frequency, and the power is less than about 10 percent of the circulating kilovolt-amperes. In this usage, the selectivity of the circuit is of no intrinsic importance. While a resonance transformer may consist of several mechanically separated sections, such as a primary and a secondary coil, the sections must act as a single resonant circuit. The effective constants of such a composite circuit, oscillating as a single unit, include the constants of all the branches interacting upon each other. Although a connection diagram of such a composite form of the singly tuned circuit of a resonance transformer may happen to look exactly like the diagram of coupled separately tuned circuits, the constants are such that an entirely different system of oscillations is produced.

This is a vital distinction, because the first mentioned class of circuits, separately tuned and coupled together, such as the Tesla coil, cannot give more than 50 percent efficiency of energy transfer from primary to secondary when driven by a self-excited oscillator tube, because of the extremely loose coupling needed between low resistance tuned circuits.

Resonance transformer superior to Tesla coil

If two resonant circuits having resistances R_P and R_S, respectively, are tuned to the same frequency f, and the coupling between the circuits consists of mutual inductance M, then the critical coupling is $2\pi fM=(R_PR_S)^{\frac{1}{2}}$. The efficiency of energy-transfer from one circuit to the other increases as M is increased, until at critical coupling an efficiency of 50 percent is reached. Further increase of coupling establishes two new stable frequencies, each of which retains this same efficiency.

Although the efficiency for the original frequency continues to increase as the coupling is increased beyond the critical value, this frequency is now unstable and cannot be used by a self-excited oscillator. Instead, a self-excited

vacuum tube will oscillate at one of the stable new inferior frequencies. Detuning one circuit favors one of these frequencies and raises the limiting efficiency slightly above 50 percent. But to adhere to the original unstable secondary frequency and obtain high efficiency by closely coupling the two tuned circuits, it is necessary that the tubes be neutralized non-regeneratively, and be driven by a master oscillator or by excitation obtained directly out of the separately tuned secondary circuit.

On the other hand, a resonance transformer operates as a single unit of inductance and capacity in spite of possible physical sub-division into separated, but coupled, sections. It has only one frequency of oscillation (aside from harmonics), and is ideal for self-excited vacuum tube operation. Energy is transferred from the primary to the secondary portion of the single oscillating system of the resonance transformer with an efficiency close to 100 percent. Clearly then, a high voltage can be generated in a resonant circuit functioning as a resonance transformer twice as efficiently as when operated as a Tesla coil, when continuously driven by a self-excited vacuum tube. Moreover, the resonance transformer construction is enormously simpler than that of a Tesla coil, because the latter has extensive stray magnetic fields arising from the very loose coupling which low-resistance tuned circuits require with a self-excited oscillator.

Moreover for other reasons, the conventional Tesla coil, when using spark excitation, is even less satisfactory for vacuum operation. A spark excited resonance transformer cannot generate a high voltage, because the coil cannot respond as a unit to the transient discharge of the condenser connected across a small portion of it. This exclusion of the resonance transformer is no drawback, for with spark excitation the energy is transferred from the separately tuned primary into the tuned secondary of the Tesla coil quite efficiently by using coupling much closer than the critical value which could be used with vacuum tube self-excitation. With suitably close coupling of the two tuned circuits, the two new frequencies which are established cause the energy to drift from primary to secondary and back at the frequency of the beat between the two frequencies. Proper quenching of the spark leaves all of the energy in the secondary, transferred there from the primary at quite high efficiency. Too much of this energy, however, is uselessly dissipated in the tail of the damped wave train. The high voltage occurs only during a very small portion of the total time. In order to impart adequate energy to the system, the necessarily large primary condenser, which stores energy preparatory to oscillating, sets a low frequency that requires a secondary of many turns of small wire. This is a serious disadvantage, for such a coil of small wire is difficult to cool in a vacuum and cannot be provided with an adequate insulating support.[1]

Oscillator Circuit

Any type of radio oscillator may be coupled to a resonance transformer by a high-frequency transmission line, but very few oscillators can be connected directly into the high-voltage resonance transformer. The Hartley circuit is adapted only to driving a resonance transformer having a high voltage step-up in applications where the inductance, which should float at grid bias potential with no voltage node at either end, is readily accessible for adjustment of its connections. Only the "tuned-plate tuned-grid" circuit is suited to driving directly a resonance transformer enclosed in a metal tank. The power output of the single-tube oscillator circuit, Fig. 1(a), is definitely limited by overheating of the

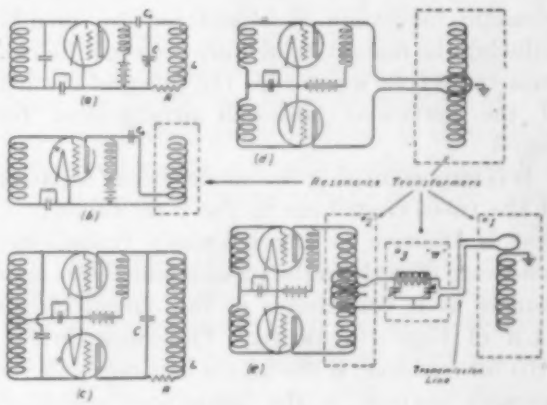

Fig. 1. Resonance transformer connections to oscillator tubes.

[1] Kossel and Eckhardt, Ann. d. Physik 17, 543 (1933).

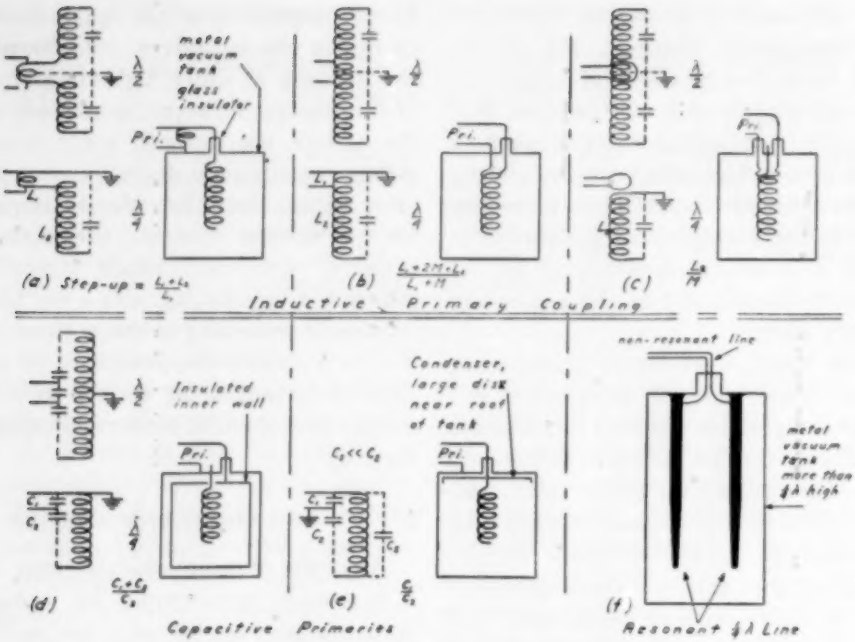

FIG. 2. Types of high-voltage resonance transformers.

condenser C_b that is used in the external high-frequency path between anode and cathode to insulate the direct anode voltage from the cathode. Hence only push-pull type oscillators are used, Fig. 1(c), because they require no such insulating condenser.

To eliminate a troublesome parasitic oscillation, only the grid input capacity is used in tuning the grid circuit, Figs. 1(b–d–e). The tuning of the grid circuit is performed by stretching the grid inductance coil. Another parasitic oscillation is eliminated by greatly reducing the mutual inductance between the two inductance coils which tune the two grid-circuits of the particular push-pull arrangement for Fig. 3.

It is important that the anode output capacity of the tubes contribute to the total capacity C that is effective in any resonance transformer connected directly to the tubes in *exactly the same manner* as it contributes to the output circuit LCR of Figs. 1(a) or 1(c). Otherwise, in Fig. 1(b) for example, if the anode capacity and the primary portion of the inductance resonated near the natural frequency of the rest of the transformer, the circuit would resolve itself into inefficient coupled resonant circuits.

With high power oscillator tubes, the physical dimensions of the leads of Fig. 1(d), for example, are not negligible compared to the operating wave-length. The leads themselves, which connect the oscillator anodes directly to the resonance transformer, act as a transmission line having waves reflected at its ends. The impedance varies along such a line, and may even be utilized in some cases to match the impedance of the oscillator tubes to the resonance transformer.

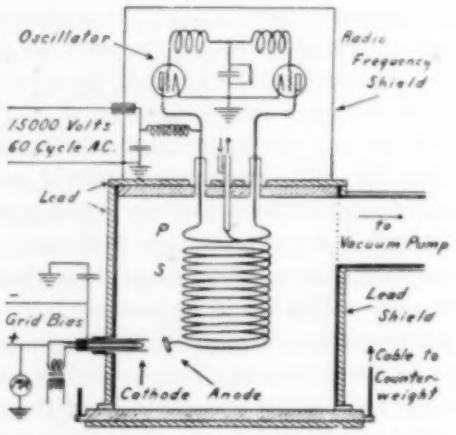

FIG. 3. X-ray arrangement with inductive primary separated from the high-voltage coil.

If the leads are very short, however, the energy in their fields is insufficient to disturb the system even when their behavior as a line is ignored.

The simple output circuit of Fig. 1(c) is actually replaced by a more complex resonance transformer, Figs. 1(d), 1(e), which may be one of the types from Fig. 2, used either to step the voltage up directly, or to step it down to match an intermediate transmission line. The intermediate line is essential for connecting the oscillator to the second class of resonance transformers mentioned below, as these transformers are $\frac{1}{4}\lambda$ resonant lines of the Lecher wire type, Fig. 2(f).

Types of Resonance Transformers

Resonance transformers consist of parallel resonant circuits which may be grouped into three classes, characterized first by "lumped" constants, secondly by evenly distributed constants, and thirdly by unevenly distributed constants plus mutual induction between elements of the circuit. Only the latter two types are of practical value for generating high voltage, the third type being especially compact and simple to adjust.

First, the "lumped constants" type has a capacity C connected across an inductance L in series with a resistance R. If R is evenly divided between the L and C branches, the impedance Z which the parallel resonant circuit offers to an e.m.f. of resonant frequency, applied across L, is a pure resistance $R'=L/RC$, being neither inductive nor capacitive at the resonant frequency. This expression is nearly true for ordinary tuned radio circuits, which by careful low-loss construction may have R' equal to about a million ohms. However, a high-voltage resonance transformer requires several million ohms impedance, which is obtained by enlarged dimensions and elimination of all C except the distributed capacity, which then results in the third class of transformer. For simplicity, the first class, with lumped constants, is assumed in approximating the step-up ratios listed with the various types in Fig. 2. M is the mutual inductance between the primary L_1 and the main inductance L_2. These voltage step-up ratios are the square-roots of the ratios of the total impedance to the primary impedance at the resonant frequency.

The second class of resonance transformers, with distributed constants, is the most efficient, but is much too expensive to build. These consist of $\frac{1}{4}\lambda$ transmission lines, open at one end and short circuited at the other, Fig. 2(f). In spite of their low ratio of L/C, the open end impedance $R'=2L/RC$ may attain enormous values because R can be made exceedingly small by using conductors of very large diameter. The exact expressions for the impedance of the open end as well as for the primary portion of the line may readily be obtained from texts on transmission line theory.

The third and most useful class of resonance transformers, having mutual inductance between elements of the circuit in addition to having the capacity unevenly distributed along the inductance, cannot be treated usefully by mathematics. The types in Fig. 2 are of this class, in actual high-voltage applications. When adjusted to maximum step-up the primary impedance is approximately equal to that of the oscillator anodes, but even the output impedance of "class C" oscillators is rather indefinite. Moreover, even if it were known, the step-up ratio is not important for quantitative use because the input voltage is very difficult to determine.

Voltage measurements

The total voltage generated by the resonance transformer is obtained roughly by the relation $W=E^2/R'$, from a measurement of the watts, W, generated in the coil whose resonant impedance R' is known only approximately. It is also easy to measure a known fraction of the generated r.m.s. voltage, but neither of these direct methods are dependable because the wave-shape due to the non-linear modulation by the unrectified anode supply-voltage is difficult to determine for each new adjustment. The known fraction of the generated voltage could be determined accurately with a peak-voltage vacuum tube voltmeter, but a more concise voltage measurement would result from a measurement of the maximum energy of photoelectrons ejected by the x-rays that arise when the coil is struck by electrons from gaseous currents or from an x-ray cathode.

It is simpler, however, to filter these x-rays through a centimeter or more of lead and plot an

aluminum absorption curve from which the absorption coefficient per electron is obtainable, and with the Klein-Nishina formula the effective wave-length of the x-rays is found, and from this the voltage of the x-rays is directly obtainable. X-rays of these energies are absorbed in aluminum almost entirely by Compton scattering and electron recoil. Therefore the absorption in aluminum is better suited to the calculation of wave-length and voltage than is an absorption in lead which has, in addition to the Compton process, a large photoelectric absorption of rapidly varying proportions that is less accurately known for this range. However, the linear absorption coefficient for lead does indicate a voltage close to that determined by absorption in aluminum.

For voltages determined from absorption coefficients, the logarithmic intensity-ratio curves for absorption in lead are found to agree with the slope of lead absorption curves obtained with other types of x-ray tubes that were operated with known voltages. From a calorimetric measurement of the kilowatts associated with an established voltage, the neighboring voltages are estimated from the change in the kilowatts in the coil.

An x-ray measurement of voltage is not needed when the voltage is used for the double acceleration of ions, for then the minimum voltage for which the ions traverse their path in synchronism with the alternating voltage is sharply defined.

Dimensions

The impedance varies as the square root of the scale of the dimensions to which the resonance transformer is built. Since the voltage varies only as the fourth root of the linear dimensions, the size of the transformer is chosen as small as the power requirements will permit, whereas the optimum geometric proportions are chosen by trial-and-error. It is difficult to obtain sufficient power below 40 meters wave-length, and furthermore, the coils of the third class of transformers cannot be adequately water-cooled if constructed for wave-lengths less than this.

It is interesting to note that one of the second class of transformers, a resonant $\frac{1}{4}\lambda$ line built for 40 meters would generate 5,000,000 volts with available oscillator tubes, compared to the 2,000,000 volts to which the coiled type of transformer could be forced, provided of course that a tube could withstand such voltages without field-current break-down. But the $\frac{1}{4}\lambda$ line would require an enormous vacuum tank 35 feet high and 15 feet in diameter, surrounding the two vertical parallel lines, Fig. 2(f). To obtain extremely low resistance each conductor of the line would be about 18″ in diameter, tapering somewhat at the high voltage end. This indicates that only the coiled third class of transformers are sufficiently compact for ordinary use.

Coil connections

Five types of resonance transformers of the third class are shown in Fig. 2 for $\frac{1}{4}\lambda$ coils; with four corresponding arrangements for $\frac{1}{2}\lambda$ coils. The types in Figs. 2(a–b–c) use three kinds of inductive primary coupling, whereas those in Figs. 2(d–e) have capacitive primary coupling. Push-pull oscillators are suited to all of the $\frac{1}{2}\lambda$ coils; but single oscillators, Fig. 1(b), are needed by all of the $\frac{1}{4}\lambda$ coils excepting the separate inductive primary of Fig. 2(c), which, like the half wave coils, will operate with either single or push-pull oscillators. In the special case of the $\frac{1}{4}\lambda$ coil with separated primary and push-pull oscillators, the load on the two tubes is more evenly balanced by providing a grounded electrostatic shield between the primary and secondary coils.

The capacitive analogue of the inductive primary of Fig. 2(c) is a voltage step-down device. However, to step the voltage down for transmission over a high-frequency transmission line, the transformer of either Figs. 2(b), or 2(c), working backwards is more practical.

The $\frac{1}{4}\lambda$ coils of Figs. 2(c) and 2(e) are simplest to construct and adjust. The latter is unique in that it may be connected directly to a single oscillator tube of unlimited size, because with a circuit corresponding to Fig. 1(b) it requires no blocking condenser. The oscillator circuit of greatest ease of adjustment and freedom from parasitic oscillations is that of Fig. 1(d), which combined with Fig. 2(c), is shown in the x-ray generator, Fig. 3, which has been used throughout most of the development.

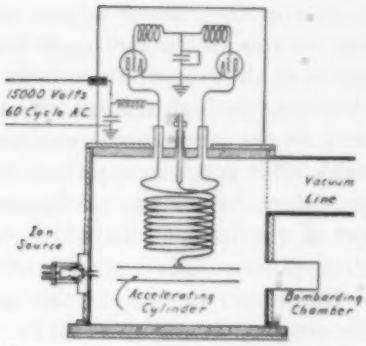

FIG. 4. System for the double-acceleration of protons, deutons or helium ions.

OSCILLATOR TUBES

A low-resistance coil inside of a copper-lined vacuum tank can form a resonance transformer whose total resonant impedance $R' = L/RC = 3$ megohms. This requires a little over 200 kilowatts to develop 800,000 volts across it. When, in addition, the coil must also support an ion-accelerator electrode, Fig. 4, the increased electrostatic capacity to the walls greatly increases the required high-frequency power, which may exceed 600 kilowatts for some accelerator systems. Higher voltages will require even more power, and this has led to the development of very large short-wave oscillator tubes, for driving the resonance transformer. The essential feature in the design of these tubes is a low inter-electrode capacity, such that the parasitic or natural frequency of the primary circuit of Fig. 3 is more than twice as high as the main resonance transformer frequency of 6000 kilocycles.

Three sizes of tubes, having continuous output ratings of 100 kw, 200 kw and 300 kw, have been constructed in the laboratory shop. The anode voltage supply is unrectified 15,000 volts r.m.s. 60 cycle a.c. This greatly reduces the heat associated with a given maximum of generated voltage, and increases the maximum to which the output power can be modulated. Thus by running the filaments exceedingly hot, a push-pull pair of these 300 kw tubes can probably deliver 1000 kw at 6000 kilocyles during the maximum of the 60 cycle voltage, although this output has not yet been required for ion acceleration.

The power dissipated in the load, averaged over a complete cycle, is much smaller than $\frac{1}{4}$ of the maximum, because of the distortion by the non-linear modulation of the output wave-shape. In the x-ray coil, for example, when generating 800,000 volts, the groups of radiofrequency oscillations reaching a peak of 200 kw have an average heating effect equal to a continuous dissipation of only 30 kw in the resistance of the coil, away from which the heat is carried by the cooling-water.

Oscillator tube construction

The six-inch diameter copper anode of each 300 kw oscillator tube is cooled by a swiftly moving sheet of turbulent water only 0.025" thick, inside of the waterjacket, which with its expansion joint is soldered around the anode. The tube undergoes no heated bake-out because it is continuously exhausted. Therefore the small clearance between the anode and the brass waterjacket can be accurately maintained. Ordinary solder is used, and because of the poisonous action of water-vapor upon the emission from tungsten filaments, the joints of the waterjacket are distinctly isolated from the soldered joints in the wall of the vacuum-tight envelope.

The cylindrical grid structure consists of a helix of copper wire wound around a frame of six water-cooled copper pipes, to which these wires are soldered. The grid is soon coated with evaporated tungsten which keeps the secondary emission reasonably low. Within the grid are placed 12 filaments of 0.050" tungsten 14 inches long. Each filament has individual spring tension, and is so easily replaceable that the unusually high temperature of 2700°K is practical, giving a total emission of 200 amperes from the filaments of each tube.

The three electrodes are insulated by two glass cylinders which form part of the vacuum wall, and which are sealed to the metal parts by red sealing wax. Each seal is protected from electric fields and radiant heat by metal shields on the inner side of the glass.

Each tube is continuously exhausted to 10^{-5} mm Hg pressure by an Apiezon oil diffusion pump system whose over-all speed is 100 liters per second.

The oscillators are mounted on waxed maple boards inside of a large copper house, with by-pass

condensers connected to all the power leads to completely prevent the escape of current which might radiate, thus eliminating any interference with radio communication.

Power Supply

Advantages of alternating current

The chief advantage of alternating current for the anode power-supply, aside from avoiding costly rectifiers, is the great ratio between the peak and the average high-frequency power output. But another almost priceless virtue of an alternating power supply is the alternate idle half-cycles which permit de-ionization of arcs that occasionally occur in the high-voltage circuit. Discharges from the high-voltage coil are harmless, because they either kill the high-voltage oscillations and cease, or else develop a parasitic oscillation and low-voltage arc, which dies out at the end of the half-cycle. Adequate de-ionization time, provided by the idle half-cycle, combined with a very fast vacuum pumping-system, prevent such momentary discharges from interrupting operation for more than one or two cycles. Far from being damaged, the all metal surfaces in the high-voltage chamber are merely cleaned by the discharge, so that even higher voltages can be used.

When the oscillator filament heating-current is shifted 90° out of phase with the alternating anode supply-voltage the emission current heats all parts of the filament evenly, just as with a center-tapped a.c. filament and d.c. anode voltage.

Methods for voltage variation

A motor-generator to operate the anode voltage-supply transformer provides the best means of varying the generated high voltage. A 150 kva transformer will supply power for a pair of 100 kw tubes driving a 800,000 volt x-ray generator in continuous operation. A transformer operated from a fixed-voltage power supply involves the simplest equipment for varying the high voltage if the transformer is connected to the anode circuit through a flowing water-column variable resistance. This resistance can use the cooling water discharged from the oscillators. A variable reactance in the power-line seriously lowers the power-factor which is already low because of the half-cycle load.

A reduction of the step-up ratio is an efficient means of lowering the high voltage for outgassing the surfaces of the resonance transformer and vacuum tank while conditioning them for operation. This is done by increasing the impedance of the part of the circuit into which the tubes deliver their power. Three good methods are available for thus decreasing the generated power. The simplest is one in which the primary of Fig. 3, for example, if mounted on sylphon supports, can be moved nearer to the main coil while outgassing. The other two systems for reducing the step-up ratio involve an intermediate transmission line.

In the circuit of Fig. 1(e), the impedances of the transmission line and of the primary and secondary of the high-voltage resonance transformer, No. 1, have permanently fixed ratios; but the impedance ratio of the auxiliary resonance transformer, No. 2, between the oscillator tubes and the line, can be varied to change the power output by providing this transformer with a tapped secondary to connect with the line. In addition to these two transformers and interconnecting line of the second method, the third method includes still another resonance transformer, No. 3, of variable ratio, inserted between the line and its connection to the secondary of the transformer that couples the line to the tubes, Fig. 1(e). This third resonance transformer is simply an impedance-matching "π" network common to transmission line practice. These two methods involving the line permit a convenient location of the oscillator at a distance from the tank, and step-up ratio-changing incurs no danger of springing leaks in the main vacuum-tank.

All three of these methods of lowering the step-up ratio permit abnormally high voltages to develop at the oscillator tubes, which may limit the extent of the reduction of the main high voltage, unless the oscillator power-supply voltage is also reduced.

Transient voltages

The presence of the direct anode voltage in the high-voltage vacuum-tank during a high

voltage discharge may momentarily short circuit the anode voltage-supply. A peculiar property of rarefied gaseous discharges is their ability to suddenly cease conducting, which could cause the momentarily short-circuited power-supply transformer to become cleared so abruptly that it would develop a tremendous surge voltage. A $\frac{1}{4}$ mfd. condenser across the supply line prevents the surge from rising to destructively high values. But now about 50 ohms is needed between this condenser and the anodes to prevent flashes in oscillator tubes, as well as flashes from the primary in the tank, from liberating sufficient gas to disrupt operation.

The transmission line, on the other hand, with a well-insulated inductively coupled resonance transformer between the oscillator and the line, Fig. 1(e), avoids the high voltage surges by not having the anode voltage enter the high-voltage tank. Hence with this system there is no need for the surge-absorbing condenser which increased the severity of the flashovers.

Grid Bias

Considerable variation in the high voltage that is generated with a fixed anode voltage can be effected by adjusting the grid-bias voltage. In fact, the reducing of an excessive bias is the most convenient means of advancing the voltage as the tank is progressively outgassed.

The grid-bias voltage is most easily obtained from a grid-leak and condenser. Since the grid-leak dissipates several kilowatts, the most satisfactory resistance is that of a flowing water-column of variable length, between graphite electrodes. When the alternating anode supply-voltage is below the operating range, the tube impedance is so great that oscillations cannot occur, and considerable power is wasted in non-oscillatory anode current. This can be minimized by maintaining a constant bias instead of the variable voltage of the grid-leak.

Rather than use a motor-generator, an effectively constant bias can be supplied during the alternate half-cycles of operation by square-wave pulses from a unique rectifier. An ordinary rectifier cannot pass the grid current because this current flows in opposition to the bias voltage. But if a large hot-cathode mercury-vapor rectifier is connected in series with a resistance across 110 volts a.c., the voltage drop across the tube during one half-cycle never rises, for example, above 15 volts. A large 110–11,000 volt transformer connected across this tube will give practically constant 1500 volts for nearly a half-cycle, with the striking property that grid current can flow *against* this voltage, and merely increase the current in the rectifier tube. The grid potential cannot become highly positive during the next half-cycle because the resistance which connects the primary to the 110 volt line limits the power which a positive grid can draw from the transformer.

To initiate oscillations, the biased oscillators must have their grids made more positive by a transient voltage which may be applied as the anode voltage nears its maximum. As few cycles of operation as are desired may be used each second. The efficiency, as an x-ray generator, is greatly increased by quadrupling the electron emission and using only every fourth cycle of the power source, with a corresponding reduction of the resonance transformer power dissipation.

Coil Construction

The coil is located in a water-cooled copper-lined steel tank more than a meter in diameter and equally high, which is exhausted to less than 10^{-6} mm Hg pressure by a 250 liter-per-second Apiezon oil diffusion pump system. The shape of the coil is chosen to give the maximum value of the ratio L/RC consistent with adequate cooling. A typical high-voltage $\frac{1}{4}\lambda$ coil has 12 turns of $\frac{3}{8}''$ diameter copper pipe wound into a cylindrical coil about 14 inches in diameter and 15 inches long. It is supported by one end which is grounded where it passes through the roof of the surrounding metal tank to connect with the cooling-water system. The resonant frequency is about 6000 kc or 50 meters wave-length.

The coil is wound of two concentric copper pipes, so that cooling water may flow down between their walls and return in the inner pipe, and also cool whatever electrode is attached to the high-voltage end of the coil. Although a peak of over 200 kw is produced in the coil by the modulated high-frequency currents when developing 800,000 volt x-rays, the average rate

of heating equals a continuous dissipation of only 30 kw, which the cooling water must carry out of this coil, in addition to the heat developed in the high-voltage electrode. Heat-transfer between the outgoing and the incoming water is reduced by covering the inner pipe with rubber tape. To protect the rubber against erosion, it is wrapped with a layer of copper tape.

For x-ray use, either the anode or the cathode may be on the high-voltage end of the coil. In the latter case the filament leads may be placed inside of one of the water passages in the pipes of which the coil is wound.

Since it has twice the impedance of a $\frac{1}{4}\lambda$ coil, a $\frac{1}{2}\lambda$ coil will generate $\sqrt{2}$ times as much voltage as will the $\frac{1}{4}\lambda$ coil, for a given power. Hence an x-ray generator superior to the $\frac{1}{4}\lambda$ coil of Fig. 3 may be obtained by using one of the $\frac{1}{2}\lambda$ coils of Fig. 2, connected as in Fig. 1(d), having an anode on one end and a cathode on the other.

A smaller $\frac{1}{4}\lambda$ coil, for twice as high frequency, is obtained if instead of using concentric pipes, a single small pipe is wound into a coil that has its cooling water discharge out of its high-voltage end into the equally high-voltage end of a similar coil, and thus return to ground. These two coils with a single voltage maximum may be located on a common axis with their high-voltage ends adjacent, in which case a reversed direction of winding of one coil improves the magnetic circuit. The simplest transformer to adjust, however, is the large $\frac{1}{4}\lambda$ coil wound with concentric cooling pipes.

X-Ray Generator

The x-ray cathode structure shown in Fig. 3 has a straight tungsten filament surrounded by a grid that has a negative bias of several thousand volts. The purpose of the grid is to prevent the escape of electrons, except when the nearby anode is near its positive voltage maximum. An emission current of 5 milliamperes, average-value, may actually consist of short pulses of current which momentarily rise to 200 milliamperes. Because of these high current densities, it is not practical to use a zero potential grid and thereby obtain a similar bias action by means of space charge alone. The ideal cathode is a very hot one whose emission is controlled solely by the grid. Since the anode potential must be near its most positive value in order that an electron current may flow to it, the x-rays are produced almost as though the anode were connected to a high-voltage direct-current supply.

The intensity of the x-rays is as great as the intensity produced by other types of high-voltage tubes. It is limited only by the overheating of the water-cooled target. Special mechanical damping of the coil is necessary to prevent the coil that supports a positive ion accelerator electrode from vibrating, but for x-rays, it is advantageous to use no damping.

The free end of the coil may be kept in sustained vibration by the magnetic and electric forces on the coil, with the amplitude of vibration controlled by the adjustment of the grid tuning coil. This movement of the high-voltage coil changes its frequency relative to the grid tuning, and the changing efficiency of oscillation alters the power output and the forces on the coil. The magnetic field is sufficient to unwind the coil through an angle of 3° in the steady vibrationless state. The motion of the x-ray target is largely at right angles to the direction of the electron stream, hence the small area of impact remains at rest in space while sweeping over a large anode surface to facilitate the heat dissipation. Without this movement of the anode, the stream of electrons can be swept over the target face by deflecting fields analogous to those of cathode-ray oscillographs.

The absorption curves of Fig. 5 indicate an operating voltage of 800,000 volts with 30 kw in the coil. The voltage is confirmed by the absorption coefficient per electron in aluminum, using the Klein-Nishina formula. These curves were obtained from a resonance transformer driven by a pair of 100 kw oscillator tubes, connected as in Fig. 3. With a filter of 5 mm steel and 5 mm lead, the intensity at 0.7 meter from the tungsten target, when using 2.8 milliamperes emission, is 20 Roentgen units per minute. As it is normally adjusted, this resonance transformer will carry an electron current of 10 milliamperes to its high-voltage end without noticeably lowering the voltage, but no target can withstand it. By virtue of the resonant circuit, the sinusoidal voltage of the useful and inverse half-cycles are equal.

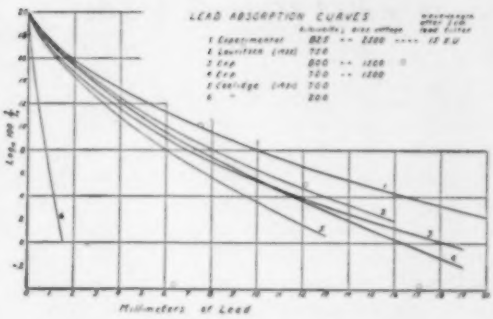

FIG. 5. Absorption of x-rays in lead.

The 700 kv and 800 kv curves were taken with the x-ray cathode-grid bias-voltage somewhat lower than the value subsequently adopted. The effect of the higher bias is clearly seen in the 825 kv curve, which lies much higher than the others, indicating a greater freedom from soft x-rays. Some earlier curves of Coolidge[2] and Lauritsen[3] are shown for comparison.

For therapeutic use, the entire tank is covered with 2″ of lead, except at the treatment port-holes, and is placed in a room walled with $\frac{1}{4}$″ lead with an additional 2″ of lead between the tube and the operator.

With increased water-cooling of the high-voltage circuit, the voltage can be raised whenever clinical observations justify the change.

POSITIVE ION ACCELERATOR

The original purpose in developing the high-voltage resonance transformer was for the multiple acceleration of ions. The most intense source of ions of gaseous elements has proved to be that type which was originated to supply mercury ions for multiple acceleration.[4] The plasma of a low-voltage high-current gaseous discharge of the hot-cathode type supplies the ions which are accelerated and focussed by the field in a positive-ion space-charge sheath of 20,000 volts or more, which the ions cross in falling toward a negative electrode that is pierced by a small hole through which emerges the ion beam of several milliamperes.

The scheme for the high-voltage double-acceleration of hydrogen or helium ions consists in having a hollow open-ended horizontal water-cooled metal cylinder attached to the high voltage end of the coil, Fig. 4. When this cylinder is highly negative, the intense beam of many milliamperes of positive ions is accelerated into one end of it from the ground-potential ion-source. These ions travel along the axis of the hollow field-free interior and emerge from the opposite end of the accelerating cylinder one half-cycle later when it is highly positive. The ions then receive a second acceleration, doubling their energy, as they pass to the wall of the tank, through which they emerge to be used at ground potential, for bombarding atomic nuclei under investigation.

The development of a high-voltage double-acceleration tube for protons and deutons has just been completed by Dr. J. J. Livingood and the writer, and is soon to be described in detail. Likewise, a description of a resonance transformer x-ray tube installed at the University of California Medical School by Dr. M. S. Livingston and M. A. Chaffee will soon be published.

The writer is deeply indebted to Dr. J. J. Livingood, Dr. F. M. Exner, and Professor E. O. Lawrence for their very active participation in developing this method. The cooperation of Dr. L. F. Fuller is highly appreciated. The work was carried on with the financial support of the Research Corporation and the Chemical Foundation, and the valuable cooperation of the Crocker Institute of Cancer Research. This opportunity is taken to thank also the General Electric Company for donating power-supply transformers, and to thank the American Smelting and Refining Company for providing the lead shielding. The writer is personally grateful to the Charles A. Coffin Foundation.

---

[2] Coolidge, Dempster and Tanis, Am. J. Roentgenol. and Rad. Therapy **27**, 405 (1932).
[3] Lauritsen, private communication.
[4] D. H. Sloan and E. O. Lawrence, Phys. Rev. **38**, 2021 (1931).

Loss and Restoration of Photoconductivity in Red Mercuric Iodide

FOSTER C. NIX, *Bell Telephone Laboratories*

(Received November 5, 1934)

Single crystals of red mercuric iodide, which normally display photosensitivity when precipitated, lose their photosensitivity on aging. This loss is accompanied by a change from the mono- to the polycrystalline fibrous state with considerable randomness of orientation of the individual crystallites. The nonsensitive crystals can be resensitized by subjecting them to an electric field for a time of the order of a few minutes. The increase in photosensitivity is accompanied by a decrease in the dark current. These correlated phenomena may not occur till after the lapse of an appreciable time after the field is first applied. The rate of decrease of the dark current with time is greater the lower the temperature. The data also suggest, but do not conclusively demonstrate, that the dark current increases with decreasing temperature. The rate of resensitization and the magnitude of the attained photosensitivity are found to increase with (a) increase in applied field strength and (b) decrease in temperature. When the light is turned on the photoelectric current is found, under certain circumstances, to rise briefly to a maximum and then descend to a permanent value at which the total current is equal to the value of the dark current prevailing when the voltage was first applied.

CRYSTALLINE materials exhibiting internal photosensitivity have been divided by Gudden and Pohl[1, 2] into two arbitrary classes, designated as "idiochromatic" and "allochromatic." The former are photosensitive in their initial and pure state while the latter acquire their photosensitivity through special treatments which (with one exception) disturb the stoichiometric chemical equilibrium.

The reaction products of these treatments are essentially the same, i.e., the photoactive centers are thought to consist of a quasi-neutral alkali atom with the valence electron more or less loosely bound. This loose binding is evident from the fact that electrons can be elicited either by heat, or light of suitable wave-length (for the most part, light of the visible spectrum possesses sufficient energy for the alkali halide crystals). Stasiw[3] has shown that the active centers when acted upon by the above agents elicit negative carriers which then move toward the anode under the influence of an applied potential. On reversal of potential the "electron cloud" reverses its direction of propagation.

Stasiw[4] and Pohl[5] were able to produce the active centers in a most ingenious way. This scheme consisted essentially in allowing electrons to enter the crystal from a pointed cathode. The electrodes of a KCl crystal consisted of a platinum foil fused onto the end of the crystal which served as an anode, while the cathode consisted of a pointed platinum wire. On impressing a potential of a few hundred volts across the crystal, when the latter was heated to a temperature of two or three hundred degrees, there resulted the flow of electrons out of the cathode into the crystal. This was accompanied by a pronounced discoloration of the crystal as could easily be seen with the unaided eye. For KCl the crystal appears violet in color. The process is though by Pohl and his collaborators to consist in the diffusion of anions out of the crystal to be replaced by electrons emerging from the pointed electrode. This process would result in an electrically neutral crystal with an anion deficit. However, it is difficult to understand how this proposed process could account for the phenomenon since numerous experiments indicate that cations[6] are the carrier of the electrolytic current in the alkali-halide crystals at temperatures up to *ca.* 500°C.

The "additive" method as introduced by Siedentopf[7] and Giesel[8] consists in heating a nonsensitive alkali-halide crystal in a closed vessel containing alkali vapor. The vapor need not necessarily be the metal forming the cation of

[1] B. Gudden, *Lichtelektrische Erscheinung* (Julius Springer) (1928).
[2] F. C. Nix, Rev. Mod. Phy. **4**, 723 (1932).
[3] O. Stasiw, Nachr. d. Ges. d. Wiss. z. Göttingen Math.-Phy. Kl. 1 (1932).
[4] O. Stasiw, Nachr. d. Ges. d. Wiss. z. Göttingen Math.-Phy. Kl. 387 (1933).
[5] R. W. Pohl, Phys. Zeits. **35**, 107 (1934).
[6] C. Tubandt, Handbuch d. Exp. Physik **12**, Part 1, Akadem. Verlags. Leipsig (1932).
[7] H. Siedentopf, Phys. Zeits. **6**, 855 (1905).
[8] F. Giesel, Ber. d. Deutsch Chem. Ges. **30**, 156 (1897).

the crystal in question; e.g., alkali vapors other than sodium can provoke discoloration and sensitization of rocksalt. This discoloration of the clear rocksalt was thought by Siedentopf to consist of a diffusion of the alkali metal atoms into the crystals; principally through places of imperfections such as holes, fissures, etc.

Still a third and important method of producing internal photosensitivity (Goldstein,[9] Röntgen and Joffé[10]) consists in the irradiation of nonsensitive crystals with light of sufficiently short wave-length (gamma-rays, x-rays and ultraviolet). This photochemical process is thought to evoke an electron transfer from anion to cation, thus producing quasi-neutral alkali and halogen atoms. The allochromatic crystals suffer a discoloration by the above treatments. Clear rocksalt becomes a yellow, while KBr becomes bluish-violet.

The concentration of the photoactive centers is found to vary from 10^{15} to 10^{17} per cubic centimeter. However, the concentration can be influenced by the past history of the material; e.g., greater concentration of centers can be obtained in materials which have been rapidly cooled or in crystals which have remained in a strained state after formation from the melt.

On plotting the velocity of propagation of the slowest of an isolated group of electrons under the influence of an applied electric field as a function of temperature, it is found that a striking similarity exists to a similar plot of electrolytic conductivity *vs.* temperature for KCl.[4, 5] At temperatures in the range of the lower branch of the curve the electrons have a velocity distribution, the spread of which decreases with increasing temperature, becoming uniform at *ca.* 670°C and remaining so for the range of still higher temperatures studied.

The agreement as to slope and point of change of slope between the two different sets of data lends strong evidence to support the contention of Pohl[5] and his collaborators, concerning the relationship existing between electrolytic dark current and emanation of electrons out of the pointed electrode, as expressed above. At least it must be admitted that there is a close connection between the electrolytic dark conduction and the velocity of propagation of the "electron cloud" under the influence of an applied electric field.

In the processes described in the foregoing paragraphs the mechanisms of sensitization have all dealt with the production of a discoloration and consequent photosensitization by either allowing foreign bodies to diffuse into the "nonsensitive" material, or by photochemical means. In the following we will describe the discovery of *loss* of internal photoelectric sensitivity with time in inherently sensitive single crystals of red mercuric iodide and with detail studies of the factors involved in their resensitization.

During the course of a study of the photoconductivity of extremely pure single crystals of red mercuric iodide, which were prepared by slow precipitation of purified material from ethyl alcohol, we observed that *after the lapse of one and one-half years of undisturbed rest the crystals had lost a considerable portion or even the whole of their photosensitivity*. During the course of a series of measurements made to ascertain the nature of the current-voltage curve (readings being taken at random in order to eliminate any effects which might result from the order in which the measurements were made) an increase in sensitivity was observed at lower voltages after readings had been made at higher voltages. We were able to obtain reproducible results in these measurements only after we had allowed the highest voltage which was used to remain impressed across the crystal for several hours. *In other words, the impressed voltage resensitized the previously desensitized crystals*. We found further that many crystals had *completely lost* their inherent photosensitive properties. These completely desensitized crystals could then be sensitized by allowing a sufficiently high voltage to remain impressed across the crystal for times comparable to those required to resensitize the partially sensitive crystals. The data used in plotting the following curves were taken on sensitization studies of crystals which had become completely nonsensitive.

These nonsensitive crystals have continued to change as regards the rate of resensitization, magnitude of the dark current, etc., ever since

[9] E. Goldstein, Zeits. f. Inst.-Kunde **16**, 211 (1896); Berl. Ber. 222 (1901).
[10] W. C. Röntgen, Ann. d. Physik **64**, 1 (1921).

FIG. 1. Experimental glass tube with amber insulation.

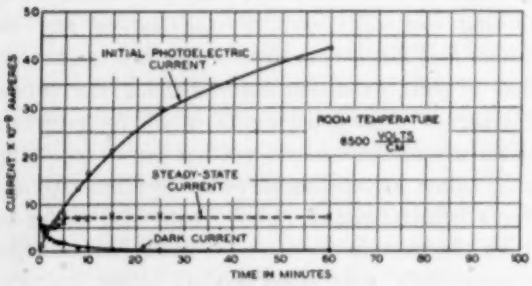

FIG. 2. Curves showing the rate of resensitization and decrease of dark current with time: Steady-state current is depicted by the dashed line. Applied electrostatic field strength 6500 volts/cm.

the effect was discovered about two years ago. In general: the older the nonsensitive crystal, the larger the dark current, the slower the rate of resensitization and the more rapid the rate of loss of photosensitivity after resensitization. The resensitized crystals lose their photosensitivity after a certain length of time. In the early stages of these studies crystals were observed to lose their photosensitivity only after many days, whereas they now lose it completely in some ten or twelve hours after resensitization. The time necessary for the disappearance of the photosensitivity after resensitization can be substantially shortened, by impressing potential of opposite polarity to that used during the resensitization, also, in the early stages of the resensitization, by irradiation with light from a tungsten lamp. We have been unsuccessful up to the present time in finding any factors which can influence the rate of loss of the original intrinsic photosensitivity.

The data to be presented in the following pages cannot be considered as quantitative. However, we have selected data made from studies on one particular crystal in a space of time small enough to permit comparable measurements to be made. Comparison of Figs. 2 and 6 will show some of the general changes that have taken place over a period of two months.

For the purpose of resensitization, the desensitized single crystal was placed between two smooth platinum-faced electrodes. The electrodes were firmly pressed against the smooth crystal faces by means of finely adjustable jaws. The amber-insulated crystal holder was mounted on the end of a re-entrant hollow copper tube which was sealed to the outer walls of the Pyrex glass tube (Fig. 1). Amber insulation was used throughout the tube. All measurements were made with the tube evacuated to a pressure less than 10^{-3} mm of Hg. The currents were measured by means of a string electrometer which registered the drop of potential across a sputtered carbon film, of 10^9 ohms resistance. The crystal was connected in a simple series circuit containing large heavy duty "B" batteries and the high resistance. The voltage was applied continuously, unless otherwise stated, during the course of the measurements. Measurements were made at temperatures (+23°C, 0°C, −33°C, −79°C, −183°C). The procedure consisted in observing (a) the dark current at the moment when the voltage was applied (hereafter to be called $t=0$) and at various times t thereafter; (b) the result of illuminating the crystal for various time-intervals beginning at various times t. In what follows, we denote the dark current by i_t^D; its value just after the voltage is applied ($t=0$) by i_0^D; the total current just after the light is turned on at instant t by $(i_t^D+i_0^\phi)$; the total current after the light has been shining for a while (see below) by i_s. We apply the name "initial photoelectric current" to i_0^ϕ (i.e., the augmentation of current occurring as soon as

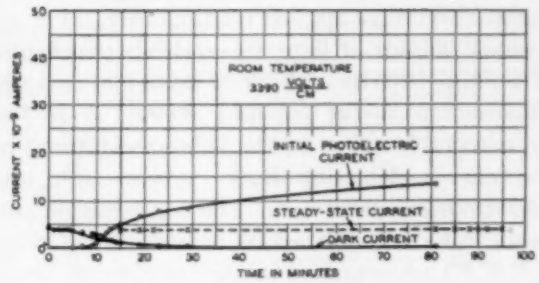

FIG. 3. Curves depicting the same relationship between decrease in dark current, rate of resensitization, with time as Fig. 2 at a lower field strength. Field strength 3390 volts/cm.

the light[11] is turned on), and the name "steady-state current" to i_s.

In Figs. 2 and 3 are plotted the values of i_t^D, i_0^ϕ and i_s observed with our crystal while the voltages there indicated were being continuously applied from $t=0$ over a period of 60 or 80 minutes, and light was being turned on occasionally for short intervals of time. It is seen that the dark current decreases steadily from i_0^D, while the initial photoelectric current increases steadily from zero.

Two cases are to be distinguished:

(I) If the light is turned on after the lapse of some minutes, i_0^ϕ is so large that in spite of the diminution of i^D, their sum is greater than i_0^D. Under these circumstances *the total current* does not remain equal to $(i_t^D+i_0^\phi)$ but *rapidly declines to a value i_s not very different from i_0^D, at which it remains constant so long as the light continues to shine.* This remarkable fact (further illustrated in Fig. 4 and further discussed) has been established for room-temperature. At lower temperatures we observe the constant value i_s, but cannot compare it with the value of i_0^D, because of the extremely rapid decrease in i^D, thus preventing reliable values of i_0^D to be obtained.

(II) For small values of t such that the sum of i_t^D and i_0^ϕ is smaller than i_0^D, the total current remains constant throughout the illumination at the value—i.e., $(i_t^D+i_0^\phi)$—which it assumes as soon as the light is turned on.

[11] The data presented were obtained with general radiation from a tungsten lamp. From numerous measurements made with monochromatic radiation from various parts of the spectral sensitive domain of red mercuric iodide it has been definitely established that the behavior described is independent of the character of the light used so long as it falls in a spectral region to which the crystal is photoelectrically sensitive.

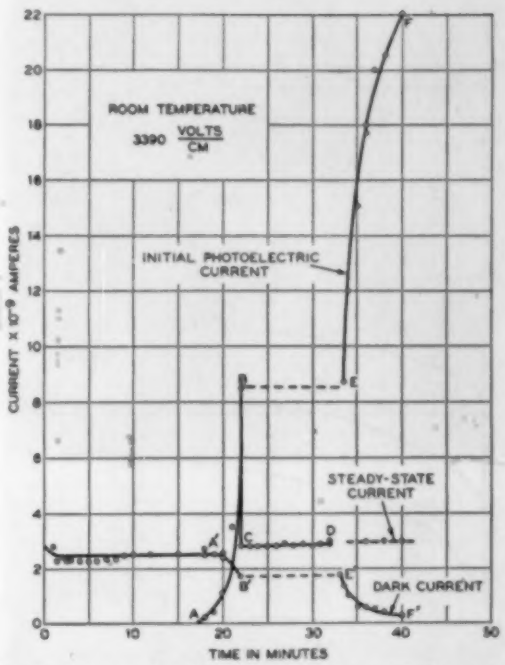

FIG. 4. Curves showing the constancy with time of the dark current during the incubation period and effect of constant illumination on the rates of change of photoelectric and dark currents.

It is seen in Fig. 3 that there is no perceptible photoelectric current for an appreciable time T after the voltage is applied; and that then there occurs an apparently simultaneous decrease in the dark current and increase of the photoelectric current. We call the period T the "incubation period." It varies in duration from zero (or a length too small to observe) up to several hours. We have not been able to obtain any data concerning the factors controlling the lengths of these incubation periods. Attempts to correlate crystallographic directions and incubation periods have proved to be futile. However, it is clear that *there exists an intimate relationship between the decrease in dark current and the resensitization process.* It is a rule illustrated in Figs. 2 and 3, that the higher the applied field the more rapid the decrease in dark current and increase in photoelectric current with lapse of time after the incubation period ends. (Note that in the case of Fig. 2, T is imperceptibly short.) It is also seen that the higher the voltage the larger the final sensitivity attained, with an accompanying increase in steady-state current (i_s) and value of the dark current at $t=0$ (i_0^D).

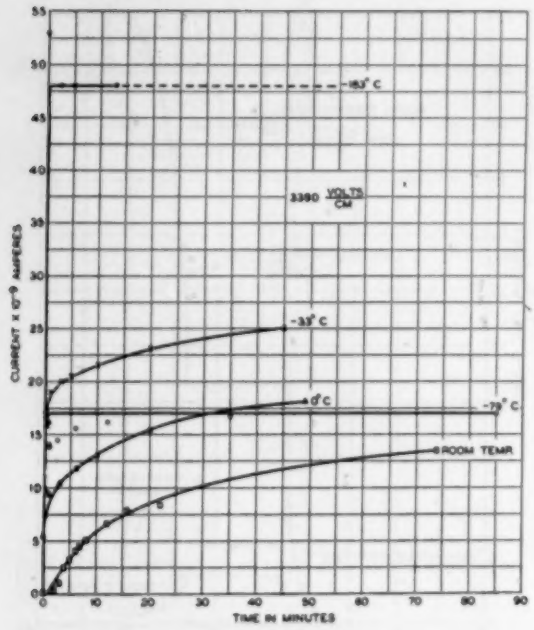

FIG. 5. Curves depicting the rate of resensitization at temperatures between and including room and liquid air temperatures.

Fig. 4 depicts the relationships between the dark, initial photoelectric and steady-state currents in a case in which an incubation period of some 17 minutes was observed. It also clearly shows the effect of steady illumination of the crystal after the incubation period is past and the photoelectric current becomes appreciable. The points A and A' mark the end of the incubation period, when the dark current begins to decrease with accompanying development of photosensitivity. Beginning at the time corresponding to BB' the crystal was irradiated continuously for 10 minutes. (Note how rapidly the photoelectric current rises to and drops from its "initial" value i_0^ϕ represented by B, and how constant it remains during the whole subsequent ten minutes at its steady-state value as shown by the points along CD.) At the time D the voltage and the light were cut off simultaneously. The voltage was then re-impressed across the crystal at the time corresponding to EE' and the light turned on again immediately for a brief flash, whereupon the initial photoelectric current (i_0^ϕ) and dark current (i_t^D) were found to be equal to E and E', respectively. The sensitization was then allowed to proceed in the normal manner—voltage applied continuously, with occasional flashes of light to establish the degree of photosensitivity. *It is to be noted that constant illumination during the time interval B–D had* no detectable effect on the subsequent trend of the curves depicting dark current (i_t^D) *and photoelectric current* (i_0^ϕ). The sensitization appears to have continued its normal course along $EF(E'F')$ accompanied by the same steady-state current, as if during the illumination it had been neither hastened nor retarded. In other words the period of constant illumination simply served to displace the extension of AB and $A'B'$ along the time axis to EF and $E'F'$. The steady-state current i_s again is equal to the value of the dark current at $t=0(i_0^D)$.

In view of the close relationship existing between the dark current and photosensitization of a desensitized crystal, it was of especial interest to study the rate of sensitization as a function of temperature. If the dark current which we measure is of an electrolytic nature we should expect it to decrease very rapidly with decreasing temperature with a consequent decrease in the rate of sensitization. However, we found the contrary to be the case. Fig. 5 shows a family of curves depicting the initial photoelectric current i_0^ϕ as function of time measured from the application of the voltage or from the end of the incubation period, at a number of temperatures between and including room and liquid air temperatures. These results show that the rate of sensitization *increases* with *decreasing* temperature. This is in strong contrast to the results of Pohl and Stasiw in which they found the "rate" of sensitization of KCl to *increase* exponentially with *increasing* temperature at a rate comparable to the increase in electrolytic conductivity with increasing temperature. At liquid air temperature the rate of sensitization is so great that the stages of the increase are not observable by the means which we have hitherto used to study the effect.

In general the lower the temperature the greater the ultimate sensitivity attainable. However, as is to be seen from Fig. 5 there exists some inconsistency in the photoresponse at CO_2 temperature ($-79°C$) for it is somewhat less than the response at liquid ammonia temperature

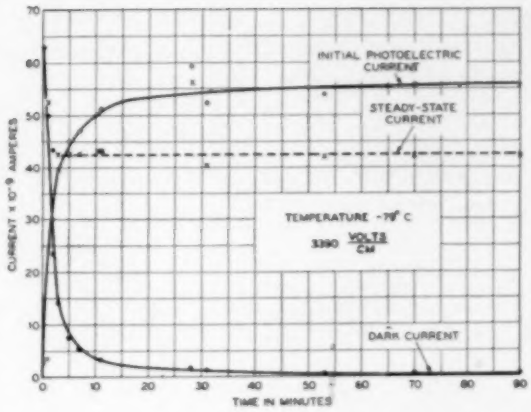

FIG. 6. Curves showing same relationships as Fig. 3 between rate of sensitization and decrease of dark current with time. These measurements were made on the same crystal as was used in Figs. 2, 3, etc. Measurements made at a date two months later.

(−33°C). Nevertheless we feel justified in concluding from numerous experiments that in general *the lower the temperature the greater the photoelectric sensitivity attainable.*

In view of the fact that the electrolytic dark current in inorganic salts, e.g., KCl, decreases exponentially with decreasing temperature, it appears improbable that the observed dark currents are of this character.

Fig. 6 shows the relations between dark (i_t^D) steady-state and initial photoelectric (i_0^*) currents as a function of time for −79°C. The same general behavior was found as in the experiments conducted at room temperature. These data were obtained some two months later on the same crystal as was used for the series of experiments given in Figs. 2 to 5. Comparison between the −79°C curve in Fig. 5 with the photoelectric current curve in Fig. 6 shows some of the effect of increase in age on the properties of the crystals. It has been generally observed that the dark conductivity tends to increase with increasing age of the crystals.

Comparison of x-ray patterns made of intrinsically sensitive (i.e., freshly-made) and desensitized crystals shows a marked difference in the physical state of the crystal: the sensitive crystals are found to be monocrystalline, whereas the desensitized ones show a polycrystalline fiber structure with considerable scattering.

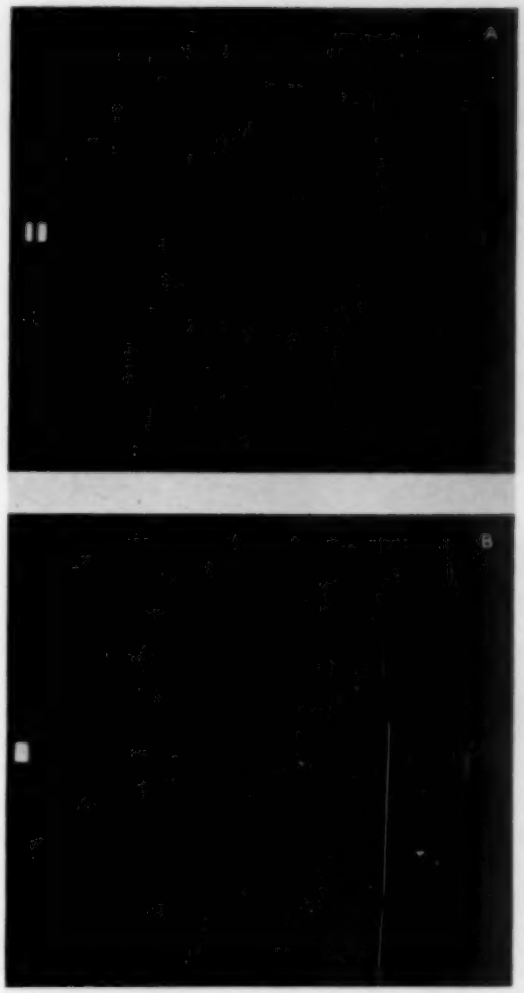

FIG. 7. X-ray diffraction patterns of (A) sensitive and (B) desensitized crystals. Retouched to bring out contrast.

Fig. 7A shows a typical x-ray diffraction pattern of a freshly-made sensitive crystal, while Fig. 7B is representative of the desensitized crystals. The lattice constants of the sensitive and desensitized crystals were found to be identical, with no detectable change in relative intensity of spots and without the appearance of new lines. The x-ray patterns of resensitized crystals were found to be identical with those of the desensitized ones, i.e., Fig. 7B.

It does not seem probable that the mechanism of sensitization used in the present work is identical with that which was used in the Stasiw and Pohl experiments; for: (1) the rate of sensitization does not increase exponentially

with increasing temperature as in the Stasiw and Pohl experiments, but on the contrary decreases with increasing temperature; (2) sensitization does not necessarily result merely from the passage of a dark current through the crystal but commences only when the dark current begins to decrease with time; (3) the dark current does not decrease exponentially with decreasing temperature but remains comparatively large at low temperatures.

In conclusion we wish to thank Dr. K. K. Darrow and Mr. E. J. Murphy for many stimulating and helpful discussions during the preparation of this manuscript.

JANUARY 1, 1935 PHYSICAL REVIEW VOLUME 47

Time Lags in Magneto-Optics

H. W. FARWELL AND J. B. HAWKES, *Columbia University*

(Received October 19, 1934)

A modification has been introduced in the apparatus usually employed for the time lag experiments, thereby enabling photometric measurements to be made. Minima were observed, but they were not confined to definite trolley positions. This apparatus has served to emphasize the variations in the exciting magnetic field, but has not disclosed evidence to support the view that sharp minima due to other causes are present.

THE problem of the time lag in the Faraday effect and of other possible related effects has been under examination for a long time, but within the past few years the results of Beams and Allison,[1] and particularly of Allison and his students,[2] have aroused much interest. The whole problem obviously demanded the attention of workers in numerous other laboratories, in order that the results might be checked, and if possible enough material obtained for a satisfactory basis to a theoretical treatment of the subject.

To assist in the study of this problem, the work reported in this article was begun about three years ago with the installation of apparatus substantially in accord with the descriptions in the references cited. On the first apparatus constructed the results were largely qualitative, and completely negative so far as sharp minima were concerned.

The qualitative results of the original set-up may be summarized in this way: First, the existence of the broad minimum for CS_2 in both cells was readily shown, and a satisfactory explanation in terms of the electrical constants of the circuit was demonstrated. This is in agreement with the findings of Slack and Breazeale[3] and of Webb and Morey.[4] Second, it was shown that temperature effects in the CS_2 cells were apt to be troublesome. Because of this water-cooled cells have been used since that time whenever measurements have been made. In addition the variability of the spark was clearly another hindrance to satisfactory observation.

Having failed to note definitely any sharp minima, one of us (H. W. F.) visited Dr. Allison's laboratory in August, 1933, where every courtesy was shown, and every opportunity given to study the apparatus, method of observing, as well as other details of the work. On the second day minima of the sharp type were seen in his apparatus. Minima were also seen a few days later in the laboratory of Professor F. G. Slack at Vanderbilt University.

Apparatus

Our apparatus was then completely rebuilt in a larger room, reproducing with extreme care every essential of the apparatus seen in Alabama. In some respects minor changes were introduced. For example the sliding bridge or "trolley"

[1] Beams and Allison, Phys. Rev. **29**, 161 (1927).
[2] Allison *et al.*, J. Chem. Ed. **10**, 2 (1932).
[3] Slack and Breazeale, Phys. Rev. **42**, 305 (1932).
[4] Webb and Morey, Phys. Rev. **44**, 589 (1933).

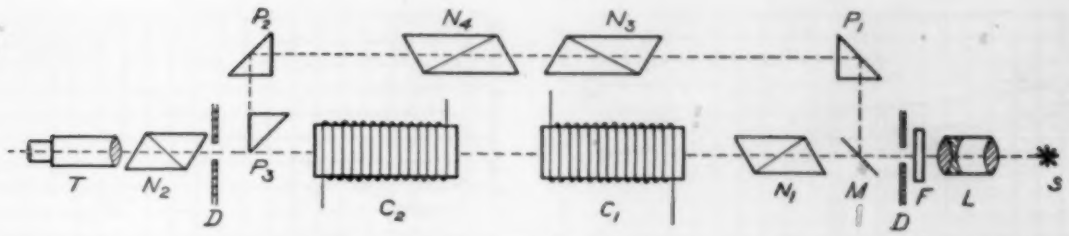

FIG. 1. Optical system used to give a comparison field. S, magnesium spark; L, lens; F, filter; D, diaphragms; N_1, polarizer for direct beam; C_1, C_2, Faraday cells inside coils; N_2, analyzer; T, telescope; M, cover glass at 45° to axis of system; P_1, P_2, P_3, right-angle prisms; N_3, polarizing Nicol in comparison train, set parallel to N_2; N_4, rotating Nicol from which scale angles are read for measuring intensities.

which moves over the long wires seemed in some of the set-ups to fail occasionally to make positive contact, and we had demonstrated that a minimum could be simulated by a contact variation. Our bridge therefore was designed to prevent such difficulty.

The hand wheel which operates the trolley by means of cords and pulleys was purposely arranged to facilitate slow motion of the trolley and no observer has been permitted to check the relation between the motion of the trolley and that of the periphery of the wheel.

After construction, the next task was to set our scale, and it was thought best to locate first the CS_2 minimum as accurately as possible and then to work from that to locate the HCl minimum generally used for setting the scale. The general region of the CS_2 minimum was found, but when HCl was used in the second cell, minima similar to those seen in Alabama were observed for many different trolley positions. Records of these minima failed to indicate any definite or favorite location and finally an attempt was made to locate them by having one of us observe while the other moved the hand wheel. The same sort of results as before were obtained, the observer at last reporting minima while the assistant had, without the observer's knowledge, ceased moving the trolley.

This led to the adoption of the arrangement shown in Fig. 1 for providing a comparison field. The light for the comparison field is thus a certain fraction of that passing through the experimental cells. Since the plane of the reflecting surface, M, is vertical, the first Nicol, N_3, in the "shunt" path was set to pass the vertical component. The second Nicol in the shunt path, N_4, has a circular scale and is initially set with its principal plane at right angles to that of N_3. The Nicol, N_4, is capable of rotation by turning either fast or slow motion knobs within easy reach of the observer. Since the analyzer, N_2, is set with its principal plane parallel to that of N_3, it follows that on rotation of N_4 through an angle θ there passes N_2 from the shunt path a horizontal component of magnitude $K \sin^2 \theta$, the value of K of course depending not only upon the source, but upon the number of reflecting surfaces and the characteristics of the media involved. Furthermore the amplitude of the light pulse passing N_2 from the direct path, as well as that from the shunt path, is directly related to the intensity of the original light from the spark, and if the optical paths are identical, the comparison of the two fields is independent of the intensity of the light from the source. (Actually in our arrangement the shunt path was about 20 cm longer, but this remained constant, and therefore introduced no great error.) As a result the rotation of N_4 is a measure of whatever takes place in the direct beam during the passage through the Faraday cells.

The angular aperture of the field observed was actually about five degrees, thus being sufficiently large to make proper comparison. While we took no measurements of field brightness, it should be stated that no measurements were taken on the apparatus until the observers had been in the dark for at least fifteen minutes. At the lowest intensities measured, the field could not be seen before fifteen or twenty minutes of dark adaptation.

If the adjustment is properly made, this arrangement should eliminate trouble caused by spark variation whether that variation is in actual brightness or in position between the

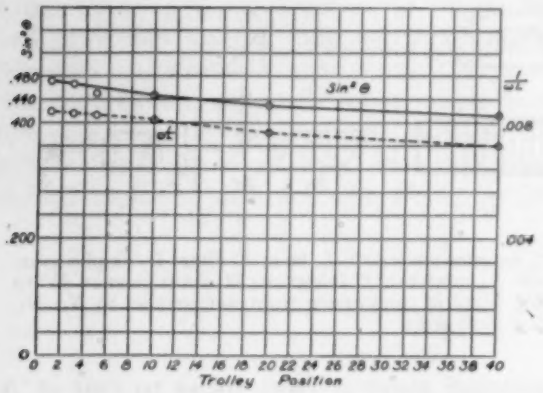

FIG. 2. Trolley position and light passed through cell C_2.

faces of the electrodes. Study of the change produced in the fields at the separating lines showed that change of spark position did not produce any abrupt change in the fields. We believe that this procedure is essential in such experiments as the one under discussion, whether the visual method or the photoelectric cell method of observation be used. Actually we used the visual method for two reasons, it was the one used by others in this work, and it is probably more satisfactory at the extremely low intensities involved. If further work on the problem is carried out, the two beams need not be brought into a single field but each may be passed through an analyzer and into a photoelectric cell, the two photo-cells being connected to oppose each other in feeding into the detector system.

TEST OF THE PHOTOMETER

Having a suitable measuring tool we first showed that the rotation produced in the Faraday cells was definitely related to spark gap width, increased intensity resulting from increased gap. An illustration of this is found in Fig. 5. Hereafter all readings were taken with gap adjusted to the same width after every two observations, the practise being to set Nicol N_4 for a match first from one side, when the comparison field was too bright, then from the other, when the comparison field was too dark. The mean of these two settings represented one reading for a photometric match.

To test the method more definitely we measured the amplitude of the light passing through

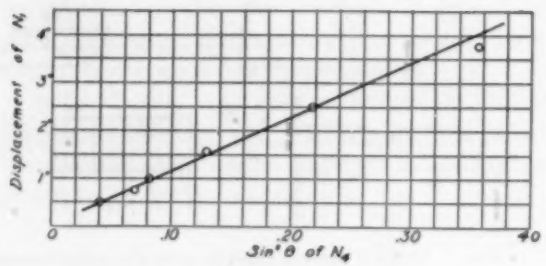

FIG. 3. Calibration of Nicol N_4.

cell C_2, whose coil was in series with the movable trolley, when cell C_1 and its coil were not used. The variation in the amplitude with trolley position is shown in Fig. 2 where the ordinate represents the square of the sine of the angle as read from the scale of N_4. The unit for the trolley scale is that usually employed and is equal to 15 cm, so that a change of position of the trolley a distance of 1 scale division means a change in electrical path amounting to 10^{-9} second. The zero on our scale is arbitrary, but very roughly, 10 on this scale corresponds to 15 on Allison's scale. Since the intensity of the light passing the analyzer N_2 is a function of the current in the coil, it should therefore be closely related to the impedance of the circuit. We have computed from our wave meter readings the values of $1/\omega L$ for different trolley positions. For the sake of comparison these are also shown in Fig. 2.

While this procedure is not quite rigorous, it is at least a very good approximation and it justifies the conclusion that the measuring apparatus is sufficiently reliable and sensitive for the purpose in hand. Further measurements with reference to electrical constants of the circuit have been quite in accord with the findings of Slack and Breazeale.[3]

A further test of the photometer consisted of a measurement of the intensity of the light passing N_2 when N_1 was set at various small angles to its normal position. This is in effect a calibration of the scale of N_4 for measuring rotation angles in the cell system. The result of this calibration is set out in Fig. 3.

MEASUREMENT FOR THE CS_2 MINIMUM

Then followed the resumption of tests to locate as accurately as possible the position of the minimum for CS_2 in both cells, since this has

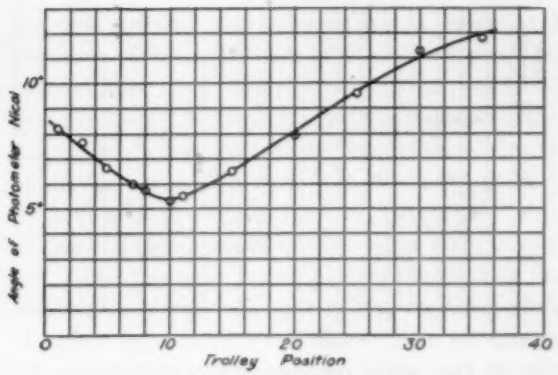

FIG. 4. Minimum observed for CS_2.

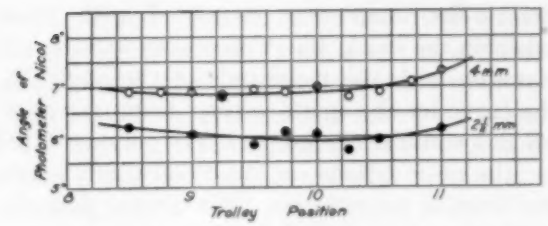

FIG. 5. Minimum observed for CS_2, enlarged scale.

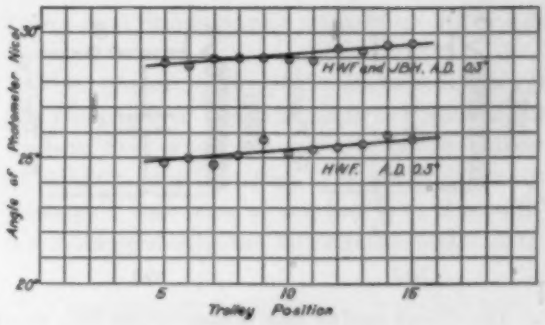

FIG. 6. Observations on HCl.

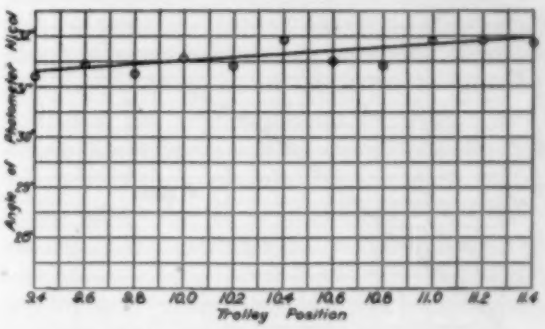

FIG. 7. Observations on HCl, enlarged scale.

been used by other observers as the standard reference point. The results of these tests are given in Figs. 4 and 5, where Fig. 4 gives a view of the test over a wide range, and Fig. 5 the results of two attempts to get more definite location. The data shown by Fig. 4 together with those from many similar runs indicate that the minimum is at 9.6 ± 0.5 scale divisions. The results shown in Fig. 5 indicate that the bottom of the curve is very flat and that this method will not give a more exact position than the one stated. Many attempts to observe fine detail in the intensity variation demonstrated only the considerable variation in the effective light, minima being frequently measured at points where later maxima appeared. Sets of observations over the same range served to average out these minima, thus proving that they represented only temporary effects. This result gave a fairly definite reference point from which the approximate position of reported minima could be calculated. This limitation of range seemed to be necessary in view of the somewhat laborious method we were using. In addition to these definite measurements we have carefully swept the region by moving the trolley slowly and watching for a change in the direct field after having set the comparison field for a match at the start. This procedure failed to indicate anything different from the results shown in our curves. It is our belief that this sweeping with the use of a comparison field is far more reliable than in the case with no comparison field.

OBSERVATIONS TO LOCATE THE HCl MINIMA

Since the sharp minima due to HCl have been given as perhaps the most pronounced and hence the most readily observed, and as located at $+0.75$ and $+0.85$ scale units from the CS_2 minimum, we felt justified in searching carefully in that region with our photometer. We have used various concentrations, but most of our measurements, including those of the diagram, were made with a concentration of HCl about 1/300 normal in the second cell. The results of various runs are given in Fig. 6 for a wide range, and in Fig. 7 for a detailed short run in the region where the minimum might be expected. Minima are thus observable, but all sharp minima fail to maintain their identity when the

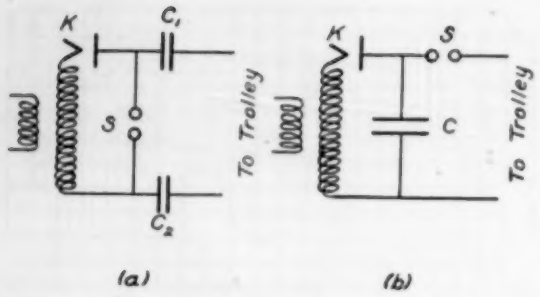

FIG. 8(a). Circuit used for most of observation; 8(b). circuit commonly used.

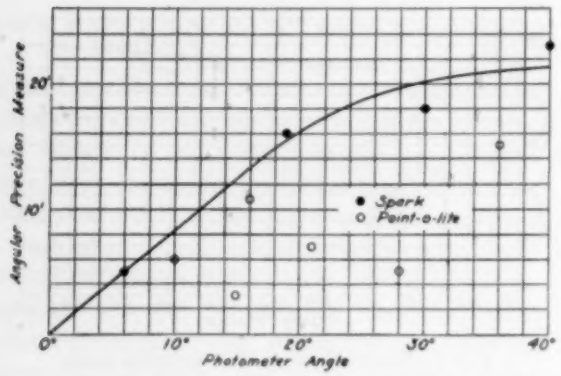

FIG. 9. Comparison of observations with different light sources.

results of repeated runs are averaged, leaving only the general form of curve to be expected from the difference in Verdet constants and the electrical constants of the circuit. No sharp minima at any characteristic trolley position were found when sweeping was employed. We are then obliged to conclude that on our set-up there are no permanent sharp minima for HCl.

FURTHER OBSERVATIONS TO CHECK RESULTS

For much of our work we used the circuit indicated in Fig. 8(a) instead of that of Fig. 8(b) which is commonly used in this experiment, but as far as our results go, the same conclusions hold with respect to both circuits.

Our condensers were normally mica condensers with small leakage and low dielectric loss, but the general results were the same with these as with glass plate condensers. The readings with the glass plate condensers were more irregular showing the influence of the factors mentioned.

Measurements on faint illuminations from a

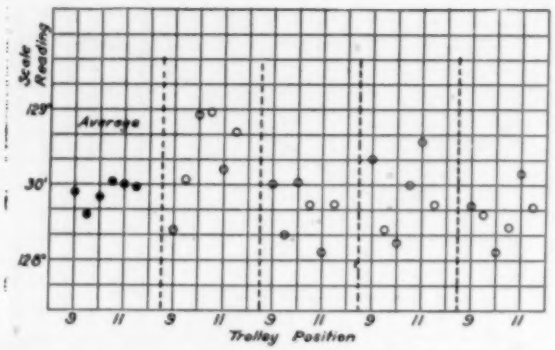

FIG. 10. Four sets of readings showing variations in Nicol readings in matching halves of the field.

Point-o-lite lamp were compared with those taken on the spark. Fig. 9 shows the variation in precision with the magnitude of the angle N_4, the curve for the spark settings being the average of a considerable number. The points plotted for the observations on the Point-o-lite source are from a normal run. This shows that the settings were more reliable if the source were constant. Since the personal errors are the same in the two cases it follows that the variations in the magnetic fields in the coils are responsible for some of the observed peculiarities.

Observation of the voltage across the primary of the high potential transformer at the time photometer settings were made indicated no changes in voltage sufficient to account for the intensity variations observed.

In practically every case our setting was made at the position where the two halves of the field showed the same general brightness, but seldom were conditions sufficiently steady to enable us to do better than to set at such a point that the direct beam was sometimes brighter and sometimes darker than the comparison beam. It is an open question as to the disadvantage suffered thereby but in view of various reports[5] on comparisons of steady fields at low illumination it seems probable that the accuracy of setting was not any the less on this account.

To illustrate further the sort of change observable we include in Fig. 10 the results of four individual runs made by the same observer. Each point is the mean of his two settings, and at the time of setting he was confident that any

[5] Blanchard, Phys. Rev. **11**, 81 (1918).

one setting was not in error by as much as 10 minutes. While the personal error is certainly present, the sensitivity is such that variations greater than 15 minutes can hardly be ascribed to personal error, but to variations for which the spark is responsible.

Our measurements further frequently show decided differences not only from day to day, but from hour to hour. For example, the first run in Fig. 10 shows most of the readings above those of later runs. We have tried to connect this with other known variables, the relative humidity for example, but so far as our records go the relation is not obvious. Careful watch of the magnesium electrodes shows that their behavior is not uniform, they wear away at a different rate at one time than another; sometimes the spark is held for quite a period at one local spot, and then it seems to wander more or less uniformly over the face of the gap. We are of the opinion that at least a portion of this difficulty can be ascribed to lack of homogeneity in the electrodes.

Further study of the temperature effects already mentioned in connection with our first set brought out some interesting facts. Part of the disturbance was clearly due to heat developed in the wire of the coils and conducted through the cylinder walls to the liquids in the cells, CS_2 being particularly sensitive on account of the large temperature coefficient of its index of refraction. The distortion observed did not occur as soon as the current began to pass through the coil, as would have been the case if eddy currents caused by impurities had produced the heating, but only after a time interval which could be prolonged by blocking the cell up a trifle from the bottom. The water-cooled coil has eliminated this difficulty.

Still another temperature effect was caused by evaporation of the CS_2 from the opening used for filling. This effect was quite distinct from the other, in that the conduction of heat to the cell was possible over a considerable area and hence caused a gradual wandering and distortion of the beam. The evaporation was of course quite local, and produced some fairly sharp contrasts in the field of view, at times making it impossible to get satisfactory photometer settings. This difficulty was remedied by sealing up completely all tubes containing liquids with large vapor pressures.

The contrast between the success in discovering the cause of such disturbances when a comparison field was used and the failure properly to diagnose disturbances of one sort or another without it has been so marked that it would be a serious oversight not to emphasize the fact.

Consideration of Subjective Effects

Slack[6] has called attention to the very considerable influence of subjective reactions in all work of this sort. It is of course not to be expected that our work is free from such difficulties, but comparison between our attempts to locate, for example, the CS_2 minimum by observing the single direct beam and by comparing the direct beam with the comparison beam, show that the latter method is far more successful. During the course of our experiments we have been aware of numerous subjective effects, such as change of size of field, pseudocolor differences and general fatigue.

In the matter of suggestion we have been most careful to keep the observer in ignorance of the trolley position, the order in which readings were taken, and the values of the readings on the scale of N_4. For example, it has not been possible for him to know on any given trial whether he was taking an observation with the same or a different trolley position. Until the run was completed, the sole task of the observer has been to match the two fields in front of him.

A peculiar result which, however, does not seem to bear upon our conclusions is the fact that almost invariably one of us sets the Nicol, N_4, at larger angles over a given run than does the other. Since the work is practically all done with filters there is no clear-cut explanation on the ground of color difference, and at present we have no suitable answer, but suggest that it will be found in physiological or psychological terms.

Conclusions

Our experiments warrant the support of the following conclusions:

(1) Observations of a single low intensity op-

[6] Slack, Phys. Rev. **45**, 126 (1934); J. Frank. Inst. **218**, 445 (1934).

tical field produced by a spark are unreliable not only on account of physiological and psychological effects, but also because of variations in the spark discharge itself, those variations being due to numerous causes.

(2) In our apparatus the intensity of the beam transmitted by the Faraday cells is consistent with predictions from the Verdet constants of the liquids used and the constants of the electrical circuit.

ACKNOWLEDGMENTS

In the course of these experiments we have enjoyed the cooperation of various members of the departments of chemistry and electrical engineering as well as of our own, and we wish particularly to thank Professor H. T. Beans of the chemistry department for his able advice and assistance and Messers. Arthur Roberts, E. H. Green and G. L. Buc for ready assistance in some of the darkest hours.

JANUARY 1, 1935 PHYSICAL REVIEW VOLUME 47

On Nuclear Moments

D. R. INGLIS, *University of Pittsburgh*

(Received November 1, 1934)

The magnetic moments of nuclei, most of them known only roughly, and their more accurately known ratios, can be fairly well explained quantum mechanically on the basis of the following assumptions: Nuclei are built of protons whose spin is 1/2 with a gyromagnetic ratio -5 (the magnitude 5/2 of the magnetic moment agreeing with deflection experiments) and of neutrons whose spin is 1/2 with a gyromagnetic ratio -1.1; according to atomic number and mass at most one of these particles with a possible "orbital" angular momentum exists outside of "closed shells" and in addition possibly two neutrons *without* "orbital" moment. The coupling scheme is selected according to physical considerations analogous to those of atomic theory, and consistent with the importance of the proton-neutron bond. Only states of lowest spin-orbit coupling energy of the proton are realized.

NUCLEI with even atomic number Z and even mass number A have no observed magnetic moment. In the light of this and other evidence for the existence of "closed shells" of protons and neutrons in nuclei, attempts have been made by Landé,[1, 2, 3] by Tamm and Altschuler[4] and by Schueler[5] to interpret observed nuclear magnetic moments as resulting from the spins and "orbits" of the few particles not in closed shells. While it is not yet clear that the interactions between particles in the nucleus are of such a nature that the magnitude of the orbital angular momentum of a single particle is conserved, there seems to be enough of value in the results[3] that the basic assumptions should be tested in as unobjectionable a manner as possible.

In several nuclei with A odd Z odd, one proton with spin and orbital momentum suffices to correlate the observed moments. It we invoke in addition to the proton two "free" neutrons (as for other nuclei it seems we must), the simplest assumption is that the extra neutrons have no orbital angular momenta, but only spins, s_n. The only orbital moment is that of the proton, l_π. Tamm and Altschuler allowed also a neutron orbital moment l_n, limited by a condition that had only an empirical meaning, their complete coupling scheme being $\{(l_\pi s_\pi)[l_n(s_n s_n)]\}$ for A odd Z odd. The strong coupling between the spins of two electrons (familiar as Russell-Saunders coupling) depends on the identity of the two particles and should not exist between the spins of a proton and a neutron. The spin-orbit coupling arises from the motion of the particle in a radially non-uniform electric field, and may be very strong for a proton (*or neutron*) in the nu-

[1] Landé, Phys. Rev. **44**, 1028 (1933).
[2] Landé (erroneously signed "Inglis and Landé") Phys. Rev. **45**, 842 (1934); **46**, 76 (1934).
[3] Landé, Phys. Rev. **46**, 477 (1934).
[4] Tamm and Altschuler, Acad. U. S. S. R. **1**, 455 (1934).
[5] Schueler, Zeits. f. Physik **88**, 323 (1934).

cleus, so that l_τ and s_τ have a constant sum j_τ (that is, j_τ^2 is a constant of the motion).

The facts of nuclear stability are interpreted[6] to show that the strongest interaction in the nucleus is that between a proton and a neutron. While the nature of this force is not completely understood, analogy with the coupling of vectors in atoms makes very plausible the assumption that the strong force between a proton and a neutron gives rise to a strong coupling between their moments—stronger than the exchange coupling between the neutrons. In a nucleus with a proton and with two neutrons (having spin moment only) outside of closed shells, the mechanical moment of the proton j_τ and that of one of the neutron spins s_τ are apt to have a constant sum j. To this the spin of the other neutron may be added to make up the total mechanical moment of the nucleus, I. The coupling of j_τ to one s_τ may be greater than to the other s_τ because the two neutrons are in general in different states.

The coupling scheme $\{[(l_\tau s_\tau)s_\tau]s_\tau\}$ may therefore be considered physically preferable.[7] It gives fairly satisfactory results only if we assume the g-values to be about $g_p=-5$ for the proton spin,[8] and $g_n=-1.1$ for the neutron spin (together with the conventional g-value 1 for the proton orbit). For a given l_τ, the proton spin may be oriented in such a way as to make $j_\tau=l_\tau-\frac{1}{2}$ or $l_\tau+\frac{1}{2}$, but with a negative value of g_p the spin-orbit interaction should be such as to make the state $j_\tau=l_\tau-\frac{1}{2}$ the lower. The formulas[9] for g-values involving these lower states are listed and evaluated in Table I. Those involving the other states appear in Table II. If the spin-orbit interaction is strong and of the type found in atomic electrons, there should be a preference for the nuclear g-values found in Table I. In Table III are listed nuclear mechanical moments I and approximate experimental g-values, together with their more accurately known ratios.

TABLE I. *Nuclear g-values, type* $l_\tau=j_\tau+1/2$.

I	j	j_τ		
1/2		I	$(4-g_p)/3$	$=3$
	1	1/2	$(8-2g_p+3g_n)/9$	$=1.63$
		3/2	$(6-g_p-2g_n)/3$	$=4.40$
3/2		I	$(6-g_p)/5$	$=2.2$
	1	1/2	$(4-g_p+6g_n)/9$	$=0.27$
		3/2	$(6-g_p+g_n)/6$	$=1.65$
	2	3/2	$(54-9g_p+5g_n)/50$	$=1.87$
		5/2	$(8-g_p-2g_n)/5$	$=3.04$
5/2		I	$(8-g_p)/7$	$=1.86$
	2	3/2	$(18-3g_p+10g_n)/25$	$=0.88$
		5/2	$(16-2g_p+g_n)/15$	$=1.66$
	3	5/2	$(160-20g_p+7g_n)/147$	$=1.72$
		7/2	$(10-g_p-2g_n)/7$	$=2.46$
7/2		I	$(10-g_p)/9$	$=1.73$
	3	5/2	$(40-5g_p+14g_n)/49$	$=1.01$
		7/2	$(30-3g_p+g_n)/28$	$=1.60$
	4	7/2	$(350-35g_p+9g_n)/324$	$=1.62$
		9/2	$(12-g_p-2g_n)/9$	$=2.15$
9/2		I	$(12-g_p)/11$	$=1.54$
	4	7/2	$(70-7g_p+18g_n)/81$	$=1.05$
		9/2	$(48-4g_p+g_n)/45$	$=1.49$
	5	9/2	$(648-54g_p+11g_n)/605$	$=1.50$
		11/2	$(14-g_p-2g_n)/11$	$=1.65$

TABLE II. *Nuclear g-values, type* $l_\tau=j_\tau-1/2$.

I	j	j_τ		
1/2		I	g_p	$=-5$
	1	1/2	$(2g_p+g_n)/3$	$=-3.7$
		3/2	$(10+5g_p-6g_n)/9$	$=-0.94$
3/2		I	$(2+g_p)/3$	$=-1$
	1	1/2	$(g_p+2g_n)/3$	$=-2.4$
		3/2	$(10+5g_p+3g_n)/18$	$=1.02$
	2	3/2	$(6+3g_p+g_n)/10$	$=-1.01$
		5/2	$(28+7g_p-10g_n)/25$	$=0.16$
5/2		I	$(4+g_p)/5$	$=-0.20$
	2	3/2	$(2+g_p+2g_n)/5$	$=-1.04$
		5/2	$(56+14g_p+5g_n)/75$	$=-0.26$
	3	5/2	$(16+4g_p+g_n)/21$	$=-0.24$
		7/2	$(54+9g_p-14g_n)/49$	$=0.50$
7/2		I	$(6+g_p)/7$	$=0.14$
	3	5/2	$(4+g_p+2g_n)/7$	$=-0.45$
		7/2	$(30-3g_p+g_n)/28$	$=1.60$
	4	7/2	$(30+5g_p+g_n)/36$	$=0.14$
		9/2	$(88+11g_p-18g_n)/81$	$=0.61$
9/2		I	$(8+g_p)/9$	$=0.33$
	4	7/2	$(6+g_p+2g_n)/9$	$=-0.13$
		9/2	$(352+44g_p+9g_n)/405$	$=0.31$
	5	9/2	$(48+6g_p+g_n)/55$	$=0.31$
		11/2	$(130+13g_p-22g_n)/11$	$=0.74$

[6] e.g., Heisenberg, Zeits. f. Physik **77**, 1 (1933); **78**, 156 (1933); **80**, 587 (1933).

[7] In behalf of the use of any simple extreme-coupling scheme wherein the vector model is valid, rather than some intermediate case, be it remarked that in atoms (Inglis and Johnston, Phys. Rev. **38**, 1642 (1931)) the variation of the g-value is at first very gradual as the type of atom varies from an extreme coupling into intermediate coupling. Validity of the result does not depend on strict realization of the extreme coupling.

[8] Suggested by Breit and Rabi, Phys. Rev. **46**, 230 (1934), whose suggested value of $g_{\text{theor.}}$ for Li appears in Table III.

[9] For the lone proton case, $j_\tau=I$, with $l_\tau=j_\tau+1/2$, $g=1+(1-g_p)/[1\pm(2I+1)]$. For the case $\{[(j_\tau s_\tau)s_\tau]s_\tau\}$, it is necessary to distinguish between the various $\pm$ signs with primes: if $j=I\pm 1/2$, $j_\tau=j\pm'\ 1/2$ and $l_\tau=j_\tau\pm''\ 1/2$, then g is given by the closed formula

$$g=\left(1+\frac{1}{1\pm(2I+1)}\right)\left(1+\frac{1}{1\pm'(2I+1\pm 1)}\right)\times\left(1+\frac{1-g_p}{1\pm''(2I+1\pm'1\pm 1)}-g_n\right)+g_n.$$

TABLE III. *Approximate "experimental"* and "theoretical" g-values.*

	I	$g_{exp.}$	$g_{theor.}$	l_v
Type $(l_v s_v)$* or $\{[(l_v s_v)s_v]s_v\}$				
Li_7^3	3/2	**2.19**	2.2*	2
F_{19}^9	1/2	3	3*	1
Na_{23}^{11}	3/2	1.4	1.65	2
Al_{27}^{13}	1/2	4	4.4	2
K_{39}^{19}	3/2	0.4	0.27	1
Cu_{63}^{29}	3/2	1.8	1.87	2
Cu_{65}^{29}	3/2	1.8	1.87	2
Ga_{69}^{31}	3/2	1.4 } **1.27**	1.65 } 1.33	2
Ga_{71}^{31}	3/2	1.8 }	2.2* }	2
As_{75}^{33}	3/2	0.6(?)	0.27(?)	1(?)
Rb_{85}^{37}	5/2	0.6 } **3.47**	0.88 } 3.46	2
Rb_{87}^{37}	3/2	2.0 }	3.04 }	3
In_{115}^{49}	9/2	1.2	1.05	4
Sb_{121}^{51}	5/2	1.1 } **1.36**	2.46 } 1.32	4
Sb_{123}^{51}	5/2	0.7 }	1.86* }	3
Cs_{133}^{55}	7/2	0.7	1.01	3
Au_{197}^{79}	3/2	0.2	0.27	1
Tl_{205}^{81}	1/2	2.8 } **1.01**	3*	1
Tl_{203}^{81}	1/2	2.8 }	3*	1
Bi_{209}^{83}	9/2	0.8	1.05	4
Type $(l_v s_v)$* or $\{l_v(s_v s_v s_v)\}$				
Cd_{111}^{48}	1/2	−1.3	−1.1*	
Cd_{113}^{48}	1/2	−1.3	−1.1*	
Sn_{119}^{50}	1/2	−1.9	−1.83	
Ba_{137}^{56}	3/2	0.6(?)	0.66	
Hg_{199}^{80}	1/2	1.1 } **−3.0**	1.1 } −3.0	
Hg_{201}^{80}	3/2	−0.4 }	−0.37* }	
Pb_{207}^{82}	1/2	1.2	1.1	

*Experimental values are taken from references 3 and 8 (trusting most Fermi and Segré, or Schueler's recent application of their formula) augmented and corrected by (Sb) Tolanski, *Proc. Roy. Soc.* **146**, 182, (1934), (F) Brown and Bartlett, *Phys. Rev.* **45**, 537 (1934); (Tl) Wills, *Phys. Rev.* **45**, 383 (1934); (K) Millman, Fox and Rabi, *Phys. Rev.* **45**, 769 (1934); and verified by (Na) Ellett and Heydenburg, *Phys. Rev.* **46**, 589 (1934); Rabi and Cohen, *Phys. Rev.* **46**, 707 (1934); and (Cs) Granath and Stranathan, *Phys. Rev.*, **46**, 317 (1934), Cohen, *Phys. Rev.* **46**, 713 (1934), but not by Barth, *Zeits. f. Physik* **91**, 272 (1934) who finds $I_{Cs}=5/2$. The magnetic moments of *elements printed in italics* have been determined from more than one configurgation, and are therefore more reliable than most of the others: Fermi and Segré *Zeits. f. Physik* **82**, 729 (1933).

In several cases the g-values are experimentally uncertain by more than ten percent, but in addition there is perhaps a greater theoretical uncertainty, due to the fact that the validity of an approximate solution of the many-electron problem is assumed in deducing g-values from experimental levels of hyperfine structure. On the fairly safe assumption that the solution is the same for two isotopes, the ratio of the g-values of two isotopes contains only the experimental uncertainty. The more accurately known data are printed in bold-faced type. The theoretical g-values in Table III were selected from Tables I and II to fit the data best.[10] *The fact that practically*[10] *all the best values are found in Table I (lower proton states) is an argument for the validity of this interpretation.*

In nuclei having one free neutron with, and possibly two without, orbital moment (A odd Z even), the spin-orbit interaction of the one neutron which has orbital moment may give rise to the strongest coupling, since the interaction between the neutrons is comparatively small. The two neutrons without orbital moment, being in similar states (analogous to s-states), may have their spins more closely coupled together than to the spin of the other neutron. This suggests as an approximation the coupling scheme $\{(l_v s_v)(s_v s_v)\}$. But the spin-orbit coupling of the neutron might be much smaller than that of a proton (g_n is smaller than g_p, and even so simple an effect as an electrostatic crowding of the protons toward the outside of the nucleus could reduce the coupling). This suggests that the coupling scheme $\{l_v(s_v s_v s_v)\}$ used by Tamm and Altschuler for this type is also possibly a reasonable approximation. The few data for this type of nucleus, among which the most important is the ratio of g-values for Hg, are interpreted almost equally successfully by either scheme. They are listed at the bottom of Table III with theoretical values according to the Tamm-Altschuler scheme $\{l_v(s_v s_v s_v)\}$.

DISCUSSION OF RESULTS

The results of our hypotheses, as listed in Table III, are in good enough agreement with the present "experimental" results so that there is no direct contradiction between them. On the other hand, if we assume all measurements to be correct, two or three cases require a greater uncertainty in the calculated value of the magnetic field at the nucleus than one might intuitionally like to admit. That part of this might be due to error in measurement seems probable in view of several changes in accepted experimental values of g and even of I within the past year. The results are most significantly adjudged in terms of the fraction of the calculated field at the nucleus which would have to be added to it (and attributed to something neglected in the approximate solution of the extra-nuclear problem) to bring about agreement; that is, in

[10] Possible exceptions are Bi, Cs and As. For Bi, Goudsmit, and for Cs, Schueler and Fermi and Segré give more favorable data than are listed. Arsenic is experimentally uncertain.

terms of $(g_{\text{theor.}}-g_{\text{exp.}})/g_{\text{theor.}}$. Aside from the quite uncertain case of As, the most adverse case is Sb, wherein, in order to get agreement of the ratio, one must suppose a 60 percent deviation from the calculated field of the electron cloud. Next to that worst case comes Cs, where a similar discrepancy of 30 percent is found. It is satisfactory that, among the cases determined from more than one atomic configuration (and printed in italics in Table III), there should be no discrepancy of more than about 15 percent (In and Cd).

The value of $g_p=-5$ is determined by the case of Li and by deflection experiments (the value 5 failing elsewhere in this scheme). Thereafter the value of $g_n=-1.1$ is determined most critically by the ratio for Rb (another possibility there, $g_n=-2$, is forbidden by discrepancies of magnitudes but not ratios in Cd and Hg). A negative gyromagnetic ratio for a positively charged particle is perhaps surprising, but not alarming in view of the failure of the Dirac value 2.

Presupposing, as we have, the applicability of the quantum mechanics to the heavy particles in the nucleus, one would like to believe that the deuton H_2^1 is a rotator stable in its zero rotational state. In that case, its moments ($I=1$, $g=0.7_5$) would be due entirely to spin and inexplicable with as small a g_n as we have here used. While simpler in number of particles, this nucleus lacks the steadying influence of a heavy charged core and may therefore be essentially a more complicated problem than the first approximation for the heavier nuclei. (For example, the spin-spin coupling may align the spins along the body axis of the rotator, making the rotation intricate.) The deuton problem being unsolved, the deuton data cannot invalidate our scheme.

The assumption that two extra neutron spins appear from closed shells when one particle will not suffice seems at first very arbitrary, but may be made plausible by consideration of possible energies. A strictly analogous assumption is made to explain the spectra of atoms of the iron group, where the lowest configuration $3d^5 5s$ of Cr follows $3d^3 5s^2$ of V. In either case, the spins of two particles which, if alone, would form a closed shell, seem to find that interaction with the spin of some other particle is energetically more advantageous than is the closed shell.

The agreement with the fairly accurately known data—the ratios and the value for Li—is satisfactory. The number of accurately known data is not sufficient to make possible a convincing array of close agreements. Since there are several ways that a coupling scheme might have been selected and several choices of values consistent with the coupling selected, a general agreement with the present data demonstrates only the possibility, not the validity, of this simple scheme. But the empirical selection of states of lowest spin-orbit energy is surprising, and quite improbable unless physically founded.

Note added to proof, December 7. THE DEUTON magnetic moment may be deduced fairly satisfactorily from the spin moments here used if one *assumes* the stability of the first rotational state. (It has been suggested that a similar assumption might account for the fact that the mass defect of the alpha-particle is much more than four times that of the deuton.) In addition to some large term representing proton-neutron binding, which leads to wave functions involving the usual spherical harmonics, we introduce into the Hamiltonian the magnetic perturbation terms

$$\mathbf{H}'=(g_n/r^3)\mu_N^2\{g_p[3(s_\pi\cdot r)(s_\nu\cdot r)/r^2-(s_\pi\cdot s_\nu)]-3(j\cdot s_\nu)\}-g_p\mu_N(s_\pi\cdot H)-g_n\mu_N(s_\nu\cdot H)-\mu_N(j\cdot H)/2$$

representing the magnetic spin-spin and rotation-spin coupling, and a small external magnetic field H. Here s_π and s_ν are Pauli spin operators, j is rotational moment, μ_N is the nuclear magneton $\mu_B/1840$, and r the proton-neutron separation. In order to deduce the factor 3 of the rotation-spin term $(j\cdot s_\nu)$ it is necessary to use the relativistic consideration applied by Thomas to atomic spin-orbit coupling, obtaining the result that the magnetic field at the neutron in the coordinate system of the neutron is 3/4 as great as it would be if the neutron were at rest, the relative motion of proton and neutron remaining unchanged. Considering only the lowest vibration state, the perturbation energy matrix reduces according to rotational states j, and according to projections M of the total angular momentum, so that we have for $j=1$ and $\pm M=1$ the submatrix

$\pm m_j$	$\pm m_{s_\pi}$	$\pm m_{s_\nu}$			
1	$\frac{1}{2}$	$-\frac{1}{2}$	$(g_p+15)A\mp\mu_1 H$	$6g_pA$	$(3g_p+30)A/\sqrt{2}$
1	$-\frac{1}{2}$	$\frac{1}{2}$	$6g_pA$	$(g_p-15)A\mp\mu_2 H$	$3g_pA/\sqrt{2}$
0	$\frac{1}{2}$	$\frac{1}{2}$	$(3g_p+30)A/\sqrt{2}$	$3g_nA/\sqrt{2}$	$2g_pA\mp\mu_0 H$.

where $A=\overline{(g_n/r^3)}\mu_N^2/10$, $\mu_1=(1+g_p-g_n)\mu_N/2$, $\mu_2=(1-g_p+g_n)\mu_N/2$, and $\mu_3=(g_p+g_n)\mu_N/2$. The perturbation term of the energy we write $\epsilon\mp g\mu_N H$, where g is the ratio of magnetic to mechanical moment of the system in the state of which the energy for $H=0$ is ϵ, in the usual perturbation procedure (setting $g_p=-5$, $g_n=-1.1$, $g_pA=a$):

$$\begin{vmatrix} -2a\mp\mu_1 H-(\epsilon\mp g\mu_N H) & 6a & -3a/\sqrt{2} \\ 6a & 4a\mp\mu_2 H-(\epsilon\mp g\mu_N H) & 3a/\sqrt{2} \\ -3a/\sqrt{2} & 3a/\sqrt{2} & 2a\mp\mu_3 H-(\epsilon\mp g\mu_N H) \end{vmatrix} =0.$$

The lowest root for $H=0$ is $\epsilon/a=-6.69$, which, inserted in the determinant, leaves only the terms in H (we neglect Paschen-Back terms in H^2), leading to

$$g=\frac{\frac{\mu_1}{\mu_N}\begin{vmatrix} 4-\epsilon/a & 3/\sqrt{2} \\ 3/\sqrt{2} & 2-\epsilon/a \end{vmatrix}+\frac{\mu_2}{\mu_N}\begin{vmatrix} -2-\epsilon/a & -3/\sqrt{2} \\ -3/\sqrt{2} & 2-\epsilon/a \end{vmatrix}+\frac{\mu_3}{\mu_N}\begin{vmatrix} -2-\epsilon/a & 6 \\ 6 & 4-\epsilon/a \end{vmatrix}}{\begin{vmatrix} 4-\epsilon/a & 3/\sqrt{2} \\ 3/\sqrt{2} & 2-\epsilon/a \end{vmatrix}+\begin{vmatrix} -2-\epsilon/a & -3/\sqrt{2} \\ -3/\sqrt{2} & 2-\epsilon/a \end{vmatrix}+\begin{vmatrix} -2-\epsilon/a & 6 \\ 6 & 4-\epsilon/a \end{vmatrix}}=-0.60, \text{ whereas } |g_{exp}|=0.7_5.$$

Erratum: Thermal Expansion and the Ferromagnetic Change in Volume of Nickel

CLARKE WILLIAMS, *Columbia University*

(Phys. Rev. **46**, 1011, 1934)

THE coordinates of the point on Fig. 5, referred to in the third paragraph of the first column on page 1014, are Temperature 450°C, and Coef. of Exp. 15.9×10^{-6}. This point was shown in Fig. 5 in the proof but disappeared subsequent to the return of the proof to the printer.

LETTERS TO THE EDITOR

Prompt publication of brief reports of important discoveries in physics may be secured by addressing them to this department. Closing dates for this department are, for the first issue of the month, the twentieth of the preceding month; for the second issue, the fifth of the month. The Board of Editors does not hold itself responsible for the opinions expressed by the correspondents.

Recent Measurements of Upper-Atmospheric Ionization

This letter is in the nature of an addendum to Dr. E. O. Hulbert's communication in the issue of this journal for November 1, 1934.

(1) In his brief account of the historical sequence of the identification of the various ionospheric regions it would appear that Dr. Hulbert has confused the main Region F_2 and the subsidiary "shelf" Region F_1. The identification of Region F_2 as a separate stratum existing above the well-known Kennelly-Heaviside layer (Region E) was made in nocturnal experiments in 1926–7.[1] In such experiments we know that Region F_1, which is of day-time occurrence only, could not have been detected. Evidence of the day-time formation of this region and of the symmetrical trend of its electron content relative to noon was first published in 1933.[2]

Since the maximum electron density in Region F_2 is always much greater than that in Region F_1, we must seek an explanation of radio skipped distances, if an electron-limitation hypothesis is accepted, in terms of Region F_2 ionization and not in terms of Region F_1 ionization, as Dr. Hulbert proposes to do. Support for such a view is found in the fact that the skipped distance has the same type of diurnal trend (asymmetry with respect to noon) as the temporal ionization variation in Region F_2 would lead one to expect. It does not follow the symmetrical variation of Region F_1 ionization relative to noon.

(2) There is substantial evidence conflicting with Dr. Hulbert's theory that the effective electrical carriers in the Kennelly-Heaviside layer are of molecular (and not electronic) mass. Effects of double refraction (echo-doubling)[3] and differential absorption of the ordinary and extraordinary reflected wave components,[4] due to the influence of the earth's magnetic field, are found for Region E as for Region F, and it may be shown that these phenomena can only be expected to occur if the effective electric charges are associated with electronic mass.

(3) The interpretation of the diurnal and seasonal trends of the critical penetration frequency for Region F_2 presents considerable difficulties. One view, urged by Kirby, Berkner and Stuart,[5] is that the measurements made when the sun is high (e.g., at summer noon) are entirely vitiated by absorption and that the ionization maximum really is greater on a summer noon than on a winter noon although the critical frequency measured in summer is not greater than that measured in winter. An alternative theory, which I put forward at a meeting of the International Scientific Radio Union in London (September, 1934) at which a world survey of ionospheric results was discussed, is that the critical frequency measurements, even allowing for a certain amount of absorptive effect, really do indicate an abnormal depression of the value of maximum ionization when the sun is high and that the occurrence of this abnormality is due to the increased temperature (and thus lower ion-production) and consequent expansion (and thus reduced *maximum* ionization content) of the outermost layers of the atmosphere.

E. V. APPLETON

Halley-Stewart Laboratory,
King's College,
London, England,
November 24, 1934.

[1] Appleton, Nature **120**, 330 (1927).
[2] Appleton, Nature **131**, 872 (1933) and Proc. Phys. Soc. **45**, 673 (1933); see also Schafer and Goodall, Nature **131**, 804 (1933).
[3] White, Proc. Phys. Soc. **46**, 91 (1934).
[4] Appleton and Ratcliffe, Proc. Roy. Soc. **A117**, 576 (1928).
[5] Kirby, Berkner and Stuart, Bur. Standards J. Research **12**, 16 (1934).

Natural Width of the $K\alpha$-Lines

The purpose of this note is to give a simple theoretical interpretation of some of the experiments dealing with the natural widths of x-ray lines. The results of Allison,[1] which exhibit an interesting variation of the widths of the $K\alpha$-doublet lines with atomic number, will be the main object of the present considerations; we hope to discuss quantitative refinements and extensions to other experimental situations in a later publication.

The widths of the $K\alpha$-lines arise almost entirely from the finite lifetimes of the energy states involved in the emission of the lines. Other effects, such as Doppler effects and perturbations due to the crystal potential, play a subordinate rôle. These lifetimes, in turn, are closely related to the probabilities of transition from the state whose lifetime is to be calculated, to energetically lower states. Under conditions[2] which are very nearly satisfied for a $K\alpha$-line, the energy width, ΔE, of such a line is the sum of the widths of two atomic states, that in which the K-electron is missing, and that in which the L-electron is removed from the atom. Subject to this interpretation, we write

$$\Delta E = \Delta E_K + \Delta E_L. \qquad (1)$$

We shall ignore the doublet structure of the lines in our present consideration.

When one K-electron is missing from the atom, the probability that an (n, l, m)-electron will fill the vacancy is given by

$$A_{K;\,n,\,l,\,m} = (64\pi^4/3)(e^2\nu^3/hc^3)\,|r_{K;\,n,\,l,\,m}|^2, \qquad (2)$$

and this probability expresses the average number of transitions of this type which occur per second. ν is the frequency of the spectral line corresponding to this transition, and $r_{K;\,n,\,l,\,m}$ the matrix element. The total number of possible transitions from the initial state of the $K\alpha$-line, i.e., the reciprocal of its lifetime Δt, is the sum of (2) over all n, l, m, including the states of the continuous spectrum:

$$1/\Delta t=\sum_{n,\,l,\,m}A_{K;\,n,\,l,\,m}=A_K. \tag{3}$$

To calculate the matrix elements in (2) would be a hopeless task. Instead, we introduce "oscillator strengths," $f_{K;\,n,\,l}$, using the relation

$$\sum_{m}|r_{K;\,n,\,l,\,m}|^2=(3h/8\pi^2m)\cdot(1/\nu)f_{K;\,n,\,l},$$

so that, because of (2) and (3),

$$A_K=(8\pi^2/c)\cdot(e^2/mc)\sum_{n,\,l}\nu^2{}_{K;\,n,\,l}f_{K;\,n,\,l}. \tag{4}$$

Since ν is independent of m, the summation over m is already completed. If the matrix elements in question involved but one electron moving in a fixed potential field, the sum rule

$$\sum_{n,\,l}f_{K;\,n,\,l}=1 \tag{5}$$

would be rigorously valid. In fact, however, we can only say that the sum of the f's connecting any one state with all other states, including multiple transitions, yields the value Z, the atomic number. Now the error made in applying the sum rule to the electrons in one closed shell is probably not very large. Thus, if both K-electrons were initially removed, we could state with fair accuracy that the sum over the f's of all possible transitions capable of filling the two vacancies is 2.[3] This sum would include numerous double jumps which are not considered when the sum rule is written for a single electron. Hence (5), while still correct as to order of magnitude, should read

$$\sum_{n,\,l}f_{K;\,n,\,l}=1-\delta, \tag{5^1}$$

where δ, a positive quantity, might be termed the "sum defect" for a K-electron.

Let us for the present suppose (5) to be correct. We can then calculate an approximate upper and a lower limit for A_K. The smallest possible frequency ν in (4) is equal to $\frac{3}{4}Z^2R$, where R is Rydberg's number, while the largest one will not be materially greater than Z^2R, which corresponds to the ionization limit for the K-electron. Thus

$$\frac{8\pi^2}{c}\cdot\frac{e^2}{mc}(\tfrac{3}{4}Z^2)^2R^2<A_K<\frac{8\pi^2}{c}\frac{e^2}{mc}Z^4R^2. \tag{6}$$

The same considerations may be applied to A_L. But here the smallest ν appearing in the sum like (4) is $(\frac{1}{4}-\frac{1}{5})Z^2R$, the largest is $\frac{1}{4}Z^2R$. We see, therefore, on inserting these values in (4) that A_L is smaller than A_K by about a factor 10 or more. This decrease is partially offset by an increase in f, for the f-sum over all the states in question is greater than one, since the f's to lower states, which are negative, must be excluded.

From Δt (cf. Eq. (3)) the natural width of the energy level and hence the frequency width is easily computed. According to the indeterminacy principle,

$$\Delta E\cdot\Delta t=h\Delta\nu\cdot\Delta t\geqq h/2\pi,$$

and one can see from the work of Weisskopf and Wigner[2] that, if the equality sign is here chosen, and Δt is defined by (3), the quantity $\Delta\nu$ refers to the full half-width of the frequency distribution. If we neglect A_L against A_K we find for the half-width of the $K\alpha$-line

$$\Delta\nu=A_K/2\pi. \tag{7}$$

According to previous remarks, ΔE_L, the width of the initial state of the L-lines, should be smaller by perhaps a factor 10 than ΔE_K, the width of the initial state of $K\alpha$. Experimental evidence on this point is available from the work of Richtmyer, Barnes and Ramberg,[4] who find for three different L-levels of Au the following values for ΔE: 8.7; 3.7; 4.4 volts, as against 40 volts for the ionized K-state. Moreover, it appears from the experiments of Richtmyer and Barnes[5] on the widths of the K-series lines for W that there is no strong variation in the width as one passes from one line to the other, indicating that it is the K-state which impresses its width upon each line.

If we plot $\Delta\nu$ from (7) against Z, with A_K given by (6), we obtain Fig. 1. The two curves indicate upper and

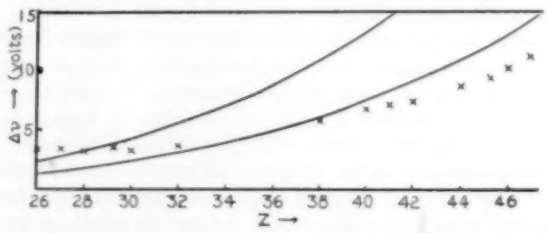

FIG. 1. Curves represent "sum rule limits" for half widths of $K\alpha$-lines. Crosses represent averages between values for $K\alpha_1$ and $K\alpha_2$ found by Allison.

lower limits in accordance with (6), the crosses are Allison's experimental points. In judging the agreement it must be borne in mind that we have neglected Auger effects which would tend to broaden the line. It is significant that the experimental widths for high atomic numbers are smaller than those given by this simple theory. This discrepancy seems to be due to what was called the sum defect, δ, arising partly from the absence of double transitions in the f-sum here used, and partly from an actual shift of oscillator strengths from inner to outer electrons as Z increases. This latter effect is also evident in the difficulties discussed by Bearden and Wheeler.[3] If experimental f-values, taken from x-ray absorption data, were substituted for the uncorrected ones here chosen, the agreement between the curves in Fig. 1 and Allison's points would be somewhat better.

HENRY MARGENAU

Yale University,
December 4, 1934.

[1] S. K. Allison, Phys. Rev. **44**, 63 (1933).
[2] Cf. V. Weisskopf and E. Wigner, Zeits. f. Physik **63**, 54 (1930).
[3] See, however, J. A. Wheeler and J. A. Bearden, Phys. Rev. **46**, 755 (1934), who find that this sum rule yields values somewhat larger than those obtainable from experiment.
[4] F. K. Richtmyer, S. W. Barnes and E. Ramberg, Phys. Rev. **46**, 843 (1934).
[5] F. K. Richtmyer and S. W. Barnes, Phys. Rev. **46**, 352 (1934).

The Fermi Proton Effect

E. Fermi and his co-workers[1] have recently discovered the remarkable effect of proton containing substances in *increasing* the yield of artificial radioelements during neutron bombardment. We had an opportunity to study this effect and some of our results are communicated below.

A silver cup was irradiated for 15 minutes with neutrons, from a Be-tube with 200 mC Rn, (1) in air, (2) filled to the rim with pure water and (3) filled and surrounded with water. The increase in activity depends to a great extent on the geometry of irradiation. The dimensions in case 3 are shown in Fig. 1.

The emitted electrons were counted by means of a He-filled Geiger-Müller tube and a thyratron operated counter. The results are plotted on logarithmic paper, as given in Fig. 2.

Filling the cup with water increases the silver activity three-fold and by surrounding it with water the activity is still further increased by a factor of 3–4. This increase is also produced in about the same degree by *n*-pentane (n-C_5H_{12}), while the effect of carbon tetrachloride (CCl_4) and carbon disulfide (CS_2) is practically negligible.

The addition of 5 percent uranyl nitrate to the water reduces the effect of pure water, as does boric acid.[1] The introduction of an Al-cylinder of 0.03 mm wall thickness between source and cup has practically no effect.

This Fermi phenomenon was also observed with iodine and aluminum cylinders. One should expect the same effect with neutrons produced by artificially accelerated ions.

In agreement with Fermi and as expressed by one of us in discussions previously, we believe that as the neutrons loose their energy by collisions they are more and more easily captured by nuclei with the production of stable or radioactive isotopes. The protons of the water absorb the energy of the neutrons by elastic collisions and the probability of capture of neutrons by protons (deutons

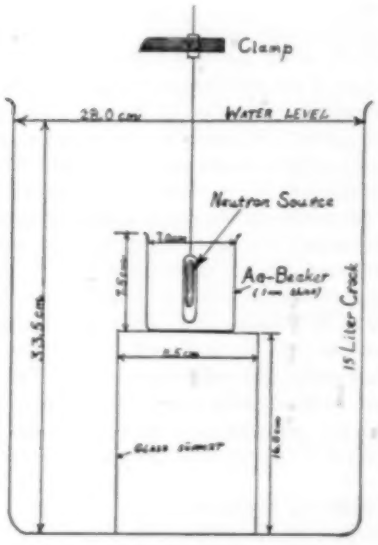

FIG. 1. Method of irradiating.

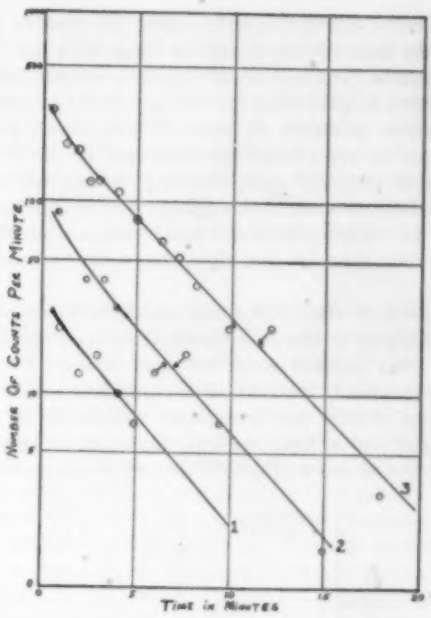

FIG. 2. Variation of the activity produced by bombarding silver with neutrons. (1) *AG*-beaker in air; (2) *AG*-beaker with water inside; (3) *AG*-beaker filled with and surrounded by water.

will be investigated) is evidently small, since a large quantity of neutrons are reflected backwards (see case 3).

It would be interesting to determine the neutron capture probability of different elements or isotopes placed between the source and the silver (or any other suitable material) and as indicated by the activity of the latter.

It is a pleasure to acknowledge our indebtedness to Dr. M. Cutler, of Michael Reese Hospital, for our sources and to Dr. W. D. Harkins for the loan of metallic beryllium.

A. v. GROSSE
M. S. AGRUSS

Kent Chemical Laboratory,
University of Chicago,
December 10, 1934.

[1] E. Fermi, E. Amaldi, B. Pontecorvo, F. Rasetti and E. Segrè, La Ricerca Scientifica **2**, No. 7–8, No. 9–10 (1934).

North-South Asymmetry of the Cosmic Radiation in Mexico

During a recent survey of cosmic-ray angular distributions, northern and southern intensities were compared at six different zenith angles in the plane of the local magnetic meridian. Measurements were made at two elevations in geomagnetic latitude 29°. The first station, referred to by the name Copilco, was on a ranch near Mexico City at an elevation of 2280 m. The second station was a camp on the summit of Nevado de Toluca, a volcano in the State of Mexico, elevation 4300 m.

The apparatus used was a new multidirectional coincidence counter which simultaneously recorded the intensi-

ties from seven different zenith angles. (Because of high horizons the data for the lowest of these have not been used.) Frequent rotations of 180° about a vertical axis at regular intervals gave data for comparing the intensities from opposite azimuths at each of the zenith angles without relying upon long-time constancy of the instrumental sensitivity, nor upon knowing the relative sensitivities of different coincidence groups. The operation and recording were wholly automatic and it was only necessary to set up the apparatus and then afterwards to read the records.

The results of the north-south comparisons represent but a small part of the data obtained on the expedition, but since they present some new and unusual features they are reported in advance of the complete account of the work. A definite southern excess was found at most zenith angles and at both stations. These are represented in Fig. 1, by the ratios of the differences of the south and

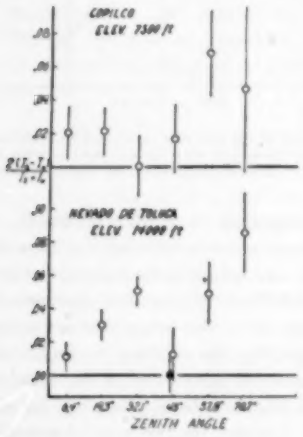

FIG. 1. Ratios of the difference to the average of south and north intensities at two stations in Mexico.

north intensities to their average value. Each point in the figure is the average of many independent determinations, and from the dispersion of the individual data the probable errors can be determined with considerable accuracy. These are represented by the vertical lines. Data for angles near the horizon are characterized by a small number of counts and the probable errors are correspondingly large. The point represented by the full dot was obtained in the same latitude at an elevation of 11,000 ft. in 1932.

A north-south asymmetry of this general character was first predicted by Lemaitre and Vallarta, though the excluded region diagrams of Störmer give a basis for the qualitative explanation. If attention is limited to rays of a particular energy which arrive from a direction parallel to the plane of the meridian this fixes the scale on which to represent the radius of the earth and it fixes the shape of the excluded regions. The component of the motion of a charged corpuscle resolved parallel to the meridian plane which rotates so as to always contain the corpuscle, is similar to that of a small ball rolling in the horn-shaped potential valley, a portion of which is represented in Fig. 2.

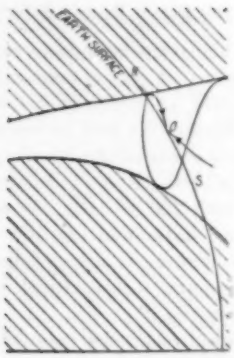

FIG. 2. Portion of the Störmer excluded region diagram for rays incident in the magnetic meridian in the latitude of Mexico, showing typical orbits incident from the north and from the south at the same zenith angle.

To be incident from the polar side of the observer at angles close to the horizon, rays would have to first pass through the earth as is indicated by the diagram, whereas from the equatorial side the orbit comes directly from external space. A lower northern intensity can thus be interpreted as a shadow effect. Since other energies are also to be taken into consideration the shadow is only a partial one. These considerations seem to account for the asymmetry at angles close to the horizon but the asymmetry near the zenith would seem to require more complicated orbits which first enter the horn on the opposite side of the equator where they penetrate the earth, thence passing out again, crossing the equator, and arriving at the point *O*. Recent calculations by Lemaitre and Vallarta have indicated the existence of such orbits and it is possible that they may account for the observed asymmetry at angles close to the zenith. It would also seem possible to account for a dip in the asymmetry such as is observed at 45° by a consideration of these same orbits. However, it is possible, though not probable in view of the similar results at both stations, that this dip is due to statistical fluctuations.

If the north-south asymmetry is to be attributed to shadow effects, along the lines indicated, it should depend upon the sum of the positives and negatives, and not upon their difference as in the case of the east-west asymmetry. The effect should disappear at the equator and should appear as a northern excess in southern latitudes.

I am indebted to M. S. Vallarta for urging me to make these further studies of the north-south intensities, as well as for his cooperation in carrying out the work. I also wish to acknowledge my gratitude to Dr. C. S. Margain for the use of his facilities at Copilco, to the Federal Government of Mexico for assistance on Nevado de Toluca, and to Mr. Lewis Fussell, Jr., for his help with the measurements and reduction of data. The work was carried out under a grant from the Carnegie Institution of Washington, administered by the Cosmic Ray Committee and the Department of Terrestrial Magnetism.

THOMAS H. JOHNSON

Bartol Research Foundation
of the Franklin Institute,
December 12, 1934.

Gamma-Ray Neutrons and the Fermi Proton Effect

We have observed that neutrons emitted by γ-rays from beryllium (Chadwick-Szillard effect) also show the Fermi proton effect.[1] Iodine was the element irradiated and a product with a half period of 24 minutes obtained.

Our neutrons were produced from 80 g of powdered Be (placed in a water-proof waxed paper cylinder of 75 mm diameter) by γ-rays from 0.50 g Ra contained in needles and filtered through 0.5 mm of Pt.

An iodine beaker was made by evenly coating the walls of a 600 cc Pyrex beaker (diameter = 8.5 cm, height = 11.5 cm) with 150 g of the element. The neutron source was placed in the iodine beaker and the latter in a 4.0 lit. beaker (diameter = 15.5 cm, height = 26.5 cm); the whole was placed in a safe protected with 2 cm of Pb.

The irradiation was run for 18 hours, (1) in *air* and (2) with the beakers filled to the rim with *water*. The results are plotted in Fig. 1.

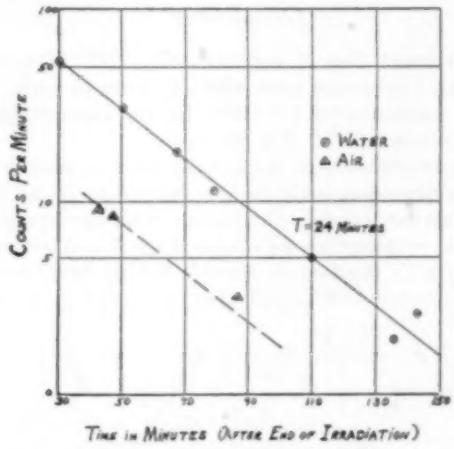

FIG. 1. Variation of time of the activity produced by bombarding iodine with neutrons produced by γ-rays.

Here, as with neutrons emitted by α-particles, the presence of water *increases* the induced radioactivity by a factor of *five*.

Again we are indebted to Dr. M. Cutler of Michael Reese Hospital for the source and to Dr. W. D. Harkins for the beryllium.

A. v. GROSSE
M. S. AGRUSS

Kent Chemical Laboratory,
University of Chicago,
December 12, 1934.

[1] E. Fermi, E. Amaldi, B. Pontecorvo, F. Rasetti and E. Segrè, La Ricerca Scientifica 2, No. 7–8, No. 9–10 (1934).

The Interaction Between Vibration and Rotation for Symmetrical Molecules

The problem of the vibration-rotation interaction in symmetrical molecules has recently been studied by Teller[1] who has shown that it will account for the anomalous spacing observed in the infrared bands of methane and of the methyl halides. We have somewhat extended the theory and have been able to revise Teller's calculations. The results appear to be of sufficient importance to warrant a preliminary report, reserving until later an account of the proofs on which they are based.

Teller has shown that the fine structure spacing of the zero branches ($\Delta K = \pm 1$, $\Delta J = 0$) in a perpendicular band of an axial symmetrical molecule has the form,

$$\Delta\nu = [(1-\zeta)/C - 1/A]h/4\pi^2,$$

where ζ is the angular momentum in units of $h/2\pi$ due to the vibratory motion alone. The value of ζ depends upon the potential constants of the molecule and may be computed in terms of them. The sum of the ζ's for all the first excited states of a given symmetry type is, however, independent of the potential constants and is a function only of the masses and dimensions of the system. Thus the sum of the line spacings of the fundamental bands of a given type (say the perpendicular bands) will yield information about the moments of inertia providing $\Sigma\zeta$ is known. Since $\Sigma\zeta$ is independent of the particular force constants it may be computed for extreme force fields where the motion of the system is readily obtainable. In this way we have found that for the symmetrical molecule YX_3, $\Sigma\zeta = C/2A - 1$, where C and A are the moments of inertia along and $\perp$ to the figure axis, respectively. For the molecule ZYX_3 (to which type the methyl halides belong) we find $\Sigma\zeta = C/2A$. Thus the sum of the line spacings of the three bands of the methyl halides should be, $\Sigma\Delta\nu = (3/C - 5/2A)h/4\pi^2$. These bands have been observed by Bennett and Meyer[2] who found the sum of the three line spacings to be, 24.65, 27.15, 28.32 and 28.5 cm^{-1} for CH_3F, CH_3Cl, CH_3Br and CH_3I, respectively. The moment of inertia A is known to be 39.5×10^{-40} for CH_3F. In the case of the other methyl halides its value has been estimated[3] to be 61, 89 and 99×10^{-40}, respectively. Combining these data we obtain $C = 5.90$, 5.65, 5.55 and 5.55×10^{-40} for CH_3F to CH_3I. The H–H distance for these molecules is accordingly 1.88, 1.84, 1.83 and 1.83×10^{-8}

The methane molecule possesses two active fundamental frequencies and for these we compute $\Sigma\zeta = \frac{1}{2}$, a result which agrees with Teller's conclusions. Using the line spacings found by Cooley[4] we obtain $I = 5.47\times10^{-40}$, H–H = 1.81 and C–H = 1.11×10^{-8}. It thus appears that the methyl group has essentially the same dimensions in the methyl halides and in methane. These values for the moments of inertia are based on the assumption that the motion is purely harmonic and hence may be subject to slight revision.

Dr. Rosenthal[5] has shown that the general potential function for the methane molecule contains five constants, A, B, C, D and E. These have not hitherto been evaluated since the molecule possesses but four normal frequencies. A fifth relation is now at hand since ζ_3 or ζ_4 may be computed as a function of the potential constants. We find

$$\zeta_i = (6\delta_i - 1)/(6\delta_i + 2) \qquad i = 3, 4,$$

where $\delta_i = 8D^2/(3m\lambda_i - A)^2$. By using this relation together

TABLE I. *Fundamental frequencies of the molecules of CH_4, CH_3D, CH_2D_2, CHD_3, CD_4.*

CH_4	(2914)	(1520)	3014			1304		
$(CH_3D)_+$	2944 ∥	1460 ⊥	2183 ∥,		3013 ⊥	1300 ∥,		1151 ⊥
$(CH_3D)_-$	2694 ∥	1406 ⊥	2993 ∥,		2796 ⊥	1036 ∥,		1289 ⊥
$(CH_2D_2)_+$	2141 M	(1317), 1424 M	2227 G,	2969 M,	3013 L	1228 G,	1019 M,	1082 L
$(CH_2D_2)_-$	2461 M	(1317), 1245 M	2768 G,	2771 M,	2536 L	989 G,	1089 M,	1285 L
$(CHD_3)_+$	2101 ∥	1286 ⊥	2992 ∥,		2222 ⊥	994 ∥,		1020 ⊥
$(CHD_3)_-$	2475 ∥	1136 ⊥	2166 ∥,		2549 ⊥	1163 ∥,		1007 ⊥
CD_4	(2061)	(1075)	2227			987		

with the four normal frequencies it is found that,

$A=7.670\times10^5$ dynes/cm $\quad D=\pm1.278$,
$B=0.476$ $\quad E=0.313$.
$C=0.341$.

The fundamental frequencies of the molecules CH_3D, CH_2D_2, CHD_3 and CD_4 may now be calculated using the equations developed by Dr. Rosenthal.[5] There are two solutions corresponding to the positive and negative values for the constant D. Our results are collected in Table I. The inactive frequencies are enclosed in brackets. In the case of CH_2D_2 the letter following the frequency indicates whether the electric moment vibrates along the axis of least, middle or greatest moment of inertia.

Professor Barker and Mr. Ginsburg have continued their investigation of the absorption spectra of the heavy methanes and they have very kindly allowed us to state that their results appear to conform very satisfactorily with the bands predicted by the solution using $D=+1.278$. The band reported by them[6] at 1090 cm^{-1} is thus probably due to CH_2D_2. If this identification is correct, it would of course invalidate their estimate of the moment of inertia of methane.

DAVID M. DENNISON
MANFRED JOHNSTON

University of Michigan,
Ann Arbor, Michigan,
December 13, 1934.

[1] E. Teller, Hand- und Jahrbuch d. Chem. Phys. **9**, 125 (1934).
[2] W. H. Bennett and C. F. Meyer, Phys. Rev. **32**, 888 (1928).
[3] S. L. Gerhard and D. M. Dennison, Phys. Rev. **43**, 197 (1933).
[4] J. P. Cooley, Astrophys. J. **62**, 73 (1925).
[5] J. Rosenthal, Phys. Rev. **45**, 538 (1934).
[6] E. F. Barker and N. Ginsburg, J. Chem. Phys. **2**, 299 (1934).

The Temperature Function of X-Ray Reflection in the Neighborhood of the Melting Point of a Crystal

In connection with some more extended work concerning the temperature variations of physical properties of metal crystals the following deviations from the Debye-Waller function concerning the temperature dependence of x-ray reflections have been observed in the neighborhood of the melting point of Bi crystals.

The apparatus used was the Bragg-spectrometer with stationary ionization chamber, described previously,[1] with added arrangements for heating the crystal in a neutral atmosphere under well controlled temperature conditions up to the melting point of Bi (272°C). The direction was along [111], the radiation used Mo $K\alpha$ in third order.

Whereas the Debye-Waller law requires a continuous decline with increasing temperature for the relative integrated intensity following:

$$I/I_0=e^{-kT\cdot\sin^2\theta}$$

it was found that at approximately 210°C I/I_0 passed through a minimum after which it *increased* with T to a value equivalent to $T\sim150$°C for the highest observed temperature (265°C) (Fig. 2).

The reversibility of the $I/I_0(T)$ function proved to be largely depending upon the thermal history of the crystal although only crystals without any indication of crystallographic irregularities were used. Figs. 1 and 3 represent the $I/I_0(T)$ function of crystals having been raised to approximately 220°C and then quenched in liquid air

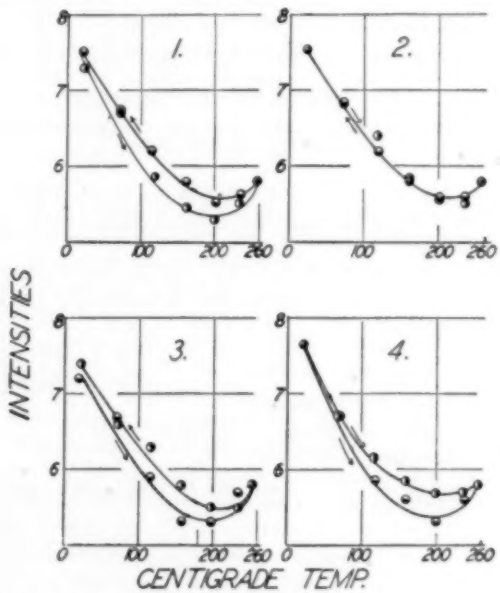

FIGS. 1–4. The ordinate represents the relative integrated intensity of third order Mo $K\alpha$ radiation reflected from Bi (111); the abscissae the temperature in C. In Figs. 1 and 3 the crystal was "quenched" before measurements with increasing temperatures were taken. In Fig. 2 the crystal was annealed before measurement. In Fig. 4 the crystal was heated after annealing (upper curve), then quenched and reheated (lower curve). The arrows indicate the temperature direction of the measurement.

previous to the heating necessary for the measurement. As is to be expected a certain "recrystallization" takes place inside the crystal indicated by a higher reflectivity for decreasing temperatures.

Fig. 2 shows the function of a crystal having been annealed at high temperature for a considerable time. Here the hysteresis is absent within the margin of experimental error.

The crystal in Fig. 4 is heated after annealing (upper curve) then immediately quenched and reheated. Here as in all other cases it will be noticed that a heated (and thus annealed) crystal being measured while cooling or a previously annealed crystal being heated shows a *higher* reflectivity, whereas the non-annealed crystal follows the power type of curve, i.e., is a less perfect reflector. It is interesting to note that this hysteresis is largest in the region of the anomaly ($d(I/I_0)/dT \sim 0$).

A detailed account of the determination of the temperature function in a temperature range from the boiling point of hydrogen to the melting point of Bi will be published soon.

ROBERT B. JACOBS
ALEXANDER GOETZ
California Institute of Technology,
December 5, 1934.

[1] R. C. Hergenrother, Physics **2**, 211 (1932).

THE AMERICAN INSTITUTE OF PHYSICS

INCORPORATED

GOVERNING BOARD

For The American Physical Society:

KARL T. COMPTON, *Chairman*
Massachusetts Institute of Technology

GEORGE B. PEGRAM, *Secretary*
Columbia University

JOHN T. TATE
University of Minnesota

For The Optical Society of America:

E. C. CRITTENDEN
Bureau of Standards

PAUL D. FOOTE
The Gulf Companies

F. K. RICHTMYER
Cornell University

For The Acoustical Society of America:

HARVEY FLETCHER
Bell Telephone Laboratories

VERN O. KNUDSEN
University of California at Los Angeles

WALLACE WATERFALL
The Celotex Company

For The Society of Rheology:

E. C. BINGHAM
Lafayette College

A. STUART HUNTER
du Pont Rayon Company

S. E. SHEPPARD
Eastman Kodak Company

For The American Association of Physics Teachers:

HOMER L. DODGE
University of Oklahoma

PAUL E. KLOPSTEG
Central Scientific Company

FREDERIC PALMER
Haverford College

ADMINISTRATIVE STAFF

HENRY A. BARTON, *Director* JOHN T. TATE, *Adviser on Publications*

MADELINE M. MITCHELL, *Editorial Secretary*
Office: 11 East 38th Street, New York, New York

JOURNALS

THE PHYSICAL REVIEW

REVIEWS OF MODERN PHYSICS

PHYSICS
JOHN T. TATE, *Editor*
J. W. BUCHTA, *Assistant Editor*
E. C. BINGHAM, *Rheology Editor*

THE JOURNAL OF THE OPTICAL SOCIETY OF AMERICA

THE REVIEW OF SCIENTIFIC INSTRUMENTS WITH PHYSICS NEWS AND VIEWS

F. K. RICHTMYER, *Editor*

JOURNAL OF THE ACOUSTICAL SOCIETY OF AMERICA

F. R. WATSON, *Editor*

THE JOURNAL OF CHEMICAL PHYSICS

HAROLD C. UREY, *Editor*

THE AMERICAN PHYSICS TEACHER

DUANE ROLLER, *Editor*

The American Institute of Physics is a membership corporation of which five societies are the founding members. These five societies are the principal national societies devoted to pure and applied physics in America. Their names, and those of their representatives who form the Governing Board of the Institute, are given above. The principal work of the Institute is the publication of journals sponsored by the societies or by itself. The names and the editors of the journals are also listed above.

The broad purpose of the Institute is to represent, in all matters of wide or common interest, the five thousand or more members and subscribers associated with the Founder Societies and the journals. It aims to advance the science and profession of physics, and to promote cooperation between pure research, the applied sciences and the industries. To achieve these aims, it is greatly in need of an endowment and is empowered by law to administer grants and funds of any kind.

CONTENTS

Phys. Rev. 47 (1935) JANUARY 1

Infra-red Absorption of Iodine Vapor. . . . . DANA T. WARREN 1

Analysis of the Hydrogen Sulfide Band at 10,100A . . . PAUL C. CROSS 7

Theories of the Spectral Selective Photoelectric Effect . CLARENCE ZENER 15

Transmutations of Sodium by Deuterons . . . . ERNEST O. LAWRENCE 17

Comparison of the Spectra of CaH and CaD . . . WILLIAM W. WATSON 27

Spectroscopic Determination of e/m C. D. SHANE AND FRANK H. SPEDDING 33

Band Structure of H_2 . . . . . FRANK H. SPEDDING, C. D. SHANE AND NORMAN S. GRACE 38

Are the Formulae for the Absorption of High Energy Radiations Valid? . . . . . J. R. OPPENHEIMER 44

Disintegration of the Nuclei of Light Atoms by Neutrons. II. Neon, Fluorine and Carbon . . . . . WILLIAM D. HARKINS, DAVID M. GANS AND HENRY W. NEWSON 52

Collisions of the Second Kind Between Magnesium and Neon. . . . . J. H. MANLEY AND O. S. DUFFENDACK 56

Low-Frequency High-Voltage Generator . . . . . DAVID H. SLOAN 62

Optical Restoration of Photoconductivity in Red Mercuric Iodide . . . . . FOSTER C. NIX 72

Polarized Light in Magneto-Optics . . H. W. FARWELL AND J. B. HAWKES 78

Nuclear Moments . . . . . D. R. INGLIS 84

Anomalous Thermal Expansion and the Ferromagnetic Change in Volume of Nickel . . . . . CLARKE WILLIAMS 88

Letters to the Editor:

Ionization Measurements of Upper-Atmospheric Ionization. . . E. V. APPLETON 89

Natural Width of the $K\alpha$-Lines . . . . . HENRY MARGENAU 89

Photoelectric Effect . . . . . A. v. GROSSE AND M. S. AGRUSS 91

North-South Asymmetry of the Cosmic Radiation in Mexico . . . . . THOMAS H. JOHNSON 91

Gamma-Ray Neutrons and the Fermi Proton Effect . . . . . A. v. GROSSE AND M. S. AGRUSS 93

Interaction Between Vibration and Rotation for Symmetrical Molecules . . . . . DAVID M. DENNISON AND MANFRED JOHNSTON 93

Interference Function of X-Ray Reflection in the Neighborhood of the Melting Point of a Crystal ROBERT B. JACOBS AND ALEXANDER GOETZ 94

LANCASTER PRESS, INC., LANCASTER, PA.